

Development of Silk Fibroin/Chitosan Based Porous Scaffolds for Cartilage Tissue Engineering

Varshini Vishwanath



Department of Biotechnology and Medical Engineering
National Institute of Technology Rourkela

Development of Silk Fibroin/Chitosan Based Porous Scaffolds for Cartilage Tissue Engineering

Dissertation submitted in partial fulfillment

of the requirements of the degree of

Doctor of Philosophy

in

Biotechnology and Medical Engineering

by

Varshini Vishwanath

(Roll Number: 510BM607)

based on the research carried out

under the supervision of

Prof. Amit Biswas

and

Prof. Krishna Pramanik



January, 2017

Department of Biotechnology and Medical Engineering
National Institute of Technology Rourkela



Department of Biotechnology and Medical Engineering
National Institute of Technology Rourkela

Certificate of Examination

Roll Number: *510BM607*

Name: *Varshini Vishwanath*

Title of Dissertation: *Development of Silk Fibroin/Chitosan Based Porous Scaffolds for Cartilage Tissue Engineering*

We the below signed, after checking the dissertation mentioned above and the official record book (s) of the student, hereby state our approval of the dissertation submitted in partial fulfillment of the requirements of the degree of *Doctor of Philosophy in Biotechnology and Medical Engineering* at *National Institute of Technology Rourkela*. We are satisfied with the volume, quality, correctness, and originality of the work.

Krishna Pramanik
Co-Supervisor

Amit Biswas
Principal Supervisor

Santanu Bhattacharya
Member, DSC

Bankim Chandra Ray
Member, DSC

Kunal Pal
Member, DSC

Examiner

Santanu Paria
Chairperson, DSC

Mukesh Kumar Gupta
Head of Department



Department of Biotechnology and Medical Engineering
National Institute of Technology Rourkela

Prof. Amit Biswas

Assistant Professor

Prof. Krishna Pramanik

Professor

January 09, 2017

Supervisors' Certificate

This is to certify that the work presented in this dissertation entitled *Development of Silk Fibroin/Chitosan Based Porous Scaffolds for Cartilage Tissue Engineering* by Varshini Vishwanath, Roll Number 510BM607, is a record of original research carried out by her under our supervision and guidance in partial fulfillment of the requirements of the degree of *Doctor of Philosophy in Biotechnology and Medical Engineering*. Neither this dissertation nor any part of it has been submitted for any degree or diploma to any institute or university in India or abroad.

Krishna Pramanik
Professor

Amit Biswas
Assistant Professor

Dedication

to

Amma

&

Appa

This is for you both.....

Varshini Vishwanath

Declaration of Originality

I, *Varshini Vishwanath*, Roll Number 510BM607 hereby declare that this dissertation entitled *Development of Silk Fibroin/Chitosan Based Porous Scaffolds for Cartilage Tissue Engineering* presents my original work carried out as a doctoral student of NIT Rourkela and, to the best of my knowledge, contains no material previously published or written by another person, nor any material presented for the award of any other degree or diploma of NIT Rourkela or any other institution. Any contribution made to this research by others, with whom I have worked at NIT Rourkela or elsewhere, is explicitly acknowledged in the dissertation. Works of other authors cited in this dissertation have been duly acknowledged under the section "References". I have also submitted my original research records to the scrutiny committee for evaluation of my dissertation.

I am fully aware that in case of any non-compliance detected in future, the Senate of NIT Rourkela may withdraw the degree awarded to me on the basis of the present dissertation.

January 09, 2017
NIT Rourkela

Varshini Vishwanath

Acknowledgement

It is often said that the roots of hard work are bitter but its fruits are sweet. After toiling hard for five long years, I have finally been able to relish my sweets of success by submitting my dissertation. Its time I penned down my gratitude towards all the wonderful people who have joined hands in making this long time dream come true.

I extent my gratitude to Dr. Sunil Kumar Sarangi, Director, National Institute of Technology, Rourkela who had been instrumental in selecting me as an eligible candidate for the project. He has been a guiding spirit for me and many of my fellow scholars alike throughout our stay, thank you sir!

My heartfelt thanks to my guide, Prof. Amit Biswas who has been there as a constant source of fortitude through my stay at NIT. He has extended his kind support and has also provided me space to chase my own ideas. He has been a good critic towards my work and dissertation which has helped me to complete my experiments and write my thesis in the best possible manner. I believe my triumphs in my future career is the best way to express my appreciation towards him.

My sincere thanks to Prof. Krishna Pramanik who is also my co-supervisor and project investigator. She has been with me through my thick and thin moments contributing to the many memorable experiences of my NIT stay. She has always kept her doors open for me in times of need. I am grateful to her for her kindness and invaluable advice she provided which has helped me to enrich my research potential.

I thank my sponsoring agency, Department of Biotechnology, Government of India, New Delhi for their complete and continual financial support through the project period. I am grateful to my institute for providing essential equipment and chemical facilities. I also thank our Sponsored Research Cell (SRICCE) for helping us manage our funding and innumerable purchases.

I thank my doctoral scrutiny committee chairman Dr. Santanu Paria (Dept.of.Chemical engg) and members Dr.Santanu Bhattacharya (Dept.of Ceramic engg), Dr. Bankim Chandra Ray (Dept. of Metallurgical and Materials engg) and Dr. Kunal Pal (Dept.of.Biotechnology& Medical engg), and for their constant monitoring and valuable

comments which have helped to complete this dissertation successfully. I also wish to express my sincere gratitude to all the faculty members and staff of my department for extending their warm support.

I would like to thank my dear friends Sahely Saha, Pallavi Pushp, Bhisham Narayan Singh, Nadeem Siddiqui, Senthiguru Kulanthaivelu, Ojaswini Mishra, Niladrinath Panda, Akalabya Bissoyi, Parinita Agrawal, Gokulanathan Kasinathan, Gautam Hari Narayana, Anupriya Bharathidasan, Trupti Patil, Rohan Bhagwat and many more who have been with me through the bittersweet moments of my stay. A special mention of thanks to Mrs.Dolly Saha for her motherly love and affection.

Words cannot suffice my gratitude to my parents who have been my backbone of untiring support and unconditional love, their sacrifices made this dissertation possible. They have always been there for me during the course of my extremely rough journey enlightening me with their words of encouragement, amidst all the pain they had undergone for me, especially during and after my encounter with Jaundice, to continue my education. For their explicit support and confidence in me, my mere expression of thanks does not stand just. I am indebted forever to my husband and best friend, Narayanan, for his unqualified, enduring love, understanding and support whenever I needed him, despite the seven seas between us. He has remained as my pillar of positive energy during all my weakest moments. I am grateful to my wonderful parents-in-law and my sister-in-law who have provided me immense geniality and the freedom to pursue my dreams. Special mention to my extended family for their love and affection across many miles. Lastly, I would like to thank this sprawling, green, wonderful campus for providing me a home away from home. The span of time I have spent in this institute has essentially been one of the most rewarding years of my academic career. This experience has enabled me to chisel out as a better student and a better person alike.

January 09, 2017
NIT Rourkela

Varshini Vishwanath
Roll Number: 510BM607

Abstract

The present research deals with the development of silk fibroin (SF) and chitosan (CS) based microporous 3D scaffolds for cartilage tissue engineering applications. Porous scaffolds prepared from SF/CS blends with varying ratio of SF and CS by freeze drying method were characterized for physicochemical, mechanical and biological properties. Among the various blend ratios, SF/CS with 80:20 blend was found to be the most favourable for achieving certain superior scaffold properties than other SF/CS blends. The scaffold possesses open pore microstructure with interconnected pore network with desired pore size (71-210 μm), average pore size ($186 \pm 32.2 \mu\text{m}$), porosity ($82.2 \pm 1.3\%$) and compressive strength ($190 \pm 0.2 \text{ kPa}$). Bioactive molecules namely glucosamine sulphate (Glu) and chondroitin sulphate (Chs), the structural components of native cartilage tissue were added individually and in combination with the aim of improving cell supportive and glycosaminoglycan (GAG) secretive properties thereby facilitating cartilage specific ECM production. Thus, SF/CS/Glu and SF/CS/Chs scaffolds with varying percentage of Chs and Glu concentrations were developed. The SF/CS/Glu scaffold with 1% (w/v) Glu was the most favourable composition have pore size of 40-190 μm , average pore size of $104 \pm 19.6 \mu\text{m}$, $79.6 \pm 4.12\%$ porosity and $202 \pm 12 \text{ kPa}$ compressive strength. A marginal improvement in scaffold property was also achieved specifically by the addition of 0.8 % (w/v) Chs. The scaffold possess a pore size of 44-196 μm , average pore size $105 \pm 19.5\%$ porosity of $87 \pm 2.13\%$ and $204 \pm 13 \text{ kPa}$ compressive strength. In-vitro cell culture study using human mesenchymal stem cell (hMSCs) derived from umbilical cord blood (UCB) has shown an enhanced cell attachment, proliferation and differentiation (GAG assay) with SF/CS/Chs scaffolds than its counterpart SF/CS and SF/CS/Glu scaffolds. An enhanced scaffold porosity, hydrophilicity, cell adhesion and cell proliferation were further achieved by the incorporation both Glu and Chs in combination into SF/CS blend. Moreover, the increased GAG secretion shown by SF/CS/Glu/Chs scaffolds represents the superiority of the scaffold than the other scaffold towards cartilage tissue regeneration. Thus, it has been demonstrated

that the scaffold comprising of SF/CS/Glu/Chs is the potential 3D polymer matrix which can be used as a suitable platform for cartilage tissue regeneration.

Key words: *Cartilage; tissue engineering; silk fibroin; chitosan; glucosamine sulphate; chondroitin sulphate.*

Contents

Certificate of Examination	ii
Supervisors' Certificate	iii
Dedication	iv
Declaration of Originality	v
Acknowledgement	vi
Abstract	viii
List of Figures	xiii
List of Tables	xviii
List of Abbreviations	xix
Chapter 1 Introduction	1
1.1 Background and significance of study	2
1.2 Scaffolds as the foundation for tissue engineering.....	4
1.3 Properties of ideal scaffolds	4
1.4 Scaffold fabrication techniques	5
1.4.1 Electrospinning.....	5
1.4.2 Phase separation	6
1.4.3 Particulate leaching	7
1.4.4 Rapid prototyping.....	7
1.5 Applications of scaffolds in cartilage tissue engineering.....	8
1.6 Biomaterials for cartilage tissue scaffold	8
1.7 Stem cells for tissue engineering.....	12
1.8 Organization of thesis.....	13
Chapter 2 Literature Review	15

Chapter 3 Scope and Objectives	23
3.1 Objectives	24
3.2 Scope of the work	24
Chapter 4 Materials and Methods	28
4.1 Materials	29
4.1.1 Chemicals for scaffold fabrication	29
4.1.2 Chemicals for cell culture study	29
4.2 Methods	29
4.2.1 Preparation of regenerated silk fibroin powder	29
4.2.2 Preparation of silk fibroin porous scaffolds by freeze drying method ...	30
4.2.3 Preparation of silk-chitosan blend porous scaffolds by freeze drying method	30
4.2.4 Preparation of SF/CS/Glu scaffolds	30
4.2.5 Preparation of SF/CS/Chs scaffolds	30
4.2.6 Preparation of SF/CS/Glu/Chs scaffolds	31
4.3 Characterization of scaffolds	31
4.3.1 Morphological characterization	31
4.3.2 Porosity and pore distribution	31
4.3.3 Structural analysis	32
4.3.4 Contact angle measurement	32
4.3.5 Swelling behavior	32
4.3.6 Biodegradation study	32
4.3.7 Compressive strength	33
4.3.8 In-vitro cell study	33
4.4 Statistical analysis	35
Chapter 5 Results and Discussion	36
5.A DEVELOPMENT OF SILK FIBROIN/CHITOSAN BLEND SCAFFOLDS	37
5.1 Results and Discussion	38
5.1.1 Scanning electron microscopy (SEM)	38
5.1.2 Porosity	40
5.1.3 Structural analysis	40
5.1.4 Swelling behavior and water contact angle	41

5.1.5 In-vitro degradation	44
5.1.6 Compressive strength	45
5.1.7 In vitro cell culture study.....	46
5.B DEVELOPMENT OF SILK FIBROIN/CHITOSAN/GLUCOSAMINE	
SULFATE SCAFFOLDS	52
5.2 Results and discussion.....	53
5.2.1 Scanning electron microscopy (SEM).....	53
5.2.2 Porosity.....	54
5.2.3 Structural analysis	55
5.2.4 Swelling behavior and water contact angle	56
5.2.5 In vitro degradation	58
5.2.6 Compressive strength	59
5.2.7 In vitro cell culture	59
5.C DEVELOPMENT OF SILK FIBROIN/CHITOSAN/CHONDROITIN	
SULFATE SCAFFOLDS	65
5.3 Results and discussion.....	66
5.3.1 Scanning electron microscopy (SEM).....	66
5.3.2 Porosity.....	67
5.3.3 Structural analysis	68
5.3.4 Swelling behavior and water contact angle	69
5.3.5 In vitro degradation	71
5.3.6 Compressive strength	72
5.3.7 In vitro cell culture	72
5.D EFFECT OF ADDITION OF GLU AND CHS IN COMBINATION ON THE	
SCAFFOLD PROPERTY	78
5.4 Results and discussion.....	79
5.4.1 Scanning electron microscopy (SEM).....	79
5.4.2 Porosity.....	80
5.4.3 Structural analysis	81
5.4.4 Swelling Behaviour	82
5.4.5 In Vitro degradation	84
5.4.6 Compressive strength	85
5.4.7 In vitro cell culture	85

Chapter 6 Summary and Conclusion	90
References	94
Dissemination	103
Biography	105

List of Figures

Figure 1.1: Schematic representation of freeze drying procedure.....	7
Figure 5.1: SEM images of (a) Pure SF, (b) SF/CS (90:10), (c) SF/CS (80:20), (d) SF/CS (70:30), (e) SF/CS (60:40) and (f) SF/CS (50:50) scaffolds. All scaffolds possessed open porous microstructure with desired pore size and interconnected pores.	39
Figure 5.2: FT-IR spectrum of (i) Pure SF, (ii) SF/CS (90: 10), (iii) SF/CS (80:20), (iv) SF/CS (70 : 30) and (v) Pure CS scaffolds. SF/CS blend scaffolds showed characteristic band of SF/CS at 1080 cm^{-1}	41
Figure 5.3 Swelling behaviour of (a) Pure SF scaffolds, (b) SF/CS (90:10), (c) SF/CS (80:20), (d) SF/CS (70:30), (e) SF/CS (60:40) and (f) SF/CS (50:50). Pure SF scaffold showed the least swelling behaviour when compared to the SF/CS blend scaffolds. Swelling was found to increase with increase in CS content.	43
Figure 5.4: Degradation pattern of (a) Pure SF, (b) SF/CS (90:10), (c) SF/CS (80:20), (d) SF/CS (70:30), (e) SF/CS (60:40) and (f) SF/CS (50:50) scaffolds. Faster degradation was observed with increase in chitosan content.	44
Figure 5.5: Compressive strength of (a) Pure SF, (b) SF/CS (90:10), (c) SF/CS (80:20), (d) SF/CS (70:30) (e) SF/CS (60:40) and (f) SF/CS (50:50) scaffolds. A gradual decrease in compressive strength was observed with increase in chitosan content.	45
Figure 5.6: Morphological changes of hMSCs observed under phase contrast microscope during (a) 1 st week, (b) 3 rd week (c) 5 th week and (d) 7 th week of culture. Initially the cells are found to be spherical in shape and slowly reached fibroblast like morphology in about 7 weeks of culture.....	46
Figure 5.7: FE-SEM images for cell attachment and proliferation of hMSCs over various scaffolds. (a) and (e) Pure SF, (b) & (f) SF/CS (90:10), (c) & (g) SF/CS (80:20) and (d) & (h) SF/CS (70:30) scaffolds after 7 and 14 days of culture respectively. hMSCs were found to spread well throughout the SF/CS (80:20) blend scaffold representing its superior cell supportive property than the other blend scaffolds.	47

Figure 5.8: Magnified FE-SEM image showing cell proliferation over SF/CS(80:20) blend scaffolds after (a) 7 days and (b) 14 days of culture.	48
Figure 5.9: Cell viability analysis by MTT assay on (a) SF, (b) SF/CS (90:10) blend, (c) SF/CS (80:20), (d) SF/CS (70:30) and (e) SF/CS (60:30) blend scaffolds. * represents significant differences at $p < 0.05$. The metabolic activity of SF/CS scaffold was increased with culture time compared to pure SF. The metabolic activity of SF/CS scaffold was increased with increase in CS content upto 20% and thereafter, a slight decrease in metabolic activity was observed with further increase in CS content in the blend	49
Figure 5.10: Live and dead assay on (a) and (c) SF scaffold; (b) and (d) SF/CS (80:20) scaffold. (a) and (b) represent 5 days and (c) and (d) represent 7 days after cell seeding. SF/CS (80:20) blend scaffold shows increased cell viability when compared to pure SF scaffold.	50
Figure 5.11: GAG assessment of (a) SF scaffold (b) SF/CS (80:20) scaffold. * represents significant difference at $P < 0.05$. The amount of GAG secreted by hMSC over SF/CS (80:20) scaffold was found to be higher throughout the culture period compared to pure SF scaffold.	51
Figure 5.12: SEM images of SF/CS/Glu scaffolds with (a) (0.2), (b) (0.4), (c) (0.6), (d) (0.8), (e) (1) and (f) (1.2) % (w/v) of Glu respectively. All scaffolds possessed open porous network with highly interconnected pore structures.....	54
Figure 5.13: FT-IR spectra of (i) SF/CS (80: 20) and (ii) SF/CS/Glu scaffolds. The additional band in SF/CS/Glu scaffold is due to the interaction of Glu with SF/CS blend.	56
Figure 5.14: Swelling behaviour (a) SF/CS (80:20) blend scaffold and SF/CS with (b) 0.2, (c) 0.4, (d) 0.6, (e) 0.8, (f) 1 and (g) 1.2 % (w/v) of Glu respectively. A drastic increase in swelling was obtained by the addition of Glu to SF/CS(80:20) scaffold and the swelling rate was increased with increase in Glu content.....	57
Figure 5.15: Degradation pattern of (a) SF/CS (80:20) blend scaffold and SF/CS with (b) 0.2, (c) 0.4, (d) 0.6, (e) 0.8, (f) 1 and (g) 1.2 % (w/v) of Glu respectively SF/CS/Glu scaffolds were found to degrade faster in comparison to the SF/CS scaffolds.....	59
Figure 5.16 FE-SEM images of cell attachment and proliferation of MSCs over various scaffolds(a) & (b)SF/CS (80:20) scaffold, (c) & (d) SF/CS/Glu 1 % (w/v) after 7 and 14	

days of culture respectively. Superior cell attachment and spreading were observed in SF/CS/Glu scaffolds than SF/CS scaffolds.	60
Figure 5.17: MTT assay of (a) SF/CS (80:20) scaffolds and SF/CS/Glu (b) 0.8, (c) 1 and (d) 1.2 % Glu (w/v). The metabolic activity of SF/CS/Glu scaffold increased with increase in Glu content.	61
Figure 5.18: Proliferation in terms of DNA quantification of hMSC over (a) SF/CS (80 : 20) scaffold; (b) SF/CS/Glu scaffolds with 1%(w/v) Glu. The hMSC proliferation on SF/CS scaffold increased with addition of Glu.....	62
Figure 5.19: Confocal images showing the cytoskeletal arrangement on (a) SF/CS (80:20) scaffold; (b) SF/CS/Glu scaffolds with 1%(w/v) Glu. The cells were found to well spread on the surface and also inside of the SF/CS/Glu scaffolds.....	63
Figure 5.20: GAG analysis of (a) SF/CS (80:20) scaffold. (b) SF/CS/Glu scaffold with 1% m (w/v) Glu. An increase in GAG content was observed with increase in culture time. The scaffold containing Glu showed higher GAG formation.....	64
Figure 5.21: SEM images of SF/CS/Chs scaffolds with (a) (0.2), (b) (0.4), (c) (0.6), (d) (0.8), (e) (1) and (f) (1.2) %(w/v) of Chs respectively. All scaffolds possessed open porous network with highly interconnected pore structures.....	67
Figure 5.22: FT-IR spectra of (a) SF/CS (80: 20), (b) Chs powder and (c) SF/CS/Chs scaffolds. The additional band in SF/CS/Chs scaffold is due to the interaction of Chs with SF/CS blend.....	69
Figure 5.23: Swelling behaviour of (a) SF/CS (80:20), (b) SF/CS/Glu with 1% (w/v) Glu and SF/CS/Chs with (c) 0.2, (d) 0.4, (e) 0.6, (f) 0.8, (g) 1 & (h) 1.2 % (w/v) of Chs respectively. The rate of swelling increased between 2-8 hrs and after that they attained state of swelling equilibrium after 10 hrs of study.	70
Figure 5.24: Degradation pattern of (a) SF/CS (80:20), (b) SF/CS/Glu with 1%(w/v) Glu and SF/CS/Chs with (c) 0.2, (d) 0.4, (e) 0.6, (f) 0.8, (g) 1 & (h) 1.2 % (w/v) of Chs respectively. All the scaffolds showed an initial faster degradation and the rate of drgradation increased with increase in Chs content.....	72
Figure 5.25: FE-SEM images showing the cell attachment & cell spreading over the scaffolds. (a) & (d) SF/CS (80:20), (b) & (e) SF/CS/Glu 1% (w/v), and (c) & (f) SF/CS/Chs	

0.8 % (w/v) scaffolds. A homogenous population of cells were present in the SF/CS/Chs scaffolds..... 73

Figure 5.26: MTT assay of (a) SF/CS (80:20) blend scaffold, (b) SF/CS/Glu scaffold with 1% (w/v) Glu and SF/CS/Chs scaffold with (c) 0.8 % (w/v) of Chs. The metabolic activity of the SF/CS/Chs scaffold was higher than SF/CS scaffold but lower than SF/CS/Glu scaffolds..... 74

Figure 5.27: DNA assay of (a) SF/CS (80:20) blend scaffold, (b) SF/CS/Glu scaffold with 1% (w/v) Glu and (c) SF/CS/Chs scaffold with 0.8%(w/v)of Chs. SF/CS/Chs scaffold showed higher DNA content than the other scaffolds..... 75

Figure 5.28: Confocal microscope images of scaffolds. (a) & (d) SF/CS (80:20), (b) & (e) SF/CS/Glu 1 % (w/v), and (c) & (f) SF/CS/Chs 0.8% (w/v) after 7 & 14 days of culture respectively. A uniform distribution of hMSCs on the SF/CS/Chs scaffolds was observed from confocal microscopic images. SF/CS/Chs scaffold showed reduced number of cells than the Glu loaded SF/CS scaffolds..... 76

Figure 5.29: GAG estimation of (a) SF/CS (80:20) blend scaffold, (b) SF/CS/Glu scaffold with 1% (w/v) Glu and (c) SF/CS/Chs scaffold with 0.8% (w/v) of Chs. GAG secretion was found to be maximum for the SF/CS/Chs scaffolds..... 77

Figure 5.30: SEM images of SF/CS/Glu/Chs scaffold with (a) Chs (0.5) (b) Chs (1) (c) Chs (1.5) % (w/v). The scaffolds showed similar pore morphology with a little variation in their pore size with various compositions..... 80

Figure 5.31: FT-IR spectra of (a) Pure SF/CS, (b) SF/CS/Glu (c) SF/CS/Chs (d) SF/CS/Glu/Chs scaffolds. The characteristic band of Glu & Chs was found in SF/CS/Glu/Chs representing the individual interaction of Glu & Chs with SF/CS blend. 81

Figure 5.32: Swelling behaviour of (a) SF/CS (80:20) (b) SF/CS/Glu (1%) (c) SF/CS/Chs (0.8%) and SF/CS/Glu/Chs scaffolds with (d) 0.5 (e) 1 (f) 1.5 % (w/v) of Chs respectively. All the scaffolds showed an initial increase in swelling during the first few hrs but the swelling equilibrium was achieved after 10 hrs of SBF treatment..... 83

Figure 5.33: Degradation pattern of (a) SF/CS (80:20) (b) SF/CS/Glu (1%) (c) SF/CS/Chs (0.8%) and SF/CS/Glu/Chs scaffolds with (d) 0.5, (e) 1 & (f) 1.5 % (w/v) of Chs respectively. The degradation of SF/CS/Glu/Chs among the group with varied Chs content increased with increase in Chs content..... 84

Figure 5.34:FE-SEM images of SF/CS/Glu/Chs scaffolds. (a) & (f) SF/CS(80:20), (b) & (g)SF/CS/Glu with 1% (w/v) of Glu, (c) & (h) SF/CS/Glu / Chs0.5 %(w/v), (d) & (i) SF/CS/Glu / Chs 1 % (w/v), (e) &(j) SF/CS/Glu/Chs1.5 % (w/v) scaffolds after 7 &14 days of culture. The cells are found to attach well on the surface and also inside the pores of the scaffold.	85
Figure 5.35: MTT assay of (a) SF/CS (80:20), (b) SF/CS/Glu (1%) (c) SF/CS/Chs (0.8%) and SF/CS/Glu (1%) with (d) 0.5, (e) 1 and (f) 1.5% (w/v) of Chs scaffolds. An increase in metabolic activity with culture period is evident with all the scaffolds with a varied degree of metabolic activity.	86
Figure 5.36: DNA quantification of (a) SF/CS(80:20) , (b) SF/CS/Glu (1%) , (c) SF/CS/Chs (0.8%), (d) Glu/Chs 0.5(%w/v) scaffolds. DNA content was found to increase in the SF/CS/Glu/Chs scaffold than the other developed scaffolds.....	87
Figure 5.37: Confocal microscopy images (a) SF/CS(80:20), (b) SF/CS/Glu (1%), (c) SF/CS/Chs (0.8%), (d) Glu/Chs 0.5(%w/v) scaffolds. after 7 days of culture. Significant cell population was observed in the SF/CS/Glu/Chs scaffolds.	88
Figure 5.38: GAG analysis on (a) SF/CS(80:20), (b) SF/CS/Glu 1%(w/v) , (c) SF/CS/Chs 0.8%(w/v) and (d) SF/CS/Glu/Chs 0.5% (w/v) scaffolds. The presence of Glu & Chs in the SF/CS scaffold significantly increase the GAG secretion over culture period.	89

List of Tables

Table 2.1: Structural components of cartilage tissue.....	17
Table 2.2: Silk Fibroin/Chitosan blends in tissue engineering applications.....	22
Table 5.1: Pore size range , average pore size and porosity of pure SF and SF/CS blend scaffolds.....	40
Table 5.2: Contact angle of SF and SF/CS scaffolds.	43
Table 5.3: Pore size, average pore size, and porosity of SF/CS/Glu scaffolds.....	55
Table 5.4: Contact angle of SF/CS/Glu scaffolds.....	57
Table 5.5: Pore size, average pore size, and porosity of SF/CS/Chs scaffolds	68
Table 5.6:.Contact angle of SF/CS/Chs scaffolds	80
Table 5.7:Pore size, average pore size, and porosity of SF/CS/Glu/Chs scaffolds	71
Table 5.8: Contact angle of SF/CS/Glu/Chs scaffolds.....	83

List of Abbreviations

ANOVA	Analysis Of Variance
BMP	Bone Morphogenetic Protein
CAD	Computer Aided Design
3D	Three Dimensional
Ca(CNS) ₂	Calcium Thiocyanate
CaCl ₂	Calcium Chloride
Ca(NO ₃) ₂	Calcium Nitrate
CH ₃ COOH	Acetic Acid
Chs	Chondroitin Sulfate
CuSO ₄	Copper Sulfate
H ₂ O	Water
DMEM	Dulbecco's Modified Eagle's Medium
DMMB	1, 9-Dimethylmethylene Blue
DNA	Deoxy Ribonucleic Acid
ECM	Extracellular Matrix
EtOH	Ethanol
FBS	Fetal Bovine Serum
FITC	Fluorescein Isothiocyanate
FT-IR	Fourier Transform Infra Red
GAG	Glycosaminoglycan
Glu	Glucosamine Sulfate
HCCOH	Formic Acid
hMSCs	Human Mesenchymal Stem Cells
LiBr	Lithium Bromide
MTT	3-[4,5-Dimethyltriazol-2-Y1]-2,5-Diphenyl Tetrazolium
MEM	4-Morpholino Ethane Sulfonic Acid
MgCl ₂	Magnesium Chloride

MWCO	Molecular Weight Cut Off
NaCl	Sodium Chloride
NaHCO ₃	Sodium Bi Carbonate
NH ₄ OH	Ammonium Hydroxide
Na ₂ HPO ₄	Disodium Hydrogen Phosphate
Na ₂ SO ₄	Sodium Sulphate
NH ₄ CNS	Ammonium Thiocyanate
KCl	Pottasium Chloride
PGA	Poly Glycolic Acid
PLGA	Poly(Lactic-Co-Glycolic Acid)
PLA	Polylactic Acid
PLLA	Poly L Lactic Acid
PVA	Polyvinyl Alcohol
RP	Rapid Prototyping
RT	Room Temperature
SBF	Simulated Body Fluid
SF	Silk Fibroin
TIPS	Thermally Induced Phase Separation
UCB	Umbilical Cord Blood
ZnCl ₂	Zinc Chloride

Chapter 1

Introduction

1.1 Background and significance of study

Cartilage tissue reconstruction has become an important area in modern medical healthcare system for functional and aesthetic surgery. Articular cartilage is predominantly avascular, aneural, and alymphatic tissue [1] which heals poorly with time. It is composed of sparsely distributed chondrocytes embedded within a dense extracellular matrix (ECM) with primarily type II collagen and proteoglycans [23]. Injuries to the cartilage tissue can occur through various mechanisms either through blunt trauma that breaks a piece of cartilage from the end of the bone or due to the constant wear and tear of cartilage tissue with aging. Current clinical methods to treat cartilage defects include arthroscopic debridement/lavage, osteochondral grafting, microfracture, osteochondral transplantation etc.[4,5]. These clinical methods have several limitations like lack of integration at the implantation site, limited mobility, and durability of the implants etc. [4,5]. Cartilage tissue can be regenerated by tissue engineering approach, which involves the combined use of scaffolds, cells and growth factors. In this technique, the scaffold with a desired set of material property is an essential component to provide a specific direction for the growth, proliferation and differentiation of cells to their desired lineages [6,7]. Specifically, scaffolds intended for cartilage regeneration require certain properties that offer adequate nutrient and waste transport, adhesion to the defect site, minimal invasive implantation or injection, biocompatibility and biodegradability [7]. A temporary three dimensional scaffold should mimic the physiological properties and perform the function of a cartilage extracellular matrix, enabling a microenvironment that can induce chondrocytes into a functional state under *in-vitro* conditions [8].

Choosing the right material for cartilage scaffold is a very important aspect for the ultimate function of the cartilage scaffold. Fabrication of scaffold utilizing the natural components of the cartilage will pave the way for better cartilage tissue regeneration [9]. In this context, a variety of natural polymers has been explored for the fabrication of scaffold matrices with desired properties [11,12,13]. Silk Fibroin (SF) is an attractive fibrous protein and has many biomedical applications because of its permeability to oxygen and water vapor and robust mechanical strength [15]. However, SF offers slow degradation, brittleness and lack of hydrophilicity, which limits its use in tissue engineering [15]. Chitosan (CS), is biocompatible and biodegradable polymer have an excellent wound healing property [16]. Moreover, CS has its inherent GAG residues that can aid in cartilage tissue growth [15,16].

However, its rapid degradation rate and low mechanical strength limits its application in tissue engineering [16]. Overall, the use of SF or CS alone is not suitable as scaffold material. In contrast, a few researchers have studied the effect of the combination of these two natural polymers and reported the resultant SF/CS blend with excellent scaffold properties [17,18,19]. However, in most of these studies, a specific ratio of SF/CS was used with the aim of exploring the suitability of the blend as scaffold material [17,19]. Therefore, a systematic study is essential to investigate the influence of SF/CS blend ratio on the properties of scaffold, targeting cartilage tissue regeneration.

Glucosamine sulfate, present in the cartilage ECM acts as a precursor for the synthesis of various molecules, including chondroitin sulfate, keratin sulfate etc [20]. It also preserves the structural integrity of the native cartilage [20]. Chondroitin sulfate, synthesized from glucosamine sulfate, predominantly has the water and nutrient absorption property, facilitates cell proliferation and also acts as an anti-inflammatory agent [21,22,23]. Both Glu and Chs are used as oral supplements for regeneration of cartilage tissue due to their synergistic effect [24,25,26]. So, the use of these components can be beneficial in the fabrication of scaffolds to provide the necessary molecules for cell attachment and promote better regeneration of cartilage.

The source of cells is another important factor in tissue engineering. Many studies have been reported on the culture of mesenchymal stem cells (MSCs) derived from the bone marrow of rats [27], adipose tissue [28,29] on SF/CS blend scaffolds for tissue regeneration. Umbilical cord blood (UCB), is a relatively cheaper source of stem cells [30,31]. The use of UCB involves limited ethical issues and has great potential in the field of stem cell engineering [32,33,34]. Thus, the use of MSCs, derived from UCB as a potential cell source for cartilage tissue regeneration using SF/CS blend scaffold is desirable.

1.2 Scaffolds as the foundation for tissue engineering

Scaffolds are engineered three dimensioned structures which provide temporary sanctuaries to colonizing cells in order to develop a complete functional tissue [35]. After implantation into the body, they degrade with time, leaving behind the newly formed tissue mass that later develops into the target tissue. Therefore, preparation of the scaffold is a challenging task as the requirements are manifold [35,36]. High cell density combined with an interactive scaffold matrix are essential to enhance cell-scaffold interactions, important for tissue generation.

1.3 Properties of ideal scaffolds

Scaffolds have the critical task of facing a complex biological and sensitive system, the human body. Therefore, these scaffolds should be biocompatible, biodegradable, sufficiently porous, and contain sufficient compressive properties [37,38]. In addition to their material properties, the developed scaffold must be designed to accommodate the seeded cells and facilitate cellular interactions [39].

Ideally the scaffold should facilitate diffusion of nutrients, gases and waste products, provide complete and controlled degradation, support cytocompatibility, cell proliferation and differentiation, create integration with the host tissue and act as temporary load bearing substrate until the new tissue is functional [40].

The foremost requirement of any scaffold is its biocompatibility, which essentially means that the scaffold should be accepted by the living cells as a favorable guest and must not elicit any kind of immunological response and cytotoxicity [38,39,41]. The geometry and morphology of the scaffold play a pivot role in the support of cellular growth, proliferation and differentiation to a particular lineage [41]. Porosity is essential as it decides the proper supply of nourishment to cells, removal of waste products, supporting cell recruitment, cell aggregation, vascularisation and cell differentiation. Interconnectivity of pores facilitates cell migration and cell signaling [41]. The swelling properties of the scaffold is important as water permeability into the scaffold determines efficient nutrient

and waste material transport [42]. The biodegradation of the scaffold is a vital process as it permits new tissue ingrowth, remodeling of the extra-cellular matrix (ECM) and matches the formation of new tissue [42]. The mechanical strength of the scaffold ensures the stability of the scaffold in withstanding the compressive behavior *in vivo* [41,42].

Biofactor delivery is also an integral feature of a successful scaffold material [43], with equal support for scaffold degradation with time, and the formation of the regenerated tissue [43,44]. Scaffolds must also be sterilizable easily, to maintain aseptic conditions during implantation [41]. Thus, the choice of the biomaterial is vital [42].

1.4 Scaffold fabrication techniques

Scaffolds are prepared using a wide range of techniques like electrospinning, phase separation, solvent casting, rapid prototyping etc. The miscellany of fabrication methods is mainly because different tissues have different structural requirements in order to regenerate to their complete capacity.

1.4.1 Electrospinning

Nanoscale scaffold matrices are integral in exercising a deliberate control over better cell growth and proliferation. Even though the ECM is not completely reconstructed by these nanofibers, this method still makes engineering at the nanoscale level possible [45]. Scaffolds made with this technique have numerous advantages like extremely high surface-to-volume ratio, controllable porosity, ability to produce nanofibers according to the size and shape required and also the ability to control the composition to obtain the desired functions [46]. A typical electrospinning system consists of a high voltage supply system, a tip (usually a syringe tip), a ground plate collector, which is either static (plate) or moving (rotating drum or mandrel). The principle of electrospinning is that when a polymer solution is introduced in a high voltage field, it is accelerated towards the collector maintained at the opposite polarity. As a result, nanofibers are produced which are deposited over the collector. Factors that control the property of the scaffolds include polymer concentration, solvent concentration, tip to target distance, voltage supplied, humidity, extrusion speed of the syringe etc [47].

1.4.2 Phase separation

Phase separation may be defined as the separation of a polymer solution into its constitutive phases due to the intervention of an external factor, in order to reduce system free energy [48]. This external factor may be pressure, temperature, solvents and nature of polymer used. As a result of the separation, two phases are produced, namely the polymer lean phase and polymer rich phase. The residual solvent is removed by evaporation or sublimation. The polymer rich phase solidifies and leaves behind a network of pores [48,49]. Polymer foams produced by phase separation can be tailor-made to meet specific needs by accordingly altering various process parameters. The various steps in phase separation process includes polymer dissolution, phase separation and gelation, solvent extraction from gel, freezing, freeze drying [49,50]. Process parameters that determine the characteristics of phase separated scaffolds are the solvent used, type of polymer used, polymer concentration, solvent exchange, thermal treatment and the order of procedures followed. Each process parameter has its own influence on the prepared porous scaffold [49,51].

The freeze drying technique, an offspring of the phase separation technique, is widely used to produce microporous scaffolds for numerous tissue engineering applications. Various types of porous materials like aligned, hybrid etc can be prepared by this method [51]. A typical freeze drying procedure includes the freezing of a solution followed by sublimation via freeze drying. The spaces occupied by the ice crystals are formed as pores, whose size can be altered by varying the freezing temperature and rate of freezing. For a larger pore size, extension of freezing time is necessary and vice versa for smaller pore sizes [51,52].

The process of freeze drying may be divided into three steps namely freezing, primary drying and secondary drying [52]. In the first step, the desired solution is frozen to a solid state. This freezing can be achieved in a deep freezer, with liquid nitrogen or under controlled freezing conditions. Since the rate of freezing has a direct effect on the rate of sublimation and the size of pores formed, freezing is considered to be one of the most important steps in lyophilisation [53]. In primary drying, the frozen solution is subjected to low temperature and vacuum atmosphere which begins the sublimation procedure. Secondary drying process deals with desorbing any unreacted or unbound solvent molecules. At the end of this step, completely dried materials can be obtained [53].

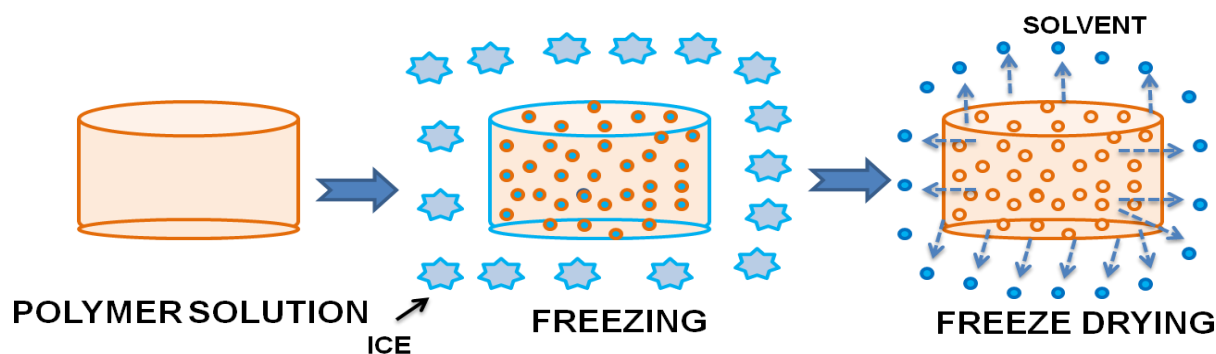


Figure 1.1: Schematic representation of freeze drying procedure

1.4.3 Particulate leaching

Particulate leaching is employed to prepare scaffolds with controlled porosity. Porogens are added to the polymeric solution with a suitable solvent. After the evaporation of the solvent, the porogens are leached out in order to create highly porous matrices [54]. Depending upon the size and morphology of the porogen, the pores are produced and organize themselves accordingly. Most commonly used porogen particulates include salt, sucrose, ammonium chloride, paraffin beads, glass beads, ice particles etc. By having control over the amount, size and shape of porogen, the pore size can be altered. It is a simple, easy technique that helps to control the pore geometry [55]. Choice of porogen size can be decided by sieving the particle to the required dimension. However, pore interconnectivity is not achieved with this process [55].

1.4.4 Rapid prototyping

Rapid prototyping, also known as solid free form technique enables the production of porous scaffolds by layer-layer manufacturing method. Scaffold models, such as images of bone defects, designed with the help of computer aided design (CAD) software [56] are expressed as cross sections. Ink jet printing technology with x and y axis technology is used to expel a binder from the jet head. The head moves according to the CAD data that has been entered into the computer, on top of a polymer powder surface. The binder dissolves and mingles with the neighbouring particles. The chamber of the piston is lowered in the z-axis and again refilled with an additional layer of powder and the entire procedure is continued. The

unbound material needs to be cleared after the final product has been completed [57]. The various other branches of rapid prototyping include 3D printing, stereolithography, selective laser sintering, fused deposition modeling, etc. Scaffolds with controlled porosity and high interconnectivity can be designed with the help of this technique. As a result, optimum mechanical and biological kinetics can be achieved [57].

1.5 Applications of scaffolds in cartilage tissue engineering

The porous scaffolds prepared from various biomaterials, using varied techniques have profound applications in tissue engineering. Various tissues in the human body namely bone, cartilage, skin, liver, cornea, urinary bladder etc. can be repaired/regenerated by utilizing the scaffold architecture [58]. Soft tissues, in particular cartilage, demand more attention as they are located in regions which are prone to constant exposure to forces and trauma. Cartilage, a predominantly avascular, aneural, and alymphatic tissue, is composed of sparsely distributed chondrocytes embedded within a dense extracellular matrix (ECM) [58,59]. As this tissue has limited possibilities of self-repair, it is considered to be an ideal candidate for tissue engineering applications [60]. Current treatment methods utilized to treat cartilage defects include arthroscopic debridement / lavage, osteochondral grafting, microfracture, osteochondral transplantation etc [61,62]. There is a persistent need to improvise these methods mainly due to the lack of sufficient compatibility and biomechanical functions. Tissue engineering based methods like combinations of chondrocytes and copolymer scaffolds and grafts that contain gelatin [63], chondroitin [64], hyaluronan [64], human fibrin [65] and PGA [66] are being used to replace the defect tissue. In another report, genetic modification was done by introducing TGF- β 1 gene into chitosan polymeric scaffolds to regenerate cartilage tissue [45].

1.6 Biomaterials for cartilage tissue scaffold

Biomaterials for scaffolding applications have a wide range of sources starting from natural and synthetic origin polymers, bioactive ceramics and hydrogels [57]. Natural origin polymers are an immediate choice for scaffolds as they are composed of structural materials of tissues. They are advantageous in terms of their biocompatibility but may sometimes cause significant immune responses. Natural polymers that are currently in use as biopolymers for scaffolding applications include alginate, agarose, collagen, cellulose,

chitosan, gelatin, heparin, hyaluronic acid, elastin, fibrin, silk etc. [65]. Synthetic biomaterials are easily available with varied physical and mechanical properties [65,66]. Synthetic polymers like polyanhydrides, PLA, PLLA, PLGA, PCL and PVA are employed for scaffold manufacture [65,66]. Composites of these natural and synthetic polymers are also exploited to prepare scaffolds for a wide range of tissue regeneration purposes. Biocomposites based on silk have also been developed including silk-HA, silk-chitosan, silk-gelatin and silk- poly (butylene succinate) [66].

The hybridization of both synthetic and natural polymers is done to evolve novel composite materials, both for physicochemical and biological benefits. Composites are prepared to utilize the properties of two or more constituents to provide a combined beneficial effect over the material and biological properties of the scaffold material. By combining various materials, it becomes easier to minimize undesirable effects and obtain materials of required features for specific applications [66]. Composite materials are chosen mainly based on the compatible blend of the composite materials [67]. The properties of the materials must correlate in a proper fashion so as to be in synchronization. Composites of polymers and ceramics improve mechanical property and tissue interaction.

i. Silk

Silk stands top on the list of advanced biomaterials used in tissue engineering owing to the reasons that it has excellent biocompatibility with robust mechanical strength [68]. It is a fibrillar protein which has the ability to be developed into a variety of forms including thin films [68], porous scaffolds [69], sponges [70] and hydrogels [70,71]. Silk possesses a molecular weight of about 370000 Da, a chain length of 150 nm and a chain diameter of 0.45 nm [71]. The two main protein constituents of silk include silk fibroin and sericin [72]. The fibroin and sericin percentage is about 60 and 40% in weight. Silk fibroin is a novel biomaterial which is biocompatible, biodegradable, non-immunogenic and mechanically strong [73].

Natural silk fibers have the ability to dissolve in limited solvents due to the presence of a large number of inter and intra-molecular hydrogen bond in fibroin and its high crystallinity [74]. Fibroin is insoluble in water and a few organic solvents, and instead, swells by 30-40%. Fibroin dissolves in concentrated aqueous, organic and

aqueous-organic salt solutions, namely LiBr, CaCl₂, Ca(CNS)₂, ZnCl₂, NH₄CNS, CuSO₄ + NH₄OH and Ca(NO₃)₂ [74].

ii. Chitosan

Chitosan (CS) is a polysaccharide found as chitin in the shells of crustaceans. It contains $\beta \rightarrow 1-4$ glucosidic linkages. CS is considered to be an excellent biomaterial with properties like wound healing, anti-microbial activity, biocompatibility and less immunogenicity [75]. It can be prepared as scaffolds in order to provide growth factors and improve chondrocyte proliferation [76]. Being positively charged in acidic medium, CS can attract the negatively charges present in the plasma thus accelerating the wound healing process [77]. CS can be processed to prepare different forms of scaffolds namely hydrogels, thin films, porous scaffolds and nanofibers [78]. However, CS has certain limitations like lack of mechanical properties and rapid degradation which hampers its utilization as a prospective scaffold material [79].

iii. Glucosamine Sulfate

Glucosamine sulfate is one of the major structural components of cartilage tissue, along with chondrocytes and hyaluronic acid [20]. The primary role of this component is to provide a structural framework to the chondrocyte network, along with sufficient nutrient balance. As a part of the proteoglycan structure, collaborated with collagen and noncollagenous glycoproteins [24], it provides the cartilage the ability to withstand compressive stress under various circumstances [24]. It also acts as the precursor molecule for the synthesis of various GAG protein including chondroitin sulfate, dermatan sulfate, keratin sulfate etc [20].

iv. Chondroitin Sulfate

Chondroitin sulfate is a predominant component of the natural ECM of cartilage which is synthesized from glucosamine sulfate [21,63,80]. It plays an important part in maintaining the water and nutrient balance of the cartilage tissue. It possess anti inflammatory properties and is found to reduce pain [81]. It also has numerous cell supportive domains that influences clustering of cells promoting cell adhesion. It is

also involved in the signaling of various growth factors and chemokines like fibroblast derived growth factors [82].

v. Collagen

Collagen is natural biopolymer found in cartilage which induces the cell-binding motifs [83]. It has versatile properties like being readily modifiable into desired shapes without disturbing the basic structure, synergy with other biomolecules and promotes blood coagulation [84]. But, it has certain disadvantages like weak mechanical and thermal stability [83,84].

vi. Polylactic acid

Polylactic acid (PLA) is an aliphatic polyester which can be degraded under physiological conditions [85,86]. It has high thermal stability and a low glass transition temperature [87]. It can form compatible blends with numerous other polymers. It finds extensive utilization in the field of controlled drug delivery [86,87].

vii. Composites for cartilage tissue regeneration

A number of researchers have worked on the composites of collagen and chondroitin sulfate as a biopolymer. The scaffolds are prepared by the co-precipitation of collagen and chondroitin sulfate or by attaching chondroitin molecules to collagen by a covalent link [88]. Since, there are studies which suggest the relation between chondroitin sulfate and chondrocyte culture, the dual influence of collagen and chondroitin sulfate produces significant results for the culture of chondrocytes. Moreover, while collagen increases the tensile strength of the scaffold, chondroitin sulfate improves cellular growth [88].

Silk fibroin and chitosan are one of the most widely used polymer blends for numerous tissue regeneration applications. Silk fibroin has sufficient mechanical stability combined with biocompatibility which can be exploited as a favorable biomaterial. But, it suffers from drawbacks like less hydrophilicity and delayed degradation [15]. Chitosan contains cell adhesion sites which can enhance the wound healing process. It also possess antimicrobial properties. But, due to its rapid

degradation and lack of sufficient mechanical properties, the utilization of chitosan in tissue engineering applications is limited [16]. However, blends of silk fibroin and chitosan have been used to obtain scaffolds with optimum mechanical, biodegradation and cell supportive properties. Also, the culture of chondrocytes on the silk chitosan blend scaffolds has been found to enhance cartilage tissue regeneration [19].

1.7 Stem cells for tissue engineering

Stem cells are an important component of the tissue engineering process. They adhere to the surface of the biomaterial, grow, proliferate and differentiate into particular lineages [29]. Mesenchymal stem cells (MSCs) are widely used in numerous tissue engineering applications. The important sources of mesenchymal stem cells include bone marrow, placenta, umbilical cord blood, adipose tissue etc. They have a great potential in the area of tissue regeneration [32].

i. Adult stem cells

Adult stem cells are undifferentiated group of cells found amongst the differentiated cells in tissues and organs [29]. They are usually found in muscle, bone marrow, skin, fat etc. These cells play a crucial role in repairing the native host tissue. Since they possess immunosuppressive ability, they can be used in allogenic transplants [33].

ii. Embryonic stem cells

These cells are found to originate from the blastocyst. They have the unique ability to differentiate into various somatic cells [34]. They possess self renewal capacity and can differentiate through precursor cells. They can differentiate into many cell types like chondrocytes, adipocytes, osteocytes etc [33]. But the usage of embryonic stem cells is limited due to ethical constraints.

iii. Mesenchymal stem cells (MSCs)

MSCs, also called as somatic cells, are undifferentiated cells which are prominent in many organs and tissues. They have originated from the mesoderm and have the ability to develop in numerous tissues like cartilage, bone, blood etc [34]. They can self renew with time and can also be readily isolated, cultured under in-vitro conditions. They possess certain similarities to fibroblasts and are readily utilized in the field of tissue engineering for numerous applications [32].

1.8 Organization of thesis

The whole thesis work has been arranged in the following chapters.

Chapter 1 describes the structure of cartilage tissue and the need for its regeneration, tissue engineering and the various strategies in regenerating cartilage tissue. This chapter focuses on different scaffold fabrication techniques along with various natural, artificial and composite polymers which can be utilized as scaffold materials for cartilage tissue engineering.

Chapter 2 presents the literature review on silk fibroin based polymer blend and composite scaffolds used for cartilage tissue engineering. Silk-chitosan based porous scaffolds with various blend ratios which have been developed till now have been briefly described.

Chapter 3 defines scope and objective of the study.

Chapter 4 describes the materials and detailed methodology adopted throughout the research work. The preparation of SF/CS based blend scaffolds and hybrid scaffolds and the various characterization techniques have been discussed in detail.

Chapter 5 describes the results and discussion consisting of 4 parts that includes

5 A: Development and characterization of SF/CS scaffolds.

The first part of the research work describes the optimization of various blend ratios of SF and CS for the preparation of SF/CS porous scaffolds, followed by the various physicochemical, mechanical and biological characterizations.

5 B: Development and characterization of SF/CS/Glu scaffolds.

The second part of the research work focuses on the improvement of cell affinity properties of SF/CS scaffolds by the addition of Glu. This part explains the preparation and characterization of SF/CS/Glu scaffolds to understand its role in cartilage tissue regeneration.

5 C: Development and characterization of SF/CS/Chs scaffolds.

The third part of the research work explains the addition of Chs to SF/CS scaffolds to validate its efficiency in improving numerous scaffold properties of SF/CS. The SF/CS/Chs scaffold preparation and characterization is described in this part.

5 D: Effect of addition of Glu and Chs in combination on the scaffold property.

The last part of the research work evaluates the effect of addition of Glu and Chs in combination towards the various SF/CS scaffold properties. This part also emphasizes the superior properties of SF/CS/Glu/Chs which can be utilized for cartilage tissue regeneration.

Chapter 6 presents a brief summary of the research work highlighting the superior in-vitro biocompatibility properties of the SF/CS based porous scaffolds which shows the potentiality of the developed scaffolds for potential cartilage tissue regeneration applications.

Chapter 2

Literature Review

Cartilage repair has become important in modern medicine for both functional and esthetic surgery. The need for treatments options is strongly associated with the fact that native cartilage is a hypocellular, avascular and not innervated tissue and thus heals poorly [89]. Defects which are confined to the articular cartilage region require restoring the structural and functional wellbeing of the tissues as it has lost its inherent capacity to regenerate. Articular cartilage forms one of the most native tissues of the human body [89,90]. Cartilage has sparsely distributed chondrocytes embedded in a dense extracellular matrix (ECM) [82]. This ECM comprises of primarily type II collagen along with proteoglycans that supply the cartilage tissue with sufficient mechanical strength for proper function [2]. As cartilage possess a limited ability to self-repair, it is considered to be an ideal application for tissue engineering. Articular cartilage, a soft tissue by nature, requires materials that can be flexible, while not necessarily providing vascularization. The material must also cater to the optimal functionality of the tissue [4]. Current treatment options like tissue grafting, mosaic plasty, autologous chondrocyte transplantation may be temporarily palliative but do not encourage long term cure [5]. A promising alternative to this treatment methods is tissue engineering which allows the regeneration of any functional tissue by employing artificial matrices (scaffolds), cells and several growth factors. Novel features are being introduced into this technique in order to achieve better cell-material and cell-cell interactions [4].

Cartilage is primarily located on the outer surface of load bearing tissues and enables smooth movement of the joints. Molecules are transported in and out of the cartilage matrix with water which helps in providing lubrication and prevents friction. Articular cartilage is a special type of hyaline cartilage which helps reduce the friction produced in the joints [5]. It is derived from the blastula stage of mesenchyme when the cells begin to secrete an extracellular cartilage matrix and form chondroblasts. These chondroblasts later come together and arrange in the dense matrix thus forming chondrocytes. Water is the major structural component and is responsible for load dependant deformation of the cartilage structure. Collagen, mainly present as collagen II offers the framework and tensile strength. Proteoglycans like chondroitin sulphate and dermatan sulphate provides electrostatic balance to the cartilage system [8]. Table 2.1 explains the basic structural components of cartilage tissue.

Table 2.1: Structural components of cartilage tissue

Component of cartilage	Proportion (%)
Chondrocytes	1-10
ECM	95
Water	60-85
Collagen	60
Proteoglycans	25-35
Glycoproteins	15-25

Materials like fibrin, collagen, alginate, chitosan, hyaluronan etc belong to the natural origin polymers that were utilized for preparing scaffolds for cartilage tissue engineering. Fibrin glue is the end product from the clot reaction which is known to enhance the growth and proliferation of chondrocytes [91]. Peretti et al. developed a fibrin based scaffold mixed with lyophilized cartilage extract which was used to culture chondrocytes. This scaffold showed enhanced biomechanical properties in addition to implant preservation [91]. Collagen is a natural component of the osteochondral framework. It therefore, has the inherent property of promoting cell attachment and proliferation in the joint areas. Hydrogels made from collagen have been utilized for the in vitro growth study of bone marrow derived mesenchymal stem cells [88]. CS is a natural polysaccharide derived from the crustacean shells which has glycosaminoglycan chains as a part of its structure. It can be prepared as scaffolds to supply growth factors and promote chondrocyte proliferation at the site of implantation [79]. Hydrogels act as injectable scaffolds as they can take up the shape of the defect in a minimal non invasive procedure. Their biomechanical properties are limited to the crosslinking density. Polyethyleneglycol hydrogels, after crosslinking and addition of specific peptide sequences support chondrogenesis [67]. CS can be prepared as scaffolds to supply growth factors and promote chondrocyte proliferation at the site of implantation [78]. Hydrogels act as injectable scaffolds as they can take up the shape of the defect in a minimal non invasive procedure. Their biomechanical properties are limited to

the crosslinking density [11]. Polyethyleneglycol hydrogels, after crosslinking and addition of specific peptide sequences support chondrogenesis [11].

Porous scaffolds, also known as sponges provide the desired porosity and surface area for cell adhesion and cell infiltration in the scaffolds. Also, the porous network is significant in providing efficient nutrient and gas exchange [68]. Nanofibrous networks also commonly called as meshes provide greater surface area and directionality for enhanced cell growth. The fiber diameter and interspace between fibers have a crucial impact over the cell behavior [47].

Wang et al investigated the effects of using silk scaffolds for potential cartilage tissue engineering applications. The chondrocytes proliferated slowly during the first 7 days of culture, with increase in the rate of cell proliferation over the next ten days. Most cell attachment was limited to the surface of scaffolds [94]. Uniform morphology and porosity was observed in freeze-dried sericin/gelatin blended scaffolds, with homogeneous pore size distributions. Enhanced mechanical properties were observed with increase in gelatin concentration. Presence of gelatin in addition to sericin also increased the number of pores and interconnectivity. Water swelling was also found to be uniform and retention was found to be up to several hours [94].

Effect of SF / hyaluronic acid blend scaffolds on the growth and proliferation of MSC's was investigated by Marcos et al. Increased swelling was observed in the blend scaffolds which may enable the infiltration of cells into the scaffolds. The enhanced cell arrangement can be attributed to a more organized pore morphology and material hydrophilicity. This, in turn, has favoured better cell attachment and proliferation [95]. Mandal et al reported the use of silk scaffolds for cell migration. Scaffolds were prepared by freezing silk solution for 24 hours, sealed on all three sides except bottom with thermocole box, for uniform cooling. The insulation cover permits controlled cooling vapours from bottom. Notable changes with regard to pore size and porosity were evident in various freezing temperatures. Pores of diameter 200–250 μm were formed due to slow cooling at -20°C and -80°C . These scaffolds had limited porosity and pore interconnectivity. But scaffolds developed by rapid freezing at -196°C were found to possess 96% porosity [95].

Nazarov et al investigated the preparation of silk fibroin porous scaffolds by different techniques. The morphology of the scaffolds varied according to the concentration of the solution and alcohol used. High alcohol concentrations caused the scaffolds to become brittle. Pore size reduced with increase in concentration of the silk solution. Higher freezing temperatures above the glass transition temperature causes longer time for ice formation. The ice particles have a direct influence in pore size namely; greater freezing time causes larger ice crystal sizes and therefore larger pore size [68]. A novel method for the preparation of silk porous membranes was studied by Nogueira et al. Foaming was induced in the silk fibroin solution by mechanical agitation. The foam was collected and compressed between polystyrene plates by applying pressure to remove excessive water. The membranes, after ethanol treatment, were stable, but became brittle at room temperature. The scaffolds had an irregular pore arrangement, with only limited visible pores. The porosity and moisture content of the scaffold were 68% and 91%, respectively. Membranes produced using this method can be considered for large scale production, use of scaffold materials in tissue engineering applications [97].

Silk scaffolds with the desired porous structure were prepared by varying the silk in methanol [98]. The increase in fibroin concentration, decreases the pore size and increases the pore density. The water molecules were restricted in their movement during freezing due to fibroin molecules and as a result, smaller ice crystals were formed at higher fibroin concentration. The compressive strength along with the compressive modulus were increased with increase in fibroin concentration. The mechanical properties also enhanced due to the increased pore wall thickness which resulted from the decreased pore size. The addition of methanol makes the fibroin molecular chains better interact and rearrange to produce a crystalline structure, which would result in structures with different morphologies. Also, scaffold morphology could be affected by freezing temperature after methanol treatment. With increase in cooling rate, aggregate formation was favoured. Therefore, the small ice crystals are formed in the spaces once occupied by water, subsequently leading to formation of smaller pores. [98]. Feng et al reported the preparation of silk fibroin porous scaffolds using the freeze drying / foaming technique. The foam was collected by mechanical agitation of the SF solution and was compressed between glass plates to remove water present. They were then allowed to partly thaw at room temperature before freeze drying. The scaffolds showed both open and closed pore structures. The

porosity increased with the decrease of fibroin solution concentration. No flake like morphology was evident. The use of foaming and freeze drying technique leads to enhanced mechanical properties of the scaffolds [99]. The effect of the freezing method on the properties of lyophilized SF porous membranes was studied by Weska et al. In order to study the effect of varying freezing methods prior to lyophilization, porous SF membranes were shock frozen in liquid nitrogen (-196°C) or slow frozen using an ultrafreezer at -80°C , for 24 hours. The main difference observed between the frozen and liquid nitrogen treated scaffolds was in the presence of water. Water was present in the samples before the freeze-drying procedure, and was the reason behind plastification of wet membranes. The quench freezing with liquid nitrogen and lyophilization caused the collapse of the membranes. On the other hand, slow cooling preserved membrane integrity. The denaturation of proteins increases under conditions when the freezing creates a large ice surface area. The observed results indicate that the freezing rate is an essential parameter that decides the integrity of lyophilized porous SF membranes [97].

Nam et al studied the effect of freezing temperature, alcohol addition and molecular weight to the morphology of regenerated SF membranes. SF porous membranes were prepared by varying freezing temperatures and solvents, followed by lyophilisation. Different freezing temperatures as such did not affect the morphology of the SF membrane. But the addition of methanol promoted aggregate particle formation which caused the random coil to change into a β -sheet conformation. At a lower cooling rate, protein aggregate formation takes place in a speed slow sufficient to synthesize an aggregate with larger voids which had been occupied by water. So, the formation of larger ice crystals would consequently lead to larger pores after lyophilization [100].

Guang et al reported modification of PCL porous scaffolds by SF. Scaffold morphology was altered due to the presence of silk fibroin, whereby increasing cell adhesion and metabolism. Liu et al studied the application of polyurethane and SF films in controlling the release of heparin. The presence of SF improved the release of heparin from the SF films [101]. Li et al analyzed the role of BMP-2 in improving the osteogenic properties of SF nanofibers. Improved osteoconductivity was noted in the BMP modified scaffolds [102]. Lee et al found that alginate improved the various material properties of SF based sponges

[103]. Yang et al analyzed the role of cellulose combined with SF and their post treatment with alkali [104].

SF/CS blends have been utilized for many tissue engineering applications (table 2.2). She et al has studied the in vitro degradation properties of SF/CS porous scaffolds. Mass % loss of scaffolds was found to be 19.28 wt% after 8 weeks of degradation [15]. Gobin et al explained the mechanical and structural properties of SF/CS porous scaffolds [69]. Altman et al described the in vitro studies on SF/CS scaffolds using human adipose tissue derived stem cells. They also explained the adhesion, migration and mechanics of human adipose-tissue-derived stem cells on these scaffolds. Enhanced wound healing and differentiation of adipose derived stem cells was observed on silk chitosan scaffold [28]. Bhardwaj studied the blend of SF/CS in preparing porous scaffolds and their characterization for tissue engineering applications [23]. They have also analyzed the potential of this scaffold blend for the culture of bovine chondrocytes and also rat derived chondrocytes. The scaffolds facilitated mesenchymal stem cell attachment, migration, cell-cell interaction and differentiation [27]. Zeng et al explained in detail the various blend ratios of SF/CS scaffolds for bone tissue engineering applications. The 40% SF-60% CS group proves the preferred ratio of scaffold material for bone tissue engineering [106].

Table 2.2: Silk Fibroin/Chitosan blends in tissue engineering applications

Biomaterials	Type of scaffold	SF/CS blend ratio	Observation	Ref
Silk fibroin & Chitosan	Film	50:50	Polymer induced conformation change observed with addition of chitosan to silk fibroin	[18]
Silk fibroin & Chitosan	Scaffold	1:1	Weight loss of scaffolds 19.28 wt% after 8 weeks of degradation	[17]
Silk fibroin & Chitosan	Scaffold	75:25	Enhanced wound healing and differentiation of adipose derived stem cells on silk chitosan scaffold	[28]
Silk fibroin & Chitosan	Scaffold	50:50	Interconnected porous structure, mechanical properties, for soft tissue engineering	[16]
Silk fibroin & Chitosan	Scaffold	75:25	Facilitates mesenchymal stem cell attachment, migration & cell-cell interaction	[29]
Silk fibroin & Chitosan	Scaffold	1:1	Scaffolds supported cell attachment and growth, and differentiation	[76]
Silk fibroin & Chitosan	Scaffold	1:1	MSC based cartilage repair	[27]
Silk fibroin & Chitosan	Scaffold	20:80, 40:60, 60:40, 80:20	The 40% silk fibroin-60% chitosan group proves the preferred ratio of cell scaffold material	[106]

Chapter 3

Scope and Objectives

In recent years, cartilage tissue engineering has been emerged as the most promising technique for the regeneration of cartilage tissue defects due to trauma and diseases through the development of biologically active 3D artificial extracellular matrix i.e tissue engineered scaffold. The design and fabrication of these scaffolds with a set of desired properties is the most challenging task. Among the various natural biopolymer, SF is considered as one of the potential candidates owing to its biocompatibility, biodegradability, non-immunogenic and robust mechanical properties [16]. However, SF lacks in hydrophilicity and delayed degradation which limits application for cartilage tissue engineering. CS, a partially de-acetylated product of chitin, is biocompatible, biodegradable and has excellent wound healing property [17]. Moreover, the inherent glycosaminoglycan residues of CS can aid in supporting cartilage tissue growth [27]. However, the rapid degradation rate and low mechanical strength warrants its application in tissue engineering [16,17]. Therefore, the present research focuses on the development of an optimal ratio of SF/CS blend and SF/CS based hybrid scaffold with bioactive molecules for cartilage tissue application.

3.1 Objectives

The objectives of the research work are as follows

- i. To develop porous scaffolds from silk fibroin/chitosan polymer blends by freeze drying method
- ii. To improve the properties of SF/CS scaffolds by incorporating bioactive molecules
- iii. To study physico-chemical and mechanical properties of the scaffolds
- iv. To study in vitro biocompatibility of the scaffold

3.2 Scope of the work

Cartilage is an integral part of the soft tissue matrix that aids the functioning of the joints. Progressive wear and tear, along with trauma leads to joint degeneration. Unlike other types of tissue, cartilage does not have its own blood supply and is aneural. Therefore, after injury, cartilage is much more difficult to self-heal and requires to be replaced completely. As a rapidly expanding field, tissue engineering may provide alternative solutions for articular cartilage repair and regeneration through development of tissue engineered scaffold.

In this context, the main challenge is the design and fabrication of a 3D scaffold as artificial ECM from a suitable biopolymer or polymer composites by an appropriate method to replace the cartilage tissue.

From the literature review, we can understand that the porous scaffolds have a potential for cartilage tissue engineering. SF and CS blends have been utilized for cartilage regeneration. However, in most of these studies, a specific ratio of SF/CS was used with the aim of exploring the suitability of the blend as scaffold material except the study of [106] on the effect of blend ratio targeting bone tissue engineering application. Therefore, the present work offers detail study on the influence of SF/CS blend ratio on the properties of scaffold targeting for cartilage tissue regeneration. Bioactive molecules like Glu and Chs are utilized as oral supplements for cartilage tissue regrowth. It is hypothesized that the use of these bioactive molecules in SF/CS blend solution for the fabrication of hybrid scaffold may pave the way for a potential artificial extracellular matrix for cartilage tissue engineering.

The various scope of the research work is summarized as follows-

1. Development of SF/CS blend scaffold

SF is an attractive fibrous protein and has many biomedical applications because of its permeability to oxygen and water vapor and robust mechanical strength. CS, a partially de-acetylated product of chitin, is biocompatible, biodegradable and has excellent wound healing property. Moreover, CS has its inherent glycosaminoglycan residues that can aid in supporting cartilage tissue growth. A specific ratio of SF/CS was used with the aim of exploring the suitability of the blend as scaffold material by most of the researchers [13, 20, 21]. Therefore, efforts will be given to establish the optimal blend ratio of SF/CS blend scaffold on the properties of scaffold targeting for cartilage tissue regeneration.

2. Characterization of scaffold

It is necessary to assess physicochemical, mechanical and biological properties of the scaffold to find their suitability for cartilage tissue engineering. The scaffold

property such as morphology, hydrophilicity, porosity, compressive strength will be characterized. The cell supportive property in terms of cell adhesion, cell proliferation and secretion of cartilage specific ECM will be evaluated.

3. Development of silk fibroin/chitosan/glucosamine sulfate scaffolds

Cartilage tissue comprises of a proteoglycan rich network which contains Glu, which acts as the backbone of proteoglycan chain. It is evident from the literature that glucosamine sulfate is usually used as an oral supplement for the regeneration of cartilage tissue [20]. Hence the cell binding affinity of the SF/CS blend scaffold shall be improved by addition of Glu in the SF/CS blend to form the hybrid scaffold. Glu can be beneficial in facilitating the cartilage specific ECM formation through GAG synthesis. The developed hybrid scaffolds will be characterized for its physicochemical and biological properties.

4. Development of silk fibroin/chitosan/chondroitin sulfate scaffolds

Like glucosamine sulfate, Chs is also used as an oral supplement for the regeneration of cartilage tissue. Chs is one of the naturally occurring GAGs present in the aggrecan region of the cartilage tissue [80]. It is an important component of extracellular matrix. The anti-inflammatory activity, water and nutrient absorption activity, wound healing property and bioactivity at the cellular level of Chs are beneficial for cartilage tissue engineering [23]. In this context, Chs will be added to SF/CS blend scaffold to investigate the effect of Chs on the SF/CS scaffold property.

5. Development of silk fibroin/chitosan/glucosamine sulfate/chondroitin sulfate scaffolds

Glu and Chs in combination are widely used for the regeneration of cartilage tissue using 1500/1200 mg of Glu and Chs respectively which reduced pain, improved the strength and movement of older people. The synergistic effects of both Glu and Chs towards cartilage regeneration was also reported [25]. The combination of Glu and Chs has alleviated pain, discomfort and improved the overall joint function in the patient groups. To make the SF/CS scaffold more effective towards cartilage tissue regeneration, cell supportive property will be improved by adding Glu and Chs together in SF/CS scaffold.

The combined effect will be assessed by physicochemical, mechanical and biological properties.

Chapter 4

Materials and Methods

4.1 Materials

4.1.1 Chemicals for scaffold fabrication

Silk cocoons (*Bombyx mori*) were purchased from Sericulture training institute, Nanjikottai, Thanjavur, Tamilnadu (India). Chitosan (degree of deacetylation > 85%), Na_2CO_3 , CaCl_2 , HCOOH , $\text{C}_2\text{H}_5\text{OH}$, CH_3COOH and Na_2HPO_4 were procured from Merck, India. Glucosamine sulfate, chondroitin sulfate, NaCl , KCl , CaCl_2 , MgCl_2 , K_2HPO_4 , NaHCO_3 and Na_2SO_4 were procured from Sigma Aldrich (USA) and used without any further purification.

4.1.2 Chemicals for cell culture study

Dulbecco's modified eagle medium (DMEM), penicillin-streptomycin solution, chondrogenic basal media with supplement, phosphate buffered saline (PBS) and trypsin were purchased from Gibco (BRL, USA). Fetal bovine serum (Hi-FBS), MTT reagent assay kit, EDTA was purchased from Hi-media. Gluteraldehyde, paraformaldehyde, papain, cysteine, 1, 9-dimethylmethylene blue (DMMB) were procured from Sigma Aldrich. Quant-it Pico green DNA kit was purchased from Thermofischer. Hoescht and TRIT-C Phalloidin were purchased from Invitrogen.

4.2 Methods

4.2.1 Preparation of regenerated SF powder

The silk cocoons were cut into fine pieces and cleaned to remove any debris. SF was extracted from the cocoons by a process called degumming in which the cut cocoon pieces are boiled in 0.02 M sodium carbonate solution for 30 mins. SF fibers thus obtained were washed thrice with distilled water and dried overnight at 40°C. The fibers were later re-dissolved in Ajisawa's reagent [$\text{CaCl}_2\text{:H}_2\text{O: EtOH}$ (1:8:2)] [115]. The SF solution was dialyzed for 3 days against deionized water using Slide-a-Lyzer dialysis cassette (Pierce, Thermo Fischer, MWCO 3500). The solution was then frozen at -80°C for 5 hours followed by freeze drying (lyophilization) for 3 days [123]. B.mori SF powder thus obtained was stored in an air tight container until further use.

4.2.2 Preparation of SF porous scaffolds by freeze drying method

Regenerated SF powder was dissolved in 0.1M HCOOH solution to obtain 2wt% SF regenerated solution. The solution was poured into plastic petridishes of size 60 mm and frozen at -20°C. The frozen samples were lyophilized at -110°C with 480 torr for 3 days to obtain freeze dried scaffolds [106].

4.2.3 Preparation of SF/CS blend porous scaffolds by freeze drying method

CS was dissolved in aqueous 0.1M CH₃COOH solution to form 2.5 wt% of polymer solution. SF and CS solutions were mixed in various volume ratios namely 90:10 (v/v), 80:20 (v/v), 70:30 (v/v), 60:40 (v/v) and 50:50 (v/v) to prepare homogeneous solutions [69]. Then the above mentioned procedure was followed to prepare SF/CS blend porous freeze dried scaffolds.

4.2.4 Preparation of SF/CS/Glu scaffolds

Glu solutions with different concentration namely 0.2, 0.4, 0.6, 0.8, 1 & 1.2 wt% were prepared. 1 ml of the prepared solutions was added to 20 ml of SF/CS blend solution and kept for stirring overnight, at room temperature, and finally the scaffolds were prepared by freeze drying method. The developed scaffolds are designated as SF/CS/Glu.

4.2.5 Preparation of SF/CS/Chs scaffolds

Chs solutions with different concentration namely 0.2, 0.4, 0.6, 0.8, 1 & 1.2 wt% were prepared with varying concentrations. 1 ml of the prepared solutions was added to 20 ml of SF/CS blend solution and kept for stirring overnight, at room temperature, and finally the scaffolds were prepared by freeze drying method. The developed scaffolds are designated as SF/CS/Chs.

4.2.6 Preparation of SF/CS/Glu/Chs scaffolds

Chs solutions with different concentration namely 0.5, 1.0 and 1.5 wt% were prepared. 1 ml of the prepared solutions was added to the solution of SF/CS/Glu, which was prepared by mixing 1% Glu in SF/CS (80:20) blend solution and kept for stirring at room temperature overnight. Scaffolds were developed using freeze drying method.

4.3 Characterization of scaffolds

4.3.1 Morphological characterization

Morphology and pore structure of the developed scaffolds were analyzed using a Scanning Electron Microscopy (SEM) [JEOL-JSM 6480 LV]. The traces of moisture present in the scaffold samples was removed by drying them using a vacuum drier for 1 hr at 40°C. The scaffolds were cut into small pieces and coated with platinum using polar on range sputter coater before imaging. The pore size of the developed scaffolds was measured by using Image J (USA) software [16]. The average pore size was determined by measuring 20 pores selected randomly through graphical measurement on SEM image.

4.3.2 Porosity and pore distribution

The distribution of pore size and porosity of the scaffolds were performed using Mercury intrusion porosimeter [(Quantachrome instruments: Pore master series, USA)] with mercury intrusion under an increasing pressure from 0.827 to 30000 psi. The instrument was degassed to remove all air from it before the intrusion of mercury. The bulk density of the scaffolds was measured by liquid displacement method using ethanol, before actual porosity analysis. The determination of porosity was based on the relationship between the applied pressure and the pore diameter into which mercury intrudes, according to the Washburn equation Washburn equation: $D = (1/P)4\gamma(\cos \phi)$. All experiments were carried out in triplicate [107].

4.3.3 Structural analysis

FT-IR spectroscopy

The structural property, molecular composition and functional groups of the developed scaffolds were evaluated by Fourier transform infrared spectroscopy (FT-IR) using an Infra red Microscope [Shimadzu AIM-8800, Japan]. Approximately 1 mg of each sample was mixed with specific amount of dry KBr powder and pelletized by using a Hydraulic press to create pellets of size about 10mm. The pellets were prepared as transparent disks which were utilized for the IR measurements. The equipment was operated in transmittance mode with wavelength from 500 to 4000cm⁻¹ with a resolution of 8cm⁻¹ [15].

4.3.4 Contact angle measurement

The contact angle of the developed SF and SF/CS based scaffolds (films) was measured by a contact angle meter K100MK3 tensiometer (KrussGmbH, Hamburg, Germany). Films were prepared for the contact angle measurement by solvent casting method. Films of width (15mm), height (10mm) and thickness (1mm) were used for the contact angle analysis. Water was used as the solvent. All the samples were analyzed at room temperature in triplicates [108].

4.3.5 Swelling behavior

Swelling ability of the developed scaffolds was evaluated in SBF till they reach equilibrium, at regular time intervals namely 1 hr, 3 hrs, 5 hrs, 7 hrs, 24 hrs and 42 hrs. The weight of the samples before immersion in water DRY_{wt} and after immersion at particular time point is denoted WET_{wt} were noted. The formula used to determine % swelling of developed scaffold is given below [109].

$$\% \text{ Swelling} = (WET_{wt} - DRY_{wt}) / DRY_{wt} \times 100 \quad \dots\dots\dots (1)$$

4.3.6 Biodegradation study

Degradation of the developed scaffolds was performed in SBF. The initial dry weight (W_o) of the sample was weighed and soaked in SBF for predetermined time intervals of 1, 7, 14 and 28 days. The sample was removed from SBF at regular time intervals and freeze dried

followed by weighing final weight W_t . The remaining weight % (W_R) was calculated using the below given formula. All the experiments were performed in triplicates [110].

$$\% \text{ Weight remaining} = 100 - [(W_o - W_t) / W_o \times 100] \dots\dots\dots (2)$$

4.3.7 Compressive strength

The compressive strength of the prepared scaffolds was performed by using Universal testing machine (H10 KS Tinius Olsen USA). The cylindrical samples with a dimension of 10 mm diameter and a thickness of 8 mm were used for analysis. A crosshead speed of 1 mm/min with a load cell of 1000N was used for compression tests. All the experiments were performed at room temperature in triplicates. Compressive strength was calculated by using the formula $S = F_{\max} / A$, where F_{\max} represents the force applied and A is the cross sectional area of the sample [16].

4.3.8 In-vitro cell study

Isolation and culture of MSCs

Umbilical Cord Blood was collected from Ispat General Hospital (IGH Rourkela), India with prior consent of the patient. Ficoll Hypaque technique was used to isolate mononuclear cells (MNCs) as described elsewhere [30, 31]. The isolated MNCs were cultured in Dulbecco's Modified Eagle Medium (DMEM) supplemented with 10% fetal bovine serum, 100U/ml penicillin and 0.1 mg/ml streptomycin. The culture condition maintained was 37 °C, 5% CO₂ with 80% relative humidity. MSCs were separated from non-adherent cells in culture flasks by discarding non adherent cells based on their unique adherent property. The adherent cells consisting of MSCs were washed thoroughly with PBS/EDTA and supplemented with freshly prepared medium. The cells were sub-cultured upto 5th passage by changing the media thrice in a week [33].

Cell seeding and culturing

Scaffolds (9x9x2mm) were sterilized prior to cell seeding by soaking in 70% ethanol followed by UV treatment and sterile PBS wash. Cells from 4th passage were seeded on sterilized scaffolds with a seeding density of 2×10^4 cells/ml by static method. The cell

seeded scaffolds were incubated in a CO₂ incubator with 5% CO₂ at 37°C. The culture medium was replenished once in every two days [34].

Cell morphology and cell attachment

Human mesenchymal stem cell (hMSCs) seeded scaffolds were treated with 2% (v/v) glutaraldehyde for fixing the cells. The samples were rinsed with wash buffer and dehydrated with series of ethanol gradations (50, 70, 80, 95 and 100%) for 5 min each [29]. Finally the samples were dried at 37°C and sputter coated with platinum for 30 sec prior to imaging. (Quorumtech, Q150RES, Czech Republic). Images were taken by Field Emission Scanning Electron Microscopy (FE-SEM) [Nova SEM-Czech Republic] in high vacuum at 5 kV.

Measurement of metabolic activity (MTT assay)

The metabolic activity of hMSCs cultured on the developed scaffolds was evaluated quantitatively by MTT [3-(4, 5-dimethylthiazol-2-yl)-diphenyltetrazolium bromide] assay [16]. Fresh media consisting of 100µl MTT solution (diluted in 1:10 PBS) was supplemented to the cells. After incubation at 37°C for 4 hrs, 0.5 ml DMSO was added to the cells and centrifuged at 1000 rpm for 5 min. The optical density (O.D) of the pink colored formazan derivative was measured using a spectrophotometric plate reader (2030 multi label reader Victor X3, Perkin Elmer, USA) at 595 nm [16].

Cell viability analysis by live and dead assay

The scaffolds were rinsed with 0.1M PBS for 20 min. The samples were later stained using calcein-AM dye and kept under incubation for a period of 30 min. The samples were removed, washed with PBS and observed under fluorescence microscope (Carl Zeiss, Axiovert 40CFL) [111].

Cell proliferation by DNA quantification measurement

hMSC proliferation on the prepared scaffolds was analysed by DNA quantification assay. In brief, cell seeded scaffold constructs were incubated at specific time periods upto 21 days in complete DMEM media supplemented with 10% fetal bovine serum, 100U/ml penicillin and 0.1 mg/ml streptomycin in a 12 well tissue culture plate. The cell scaffold constructs were rinsed with DMEM and PBS repeatedly followed by lysis with 0.5 ml of Lysis buffer

(10 mM tris and 2% triton) for 1 hr. The cell lysate was sonicated. 100 μ L of Quant-it PicoGreen reagent was added to equal amount of sonicated cell lysate and incubated at 37°C for 10 mins. The excitation and emission wave lengths of fluorescence were 528 nm and 485 nm respectively. The readings were then compared with the number of cells with the help of a calibration curve created with known concentration of hMSCs [111].

Cell distribution and cytoskeletal organization

Confocal laser scanning microscopy was used to analyse the cell distribution and cytoskeletal analysis of hMSCs on the developed scaffolds. Hoescht and Trit C Phalloidin were used according to the protocol followed elsewhere. Briefly, cell seeded scaffolds after 7 and 14 days of study were harvested and fixed with 4% paraformaldehyde solution. Permeabilization with Triton X was performed followed by PBS wash. Hoechst nuclear stain was then performed for a minute and the constructs were further stained with TRIT C conjugated Phalloidin. The samples were examined by confocal laser scanning microscope (Olympus IX 81) [96].

Estimation of GAG (Glycosamino glycan)

The scaffolds seeded with hMSCs were cultured in freshly prepared chondrogenic differentiation media. The cell seeded scaffolds were incubated in a CO₂ incubator with 5% CO₂ at 37°C. The culture medium was replenished once in every two days.

GAG content of the cell seeded scaffolds was evaluated by GAG assay using the 1, 9-dimethylmethylene blue (DMMB) reagent. At specific time intervals, GAG was harvested from the cells by digestion with papain solution (125 μ g/mL of papain, 5 mM L-cystein, 100 mM Na₂HPO₄, 5 mM EDTA) maintaining a pH of 6.8 at 60°C for 16 hrs. Absorbance was measured at 525nm [112].

4.4 Statistical analysis

Statistical analysis of data was performed with ANOVA considering $p < 0.05$ as statistically significant. All data is presented as mean \pm standard deviation with $n = 3$.

Chapter 5

Results and Discussion

5.A DEVELOPMENT OF SILK FIBROIN/CHITOSAN BLEND SCAFFOLDS

SF is a fibrous protein and has many biomedical applications because of its permeability to oxygen and water vapor and robust mechanical strength [9]. However, because of its slow degradation, brittleness and lack of hydrophilicity, its use in tissue engineering is limited [17]. CS, a partially de-acetylated product of chitin, is biocompatible, biodegradable and has excellent wound healing property [16]. Moreover, CS has its inherent glycosaminoglycan residues that can aid in supporting cartilage tissue growth [16]. However, the rapid degradation rate and low mechanical strength warrant its application in tissue engineering [111]. Therefore, the use of SF or CS alone is not suitable as scaffold material. Therefore, a number of researchers have given effort to study the effect of combination of these two natural polymers and reported the resultant blend with excellent scaffold properties [69,77]. However, in most of these studies, a specific ratio of SF/CS was used with the aim of exploring the suitability of the blend as scaffold material [27,69,76,77] except the study of Zeng. et. al on the effect of blend ratio targeting bone tissue engineering application [106].

Therefore, efforts are given in this phase of dissertation to develop SF/CS blend scaffolds by freeze drying method. The influence of volume ratio of SF/CS on various scaffold properties is investigated by physicochemical, mechanical and biological characterizations, targeting for cartilage tissue regeneration. The results and discussion of this experimental is presented in this chapter.

5.1 Results and Discussion

5.1.1 Scanning electron microscopy (SEM)

Sufficient pore size and pore interconnectivity are important for the supply of nutrient and oxygen to the cells and also for the release of wastes [48]. Figure 1 shows the SEM images of the developed freeze dried pure SF and SF/CS blend scaffolds. As it is seen in figure, all the scaffolds possess open microporous structures with varying pore sizes and high pore interconnectivity. Table 5.1 shows the pore size and average pore size of the developed scaffolds. A gradual increase in average pore size from 95 ± 25.2 to 230 ± 20.4 μm was observed with increase in CS content in the scaffold. The pore size of scaffold depends on the formation of ice crystal which results from the water content of the polymeric blend [29]. CS, being a hydrophilic polymer, increases the water content during freezing process

thereby forms large ice crystals which in turn create large pores upon sublimation during freeze drying. The measured pore sizes of the developed scaffolds are within the desired range of pore size suitable for cartilage tissue engineering [113]. The increase in pore size with increase in CS volume in SF/CS blend scaffold has also been reported earlier [16].

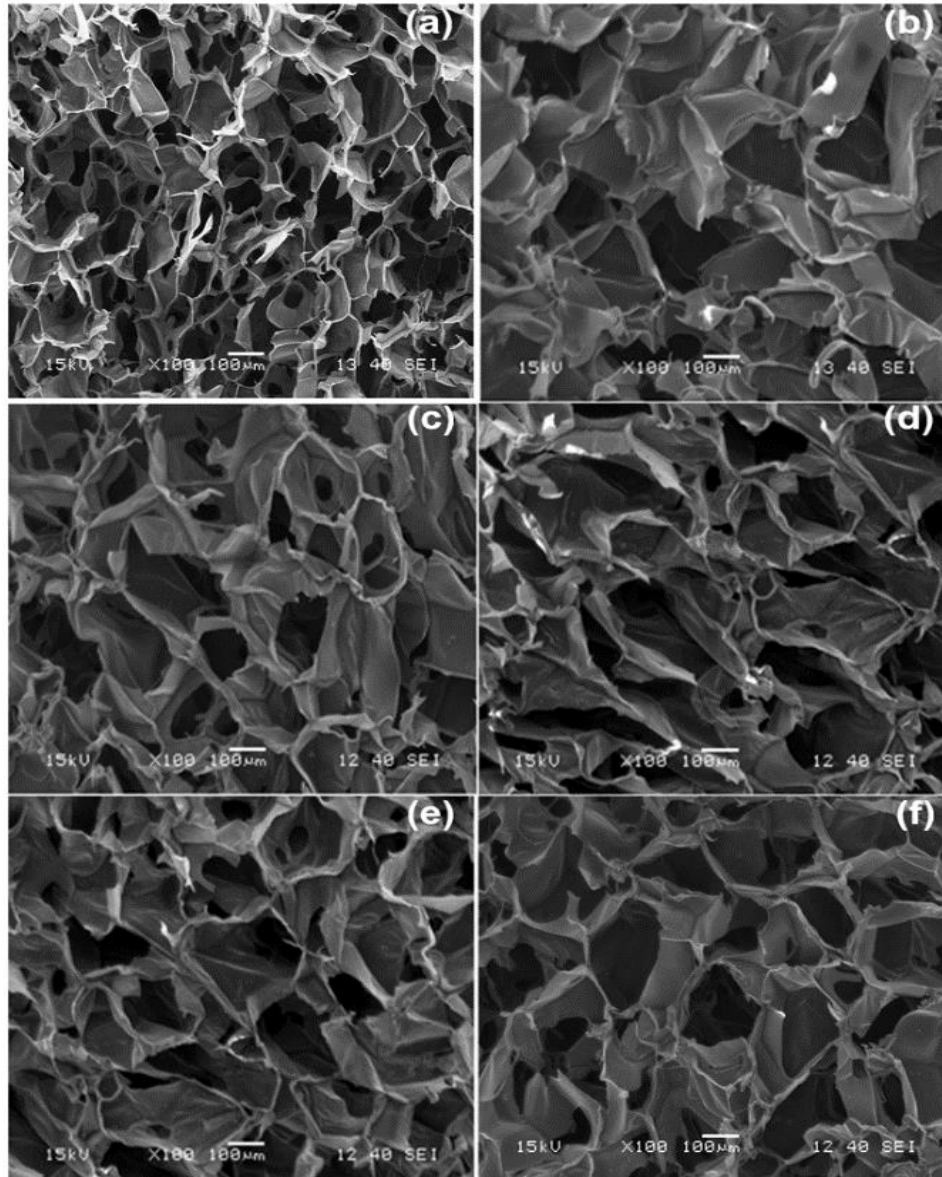


Figure 5.1: SEM images of (a) Pure SF, (b) SF/CS (90:10), (c) SF/CS (80:20), (d) SF/CS (70:30), (e) SF/CS (60:40) and (f) SF/CS (50:50) scaffolds. All scaffolds possessed open porous microstructure with desired pore size and interconnected pores.

5.1.2 Porosity

Porosity of scaffold is an important parameter in tissue engineering. The higher porosity provides higher cell proliferation, cell migration and fosters nutrient delivery [107]. Both pure SF and SF/CS blend scaffolds exhibit porous structures with desired porosity. Table 5.1 shows the porosity of the SF and SF/CS blend scaffolds. Pure SF scaffolds exhibited maximum porosity of $93.3 \pm 1.6\%$. The porosity of the SF/CS blend scaffold was decreased with increase in CS content. Among the prepared blend scaffolds, the maximum porosity ($87.9 \pm 1.2\%$) was observed with the scaffold having SF/CS volume ratio of 90:10, followed by 80:20. The hydrophilic nature of CS increased the water content of the scaffolds, creating bigger pores thus offered decreased porosity, which was also reported earlier [16]. However, the prepared blend scaffold still possess adequate porosity and thus suitable for tissue engineering applications.

Table 5.1: Pore size range, average pore size and porosity of pure SF and SF/CS blend scaffolds

Sample	Pore size (μm)	Average pore size (μm)	Porosity (%)
SF	45-122	95 ± 25.2	93.3 ± 1.6
SF/CS (90:10)	52-165	155 ± 30.3	87.9 ± 1.2
SF/CS (80:20)	71-201	186 ± 32.2	82.2 ± 1.3
SF/CS (70:30)	78-221	202 ± 26.1	78.0 ± 1.9
SF/CS (60:40)	84-229	216 ± 23.5	73.5 ± 2.8
SF/CS (50:50)	91-236	230 ± 20.4	71.2 ± 2.0

5.1.3 Structural analysis

FT-IR spectroscopy

Fourier transform infrared spectroscopy is a useful tool in determining the interactions between the various chemical groups present in the blend solutions. Figure 5.2 represents the FT-IR spectra of SF, CS and SF/CS blend scaffolds. FT-IR spectra reveals that the amide

V absorption band at 700 cm^{-1} , amide III band at 1260 cm^{-1} , amide II band at 1525 cm^{-1} and amide I band at 1625 cm^{-1} relate to the β sheet conformation of SF. Whereas the band at 1598 cm^{-1} corresponds to the amino group of CS. The additional band at 1080 cm^{-1} in SF/CS blend scaffolds is the characteristic band of the SF/CS blend scaffold [16].

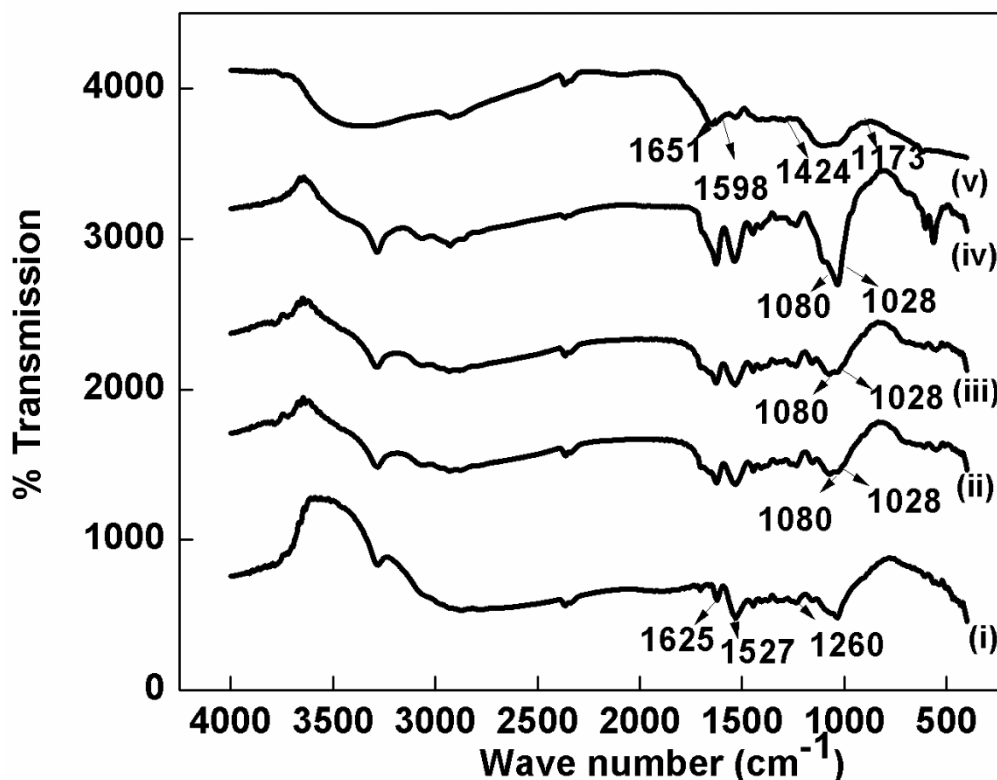


Figure 5.2: FT-IR spectrum of (i) Pure SF, (ii) SF/CS (90: 10), (iii) SF/CS (80:20), (iv) SF/CS (70: 30) and (v) Pure CS scaffolds. SF/CS blend scaffolds showed characteristic band of SF/CS at 1080 cm^{-1} .

5.1.4 Swelling behavior and water contact angle

The swelling behavior of scaffolds enables the cells to utilize the interior architecture of the scaffold to a maximum extent [18]. The swelling ability of a scaffold is essential to support numerous cellular activities. Figures 5.3 shows the % swelling of pure and blend scaffolds. Pure SF scaffold showed the least swelling behaviour ($\sim 204\%$) when compared to the SF/CS blend scaffolds. Swelling was found to increase with increase in CS content ($\sim 222\text{--}262\%$), as shown in figure 5.3. The increase in swelling ratio is attributed to the increase in

hydrophilic CS. Similar trend in swelling behavior of SF/CS blend scaffolds were reported earlier in the literature [17,18]. The percentage of swelling was found to increase with an increase in CS content (Fig. 5.3), which may be partly due to the increase in pore size thereby enhancing the water uptake capacity [17] and partly due to increased hydrophilicity of the scaffold material. Change in swelling ability with different volume ratios of silk fibroin and chitosan is due to the varying amounts of chitosan which is hydrophilic in nature. The intermolecular interaction between silk fibroin and chitosan changes with difference in chitosan percentage. SF, being a fibrous protein, exhibits less hydrophilicity due to the presence of β -sheet conformation. CS has a unique structural feature that is the presence of a primary amine at the C-2 position of the glucosamine residues. CS has improved water uptake capacity due to the presence of a high content of primary amines [15]. Further, due to its more degradation ability than SF, greater CS content will hamper the stability of the blend scaffolds in water [17].

However, the contact angle of water measured on SF/CS scaffold decreased from $55.3 \pm 0.1^\circ$ to $51.5 \pm 1.2^\circ$ on increasing CS from 10 to 50 (v/v) as compared to pure SF scaffold ($56.2 \pm 0.2^\circ$), as shown in table 5.2. This further supports the high hydrophilicity of SF/CS blend scaffolds that increases with increase in CS content and thereby possess superior surface property.

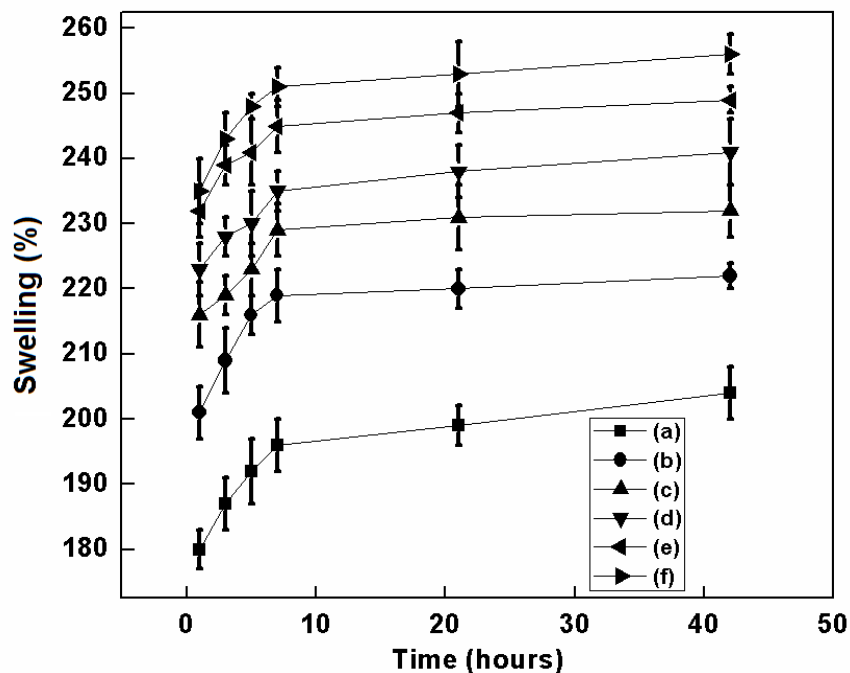


Figure 5.3 Swelling behaviour of (a) Pure SF scaffolds, (b) SF/CS (90:10), (c) SF/CS (80:20), (d) SF/CS (70:30), (e) SF/CS (60:40) and (f) SF/CS (50:50). Pure SF scaffold showed the least swelling behaviour when compared to the SF/CS blend scaffolds. Swelling was found to increase with increase in CS content.

Table 5.2: Contact angle of SF and SF/CS scaffolds.

Sample	Contact angle(degree)
SF	56.2 ± 0.2
SF/CS (90:10)	55.3 ± 0.1
SF/CS (80:20)	54.2 ± 0.3
SF/CS (70:30)	53.6 ± 0.8
SF/CS (60:40)	52.5 ± 0.6
SF/CS (50:50)	51.5 ± 1.2

5.1.5 In-vitro degradation

The ability of a scaffold material to degrade with time, inside a biological system is a promising feature in order to facilitate growth of neo tissue [14]. Nevertheless, an optimum degradation rate is essential which needs to match the growth rate of the new tissue and sustainability at the site of implant [15]. Figure 5.4 presents the *in-vitro* degradation of the pure SF and SF/CS blend scaffolds. Pure SF, being a less hydrophilic polymer, shows a very slow and stable degradation, with 93.2% remaining after 28 days of study. As the volume ratio of CS was increased, the degradation behaviour also shifted to a faster pace, owing to the water absorbing nature of chitosan [15]. Blends of 90:10 and 80:20 SF/CS show residual % mass remaining of 88 % and 87.9 % respectively followed by 70:30 and 60:40 with 84 and 82 % in 4 weeks. The least mass remaining is observed with the blend ratio of 50:50 where 76% of the total mass was present. The number of hydrogen bond interactions between SF and CS increases with CS, which enhances the tendency to attract water molecules towards them, thereby causing rapid degradation [17].

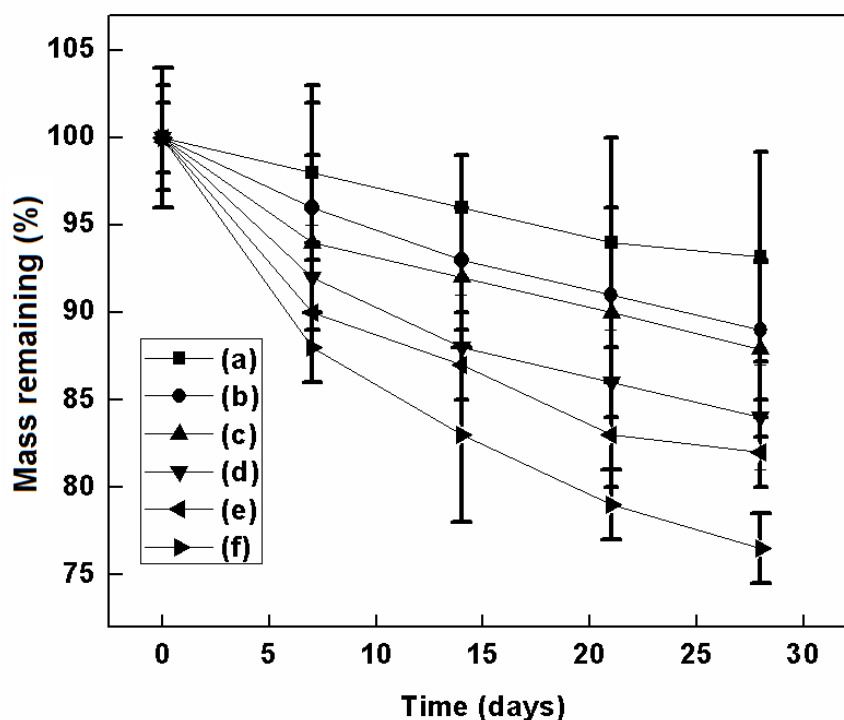


Figure 5.4: Degradation pattern of (a) Pure SF, (b) SF/CS (90:10), (c) SF/CS (80:20), (d) SF/CS (70:30), (e) SF/CS (60:40) and (f) SF/CS (50:50) scaffolds. Faster degradation was observed with increase in chitosan content.

5.1.6 Compressive strength

Compressive strength is one of the properties which is used to assess whether the scaffolds possess sufficient strength to cater the stress imparted by the native tissue formed [35]. Figure 5.5 shows the compressive strength of both pure SF and SF/CS blend scaffolds. In comparison to pure SF (160 ± 0.3 kPa), a higher compressive strength of 210 ± 0.9 kPa was obtained by addition of CS to SF with 90:10(v/v) blend ratio (fig.5.5). However, a gradual decrease in compressive strength was observed with increase in CS in blend. The initial increase in compressive strength as observed with SF:CS (90:10), may be attributed to the strong ionic bond formation between SF with a lesser amount of CS. But as CS increased, the formation of weaker ionic interactions occurred and consequently, compressive strength decreased. A similar trend in compressive strength was also reported earlier [116]. Overall, the compressive strength of the developed scaffolds is within the range of 0.01-3MPa suitable for cartilage tissue engineering application [116].

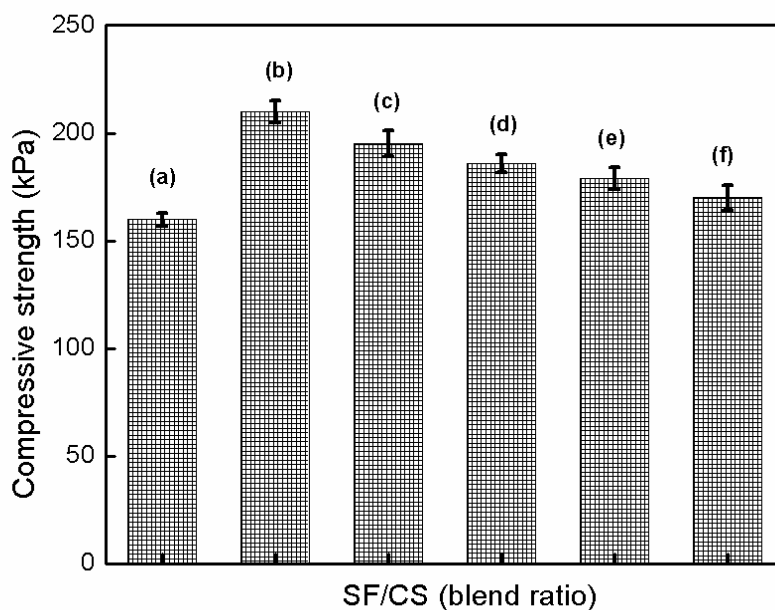


Figure 5.5: Compressive strength of (a) Pure SF, (b) SF/CS (90:10), (c) SF/CS (80:20), (d) SF/CS (70:30) (e) SF/CS (60:40) and (f) SF/CS (50:50) scaffolds. A gradual decrease in compressive strength was observed with increase in chitosan content.

5.1.7 In vitro cell culture study

Morphological study of hMSCs

Figure 5.6 shows the phase contrast microscope images of hMSCs after 1st week, 3rd week, 5th week and 7th week of culture. The isolated MSCs were cultured in DMEM media upto 4th passage. Initially, during the first week of culture, the cells were round in morphology. In subsequent passages, the cells slowly attained elongated morphology, which is a characteristic feature of hMSCs. At the end of 3rd passage, it was observed that all the cells acquired the desired morphology of hMSCs. These were maintained and used for further *in-vitro* cell culture studies.

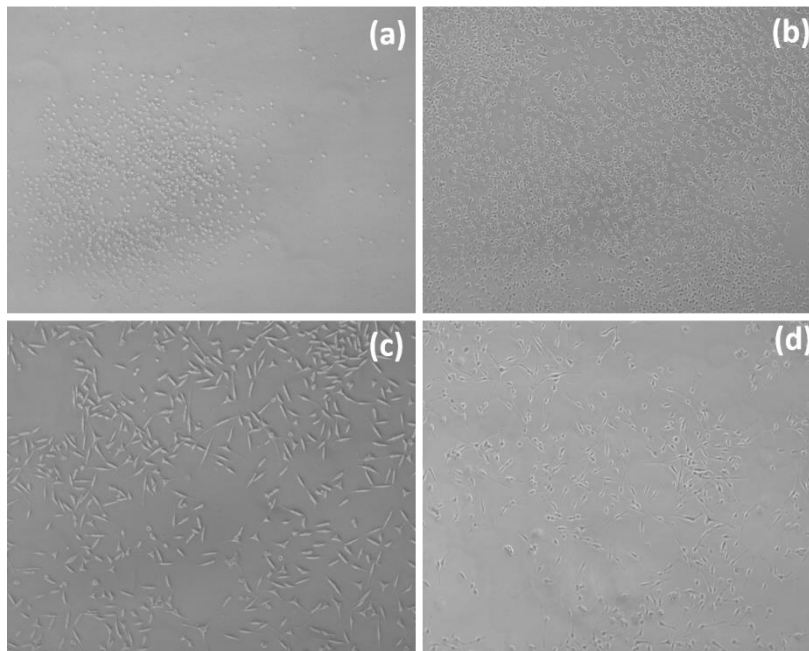


Figure 5.6: Morphological changes of hMSCs observed under phase contrast microscope during (a) 1st week, (b) 3rd week (c) 5th week and (d) 7th week of culture. Initially the cells are found to be spherical in shape and slowly reached fibroblast like morphology in about 7 weeks of culture

Cell morphology and cell attachment

Cell attachment and cell morphology study generally indicate the cordial relationship between the seeded cells and the scaffold environment. It is, therefore, important to analyze the suitability of the biomaterial towards cellular behavior in culture condition. SEM

micrographs in Figure 5.7 shows the attachment and spreading of MSCs on the scaffold during 7 (a-d) and 14 (e-h) days of culture. Cells were found to be initially adhered to the scaffold matrix. With increase in culture time, the hMSCs were found to spread well throughout the SF/CS (80:20) blend scaffold representing its superior cell supportive property than the other blend scaffolds (Figure 5.8). A slightly lower cell density was observed with increase in CS content in the SF/CS (70:30) blend which may be due to the lower porosity of the scaffold resulting in lower volume that decreased the cell migration and nutrient delivery [114].

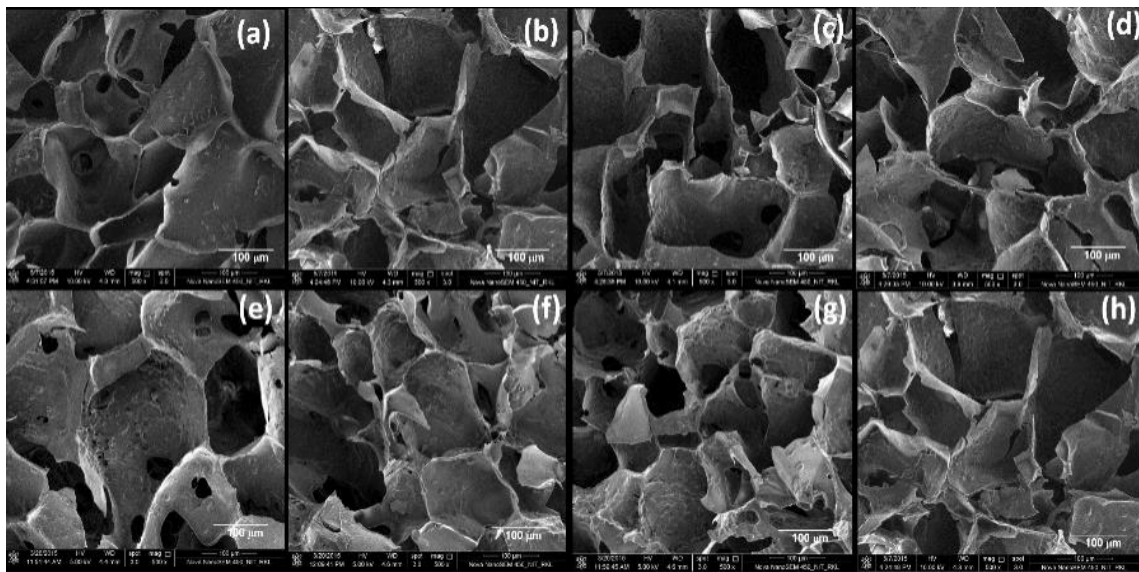


Figure 5.7: FE-SEM images for cell attachment and proliferation of hMSCs over various scaffolds. (a) and (e) Pure SF, (b) & (f) SF/CS (90:10), (c) & (g) SF/CS(80:20) and (d) & (h) SF/CS (70:30) scaffolds after 7 and 14 days of culture respectively. hMSCs were found to spread well throughout the SF/CS (80:20) blend scaffold representing its superior cell supportive property than the other blend scaffolds.

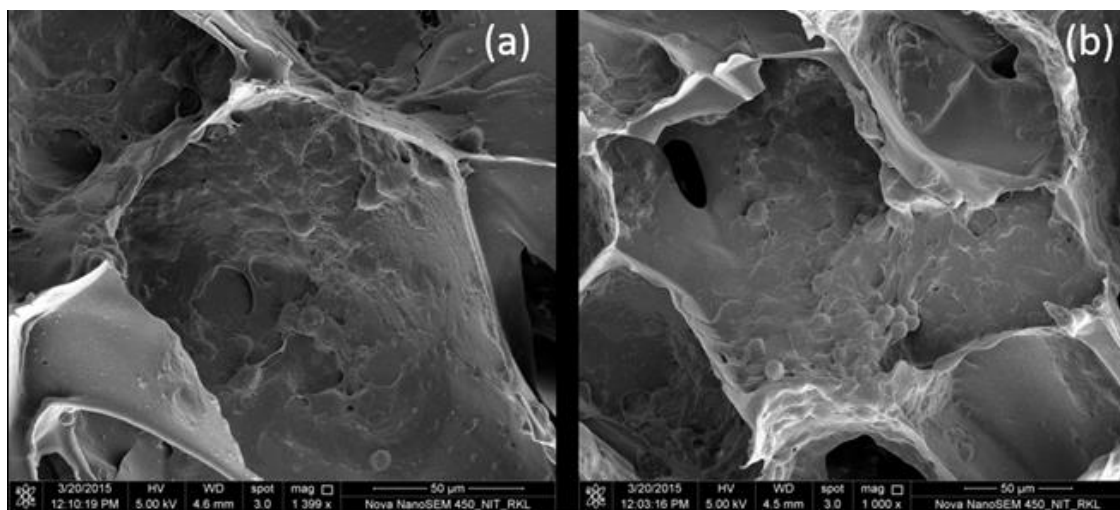


Figure 5.8: Magnified FE-SEM image showing cell proliferation over SF/CS (80:20) blend scaffolds after (a) 7 days and (b) 14 days of culture.

Cellular metabolic activity by MTT assay

The metabolic activity of hMSCs seeded on scaffolds is a direct recognition of their ability to express progress as a living entity [111]. Relative cellular metabolic activity for various SF/CS blend scaffolds was measured by MTT assay at 3, 5 and 7 days of culture as shown in fig 5.9. In comparison, SF/CS (80:20) scaffold showed higher proliferation compared to the 70:30 and 60:40 scaffolds ($p < 0.05$) (Figure 5.9). This may be attributed to the fact that there is more distinct interaction between the positive amino groups of chitosan and the negative charges located in the cells. The 80:20, 70:30 and 60:40 blend scaffolds showed better cell proliferation in day 5 and day 7, but 80:20 blend showed more cell proliferation compared to the 70:30 and 60:40 blend scaffolds ($p < 0.05$).

The metabolic activity of SF/CS scaffold was increased with increase in CS content upto 20% which may be attributed to the higher cell binding ability of CS than SF. However, a slight decrease in metabolic activity was observed with further increase in CS content in the blend (SF/CS 70:30 and 60:40). The decrease in metabolic activity representing the lower proliferation of MSCs on these scaffolds is probably due to having lower porosity which has concealed the benefit of higher cell binding ability of CS. The decreased cell proliferation may be attributed to reduced pore volume that resulted in lower cell migration and nutrient delivery on to the scaffold [111,114].

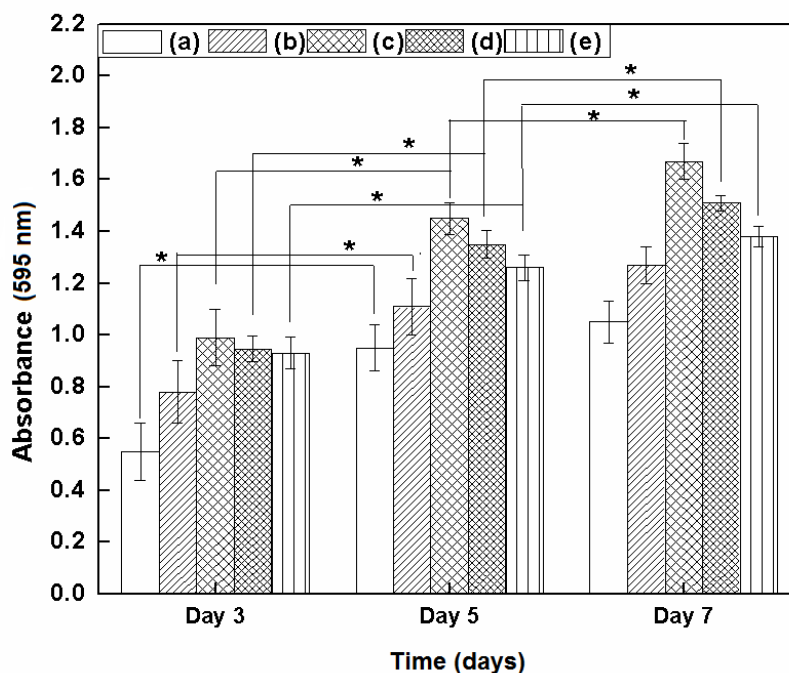


Figure 5.9: Cell viability analysis by MTT assay on (a) SF, (b) SF/CS (90:10) blend, (c) SF/CS (80:20), (d) SF/CS (70:30) and (e) SF/CS (60:30) blend scaffolds. * represents significant differences at $p < 0.05$. The metabolic activity of SF/CS scaffold was increased with culture time compared to pure SF. The metabolic activity of SF/CS scaffold was increased with increase in CS content upto 20% and thereafter, a slight decrease in metabolic activity was observed with further increase in CS content in the blend

Cell viability studies by live/dead assay

Cell viability study is crucial to determine the biocompatibility of the developed scaffold matrices. Increased growth of cells over culture time signifies the non-cytotoxic behavior of the cell supportive material [111]. Figure 5.10 represents the live/ dead assay of SF and SF/CS blend scaffolds. When compared to pure SF scaffolds, SF/CS (80:20) blend scaffolds showed increased cell viability which is due to the increased percentage of cell supportive domains in the blend scaffolds [111].

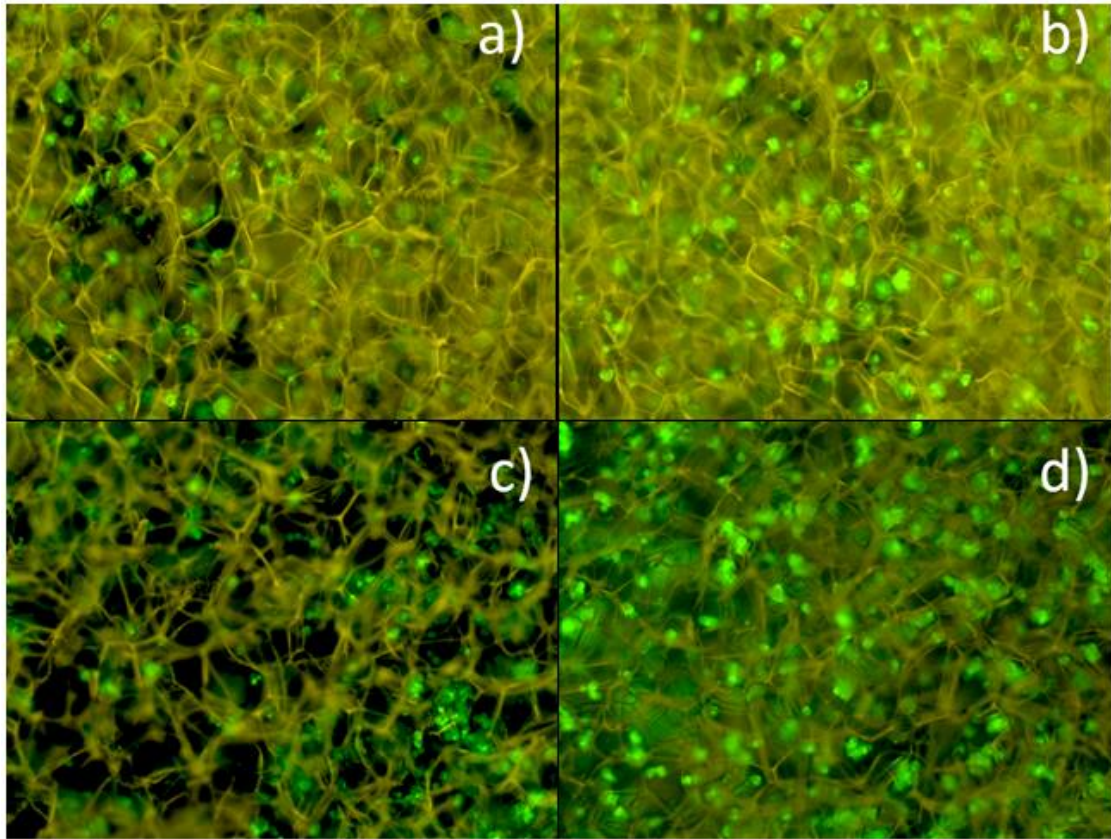


Figure 5.10: Live and dead assay on (a) and (c) SF scaffold; (b) and (d) SF/CS (80:20) scaffold. (a) and (b) represent 5 days and (c) and (d) represent 7 days after cell seeding. SF/CS (80:20) blend scaffold shows increased cell viability when compared to pure SF scaffold.

GAG estimation

The presence of GAG secretion is a clear indication of the differentiation of hMSCs into chondrogenic lineage [96]. Figure 5.11 shows the GAG content in SF/CS (80:20) scaffolds and pure SF scaffolds used as control. The amount of GAG secreted by MSCs seeded on the SF/CS scaffolds ($18\mu\text{g}/\text{mg}$ of scaffold) is higher than the pure SF scaffolds ($14\mu\text{g}/\text{mg}$ of scaffold) ($p < 0.05$). The presence of glycosaminoglycan groups in CS has promoted chondrogenic differentiation of hMSCs over blend scaffolds that lead to improved GAG production [27]. This study validates synergistic effect of both SF and CS that has directed cell proliferation and their consecutive differentiation towards the cartilaginous lineages. It has been demonstrated that the developed SF/CS scaffold with optimal blend ratio of 80:20 is a potential scaffold material for cartilage tissue engineering applications.

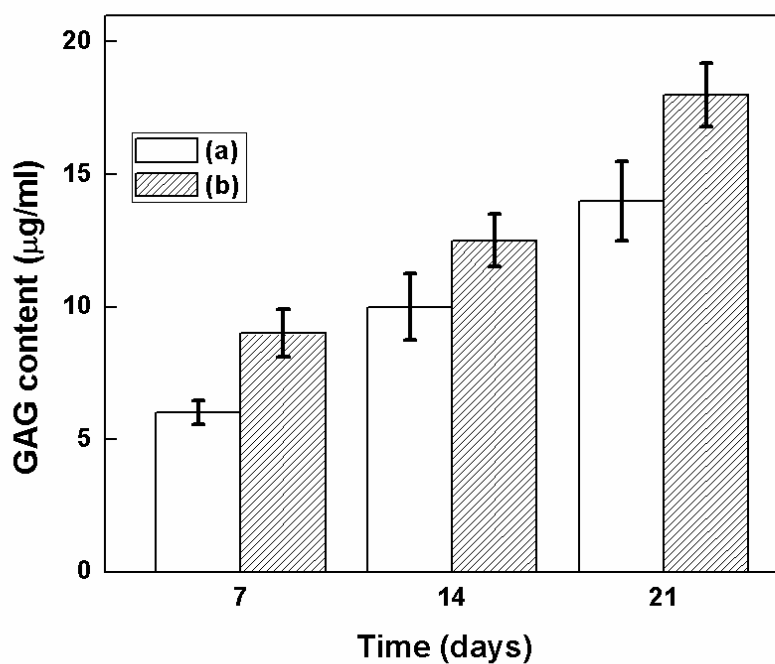


Figure 5.11: GAG assessment of (a) SF scaffold (b) SF/CS (80:20) scaffold. * represents significant difference at $p < 0.05$. The amount of GAG secreted by hMSC over SF/CS (80:20) scaffold was found to be higher throughout the culture period compared to pure SF scaffold.

5.B DEVELOPMENT OF SILK FIBROIN/ CHITOSAN/ GLUCOSAMINE SULFATE SCAFFOLDS

In the previous section, SF/CS blend scaffolds with optimal blend ratio of 80:20 was developed by freeze drying method. The cell binding affinity which can mimic the natural environment of cartilage has been reported to be improved by the incorporation of active biomolecules [5]. Glu is a amino monosaccharide present in the cartilage tissue [26]. It has a major role in acting as a precursor for glycoprotein and GAG synthesis [24]. Glu is also usually used as an oral supplement for the regeneration of cartilage tissue. Therefore, it has been hypothesized that the addition of Glu might be beneficial in facilitating the cartilage specific ECM formation through GAG synthesis.

The aim of the present phase of research work is to investigate the effect of Glu with varied content on the properties of SF/CS (80:20) scaffolds with the intention to improve cell viability, cell attachment and cartilage specific ECM formation ability of the SF/CS scaffolds. The results and discussion of this experimental work is described in this chapter.

5.2 Results and discussion

5.2.1 Scanning electron microscopy (SEM)

SEM images has revealed that the addition of Glu does not show any negative impact on the morphology of SF/CS scaffold which is evident from the open and well interconnected porous structure (figure 5.12). Table 5.3 shows the pore size and average pore size of the Glu added SF/CS (80:20) scaffolds. A marginal change in pore size was observed with change in Glu content. The pore size and average pore size were measured to be decreased with increase in Glu content from 0.2 to 1.2 % (w/v). Though the pore size was lower than the SF/CS scaffold, the scaffold containing Glu content still possess pore size adequate for supporting tissue regeneration.

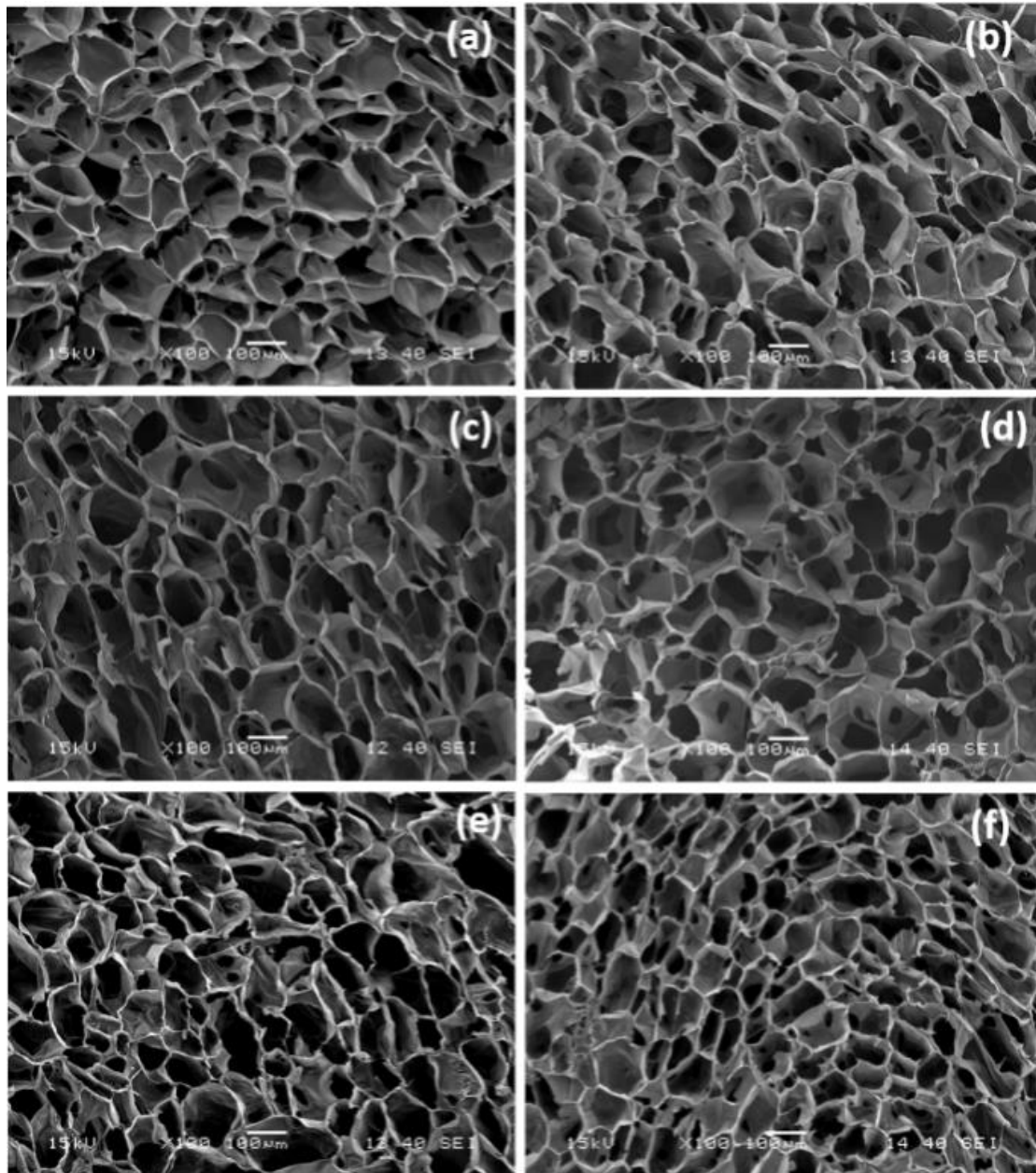


Figure 5.12: SEM images of SF/CS/Glu scaffolds with (a) (0.2), (b) (0.4), (c) (0.6), (d) (0.8), (e) (1) and (f) (1.2) % (w/v) of Glu respectively. All scaffolds possessed open porous network with highly interconnected pore structures.

5.2.2 Porosity

As observed in Table 5.3, the porosity of the SF/CS scaffold was increased with increase in Glu concentration, though the variation in porosity is not statistically significant between the concentration range. However, the maximum porosity (79.8 ± 3.26) was achieved with 1.2 % (w/v). A comparable porosity was also shown by scaffold with 1 % (w/v) Glu

(79.6±4.12). Furthermore, in comparison, the porosity of the SF/CS/Glu 1% (w/v) and SF/CS/Glu 1.2% (w/v) was slightly lower than the SF/CS scaffolds (control) confirming that the addition of Glu did not show much impact on the scaffold porosity.

Table 5.3: Pore size, average pore size, and porosity of SF/CS/Glu scaffolds.

Sample	Pore size (μm)	Average pore size (μm)	Porosity (%)
Glu 0.2 (w/v)	60-210	107±24.2	75.6±2.96
Glu 0.4 (w/v)	55-204	106±18.6	76.3±3.21
Glu 0.6(w/v)	51-200	105±30.8	76.5±3.61
Glu 0.8 (w/v)	45-195	104±25.3	78.9±3.56
Glu 1 (w/v)	40-190	104±19.6	79.6±4.12
Glu 1.2(w/v)	38-184	101±23.4	79.8±3.26

5.2.3 Structural analysis

FT-IR spectroscopy

The interaction between the functional groups present in SF/CS/Glu scaffolds was assessed by FT-IR spectroscopy as shown in figure 5.13. The absorption band at 1080 cm⁻¹ suggests that the NH groups of SF and C=O and NH₂ groups of CS have specific intermolecular interactions. An additional band at 1614 cm⁻¹, which corresponds to the addition of Glu in SF/CS/Glu scaffolds [20,116]. The FT-IR analysis confirms the molecular interaction of Glu in the SF/CS blend.

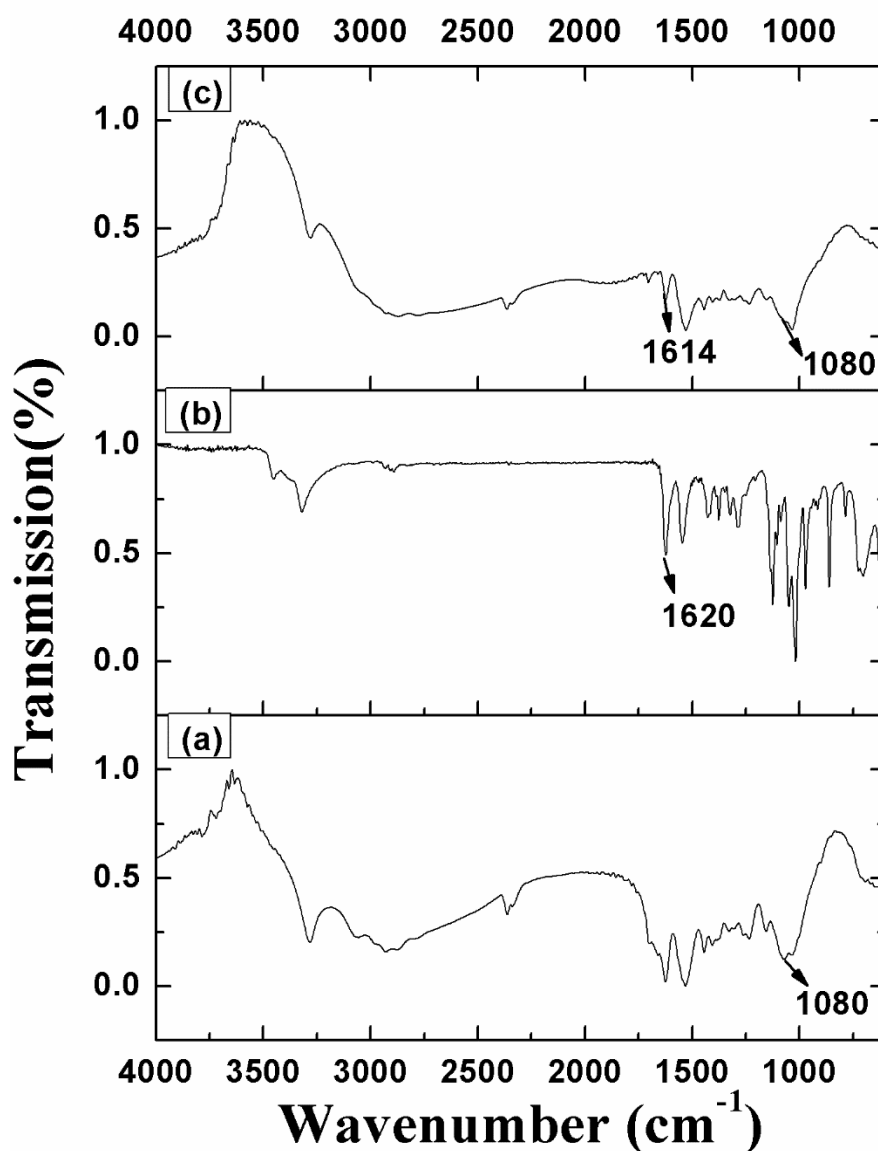


Figure 5.13: FT-IR spectra of (a) SF/CS (80: 20), (b) Glu powder and (c) SF/CS/Glu scaffolds. The additional band in SF/CS/Glu scaffold is due to the interaction of Glu with SF/CS blend.

5.2.4 Swelling behavior and water contact angle

The % swelling behaviour of SF/CS/Glu scaffolds has been depicted in figure 5.14. A drastic increase in swelling was obtained by the addition of Glu to SF/CS (80:20) scaffold and the swelling rate was increased with increase in Glu content. An equilibrium state of swelling was observed with all the scaffolds after 10 hrs of SBF treatment. The higher hydrophilicity of the scaffold material was responsible for the increased swelling which was

resulted from the enhanced interaction between amine groups present in Glu and the hydroxyl groups of water [17]. The role of Glu (hydrophilic in nature) might be the main controlling factor in swelling which may be due to the presence of double bonds of Glu.

The wettability and thus the hydrophilicity of the SF/CS scaffold was slightly improved by the addition of Glu to the scaffold as reflected from the contact angle data presented in table 5.4. SF/CS/Glu (0.2 -1.2 w/v) showed a decrease in contact angle in the range 53.5-49.1° in comparison to SF/CS (80:20) ($54.2 \pm 0.3^\circ$). The contact angles were found to be decreased in a narrow range with increase in Glu content. This decrease in contact angle is possibly due to the hydrophilic property of Glu that improves the wettability of the scaffold. Interestingly, the difference between the contact angles obtained with 1% and 1.2% Glu is not statistically significant representing similar hydrophilicity property of both the scaffolds.

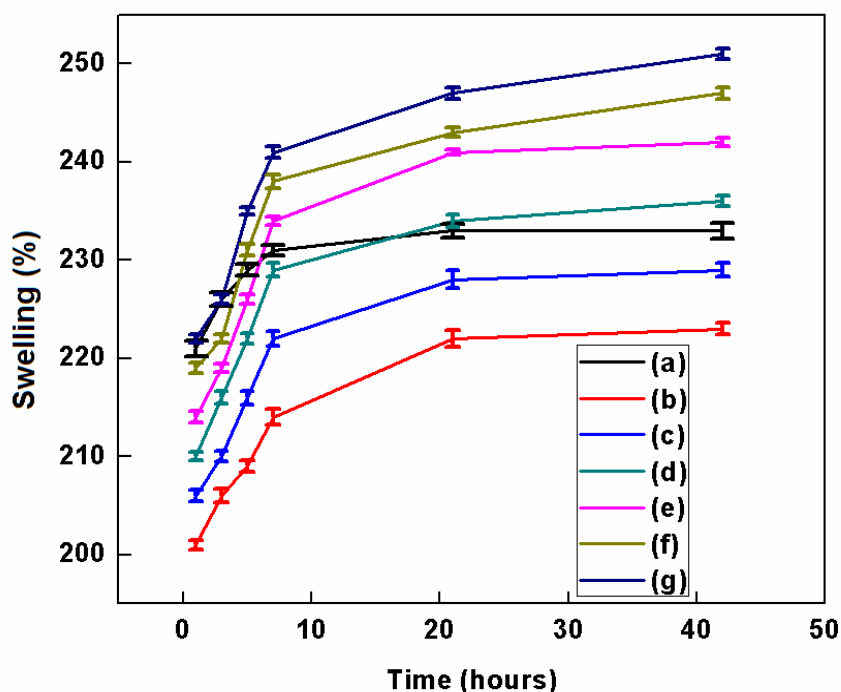


Figure 5.14: Swelling behaviour (a) SF/CS (80:20) blend scaffold and SF/CS with (b) 0.2, (c) 0.4, (d) 0.6, (e) 0.8, (f) 1 and (g) 1.2 % (w/v) of Glu respectively. A drastic increase in swelling was obtained by the addition of Glu to SF/CS (80:20) scaffold and the swelling rate was increased with increase in Glu content.

Table 5.4: Contact angle values of SF/CS/Glu scaffolds

Sample	Contact angle(degree)
SF/CS (80:20)	54.2±0.3
SF/CS/Glu 0.2 (w/v)	53.5±0.2
SF/CS/Glu 0.4 (w/v)	52.3±0.3
SF/CS/Glu 0.6(w/v)	51.1±0.1
SF/CS/Glu 0.8 (w/v)	50.2±0.7
SF/CS/Glu 1 (w/v)	49.5±0.8
SF/CS/Glu 1.2 (w/v)	49.1±0.2

5.2.5 In vitro degradation

The effect of addition of Glu to SF/CS scaffold on degradation is shown in figure 5.15. It is observed that all the scaffolds showed a steady degradation pattern during the entire time period. SF/CS/Glu scaffolds were found to degrade faster in comparison to the SF/CS scaffolds, as shown in figure 5.15. SF/CS scaffolds showed 87.9 % mass remaining in 28 days, whereas, the scaffolds with Glu content showed a mass remaining in the range 79-69.4 % with varied % of Glu (0.2 - 1.2 % w/v). The reason behind the enhanced degradation of SF/CS/Glu scaffolds is the additional hydrophilic groups present in the scaffold due to addition of Glu.

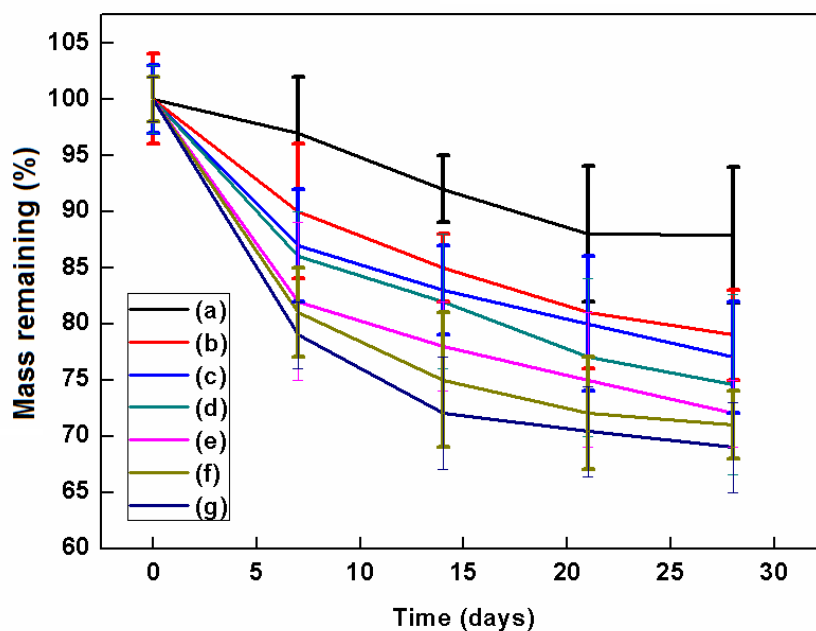


Figure 5.15: Degradation pattern of (a) SF/CS (80:20) blend scaffold and SF/CS with (b) 0.2, (c) 0.4, (d) 0.6, (e) 0.8, (f) 1 and (g) 1.2 % (w/v) of Glu respectively. SF/CS/Glu scaffolds were found to degrade faster in comparison to the SF/CS scaffolds.

5.2.6 Compressive strength

The compressive strength of the SF/CS/Glu scaffolds was measured as 199 ± 13 , 200 ± 17 , 201 ± 13 , 202 ± 16 , 202 ± 12 and 201 ± 10 kPa with Glu content of 0.2, 0.4, 0.6, 0.8, 1 and 1.2% (w/v) respectively. Thus, the addition of Glu in SF/CS scaffold did not show any significant influence on the compressive strength that means the mechanical integrity of the SF/CS scaffold remain intact with addition of Glu. This may be attributed to the fact that a little amount of Glu added to the blend is not sufficient enough to have any impact on the compressive strength.

5.2.7 In vitro cell culture

Cell attachment and morphology

The morphology and cellular attachment of hMSCs over SF/CS/Glu scaffolds are shown in figure 5.16. On close observation, hMSCs were found to attach and spread on the scaffold surface during the entire 14 days culture period on the scaffold. Better cell attachment is observed with SF/CS/Glu scaffolds in comparison to SF/CS (80:20) scaffold used as

control. The cells were also well spread throughout the scaffold and colony formation was observed on day 14. The enhanced cell attachment and spreading on scaffolds loaded with Glu can be attributed to the fact that Glu is the precursor of GAG formation [24], thus created a cell friendly microenvironment for the growth and proliferation of MSCs. The superior cell attachment and spreading observed with SF/CS/Glu scaffold represents its better cytocompatibility than the SF/CS scaffold.

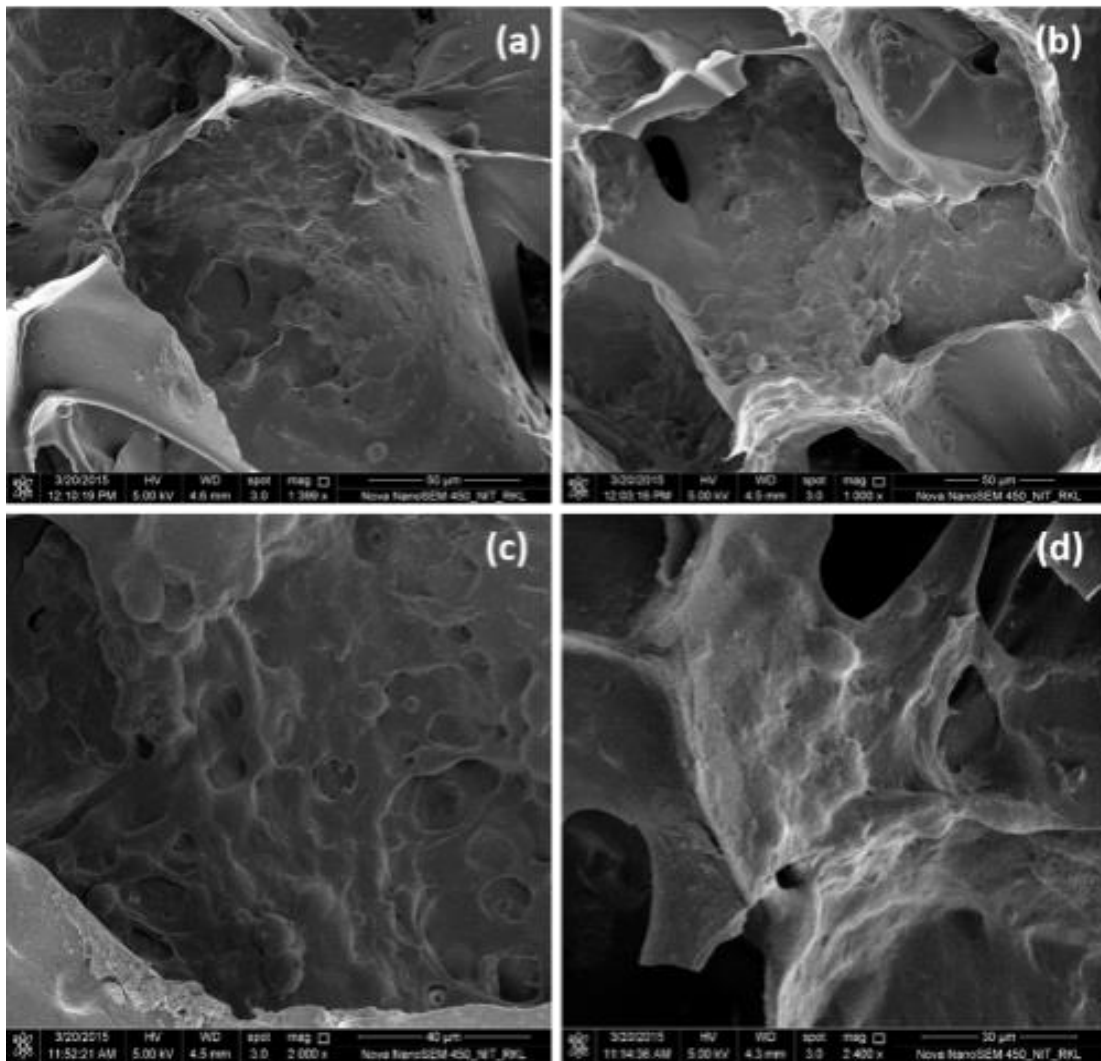


Figure 5.16 FE-SEM images of cell attachment and proliferation of MSCs over various scaffolds (a) & (b) SF/CS (80:20) scaffold, (c) & (d) SF/CS/Glu 1% (w/v) after 7 and 14 days of culture respectively. Superior cell attachment and spreading were observed in SF/CS/Glu scaffolds than SF/CS scaffolds.

Cellular activity by MTT assay

The cellular viability in terms of metabolic activity of the MSCs seeded on the SF/CS/Glu scaffolds was evaluated by MTT assay is shown in figure 5.17. As expected, the metabolic activity was found to increase with the progress of the culture upto 7 days and the metabolic activity of SF/CS/Glu was higher than the SF/CS scaffolds. The improved metabolic activity shown by SF/CS/Glu can be attributed to the presence of increased Glu residues providing suitable cell recognition sites thereby attracted more number of cells on the scaffold surface [26]. Since there is no significant difference in cell viability between SF/CS/Glu scaffolds containing 1 and 1.2 % (w/v) of Glu, SF/CS/Glu scaffolds with 1% (w/v) was selected for further study.

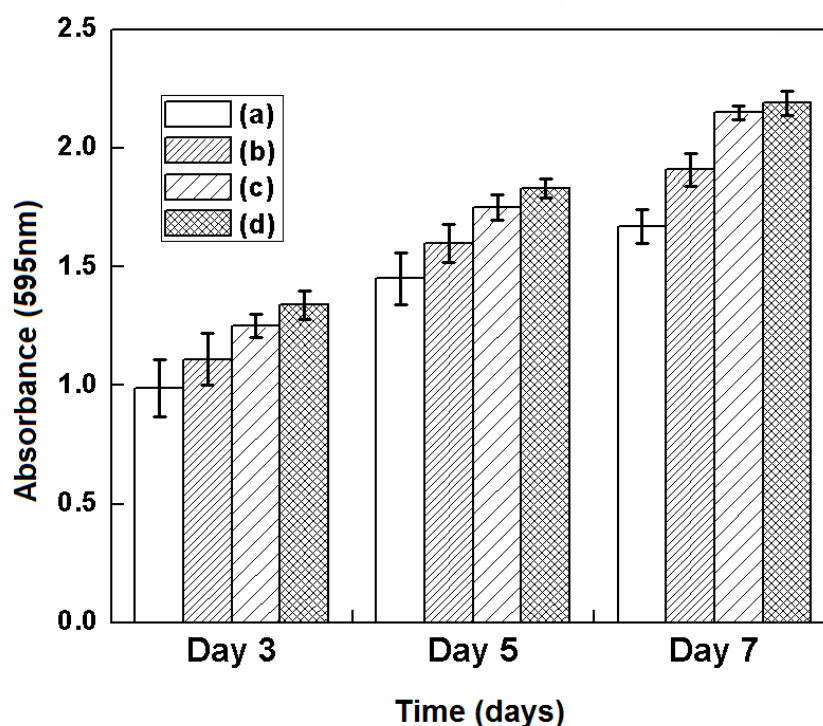


Figure 5.17: MTT assay of (a) SF/CS (80:20) scaffolds and SF/CS/Glu (b) 0.8, (c) 1 and (d) 1.2 % Glu (w/v). The metabolic activity of SF/CS/Glu scaffold increased with increase in Glu content.

Cellular proliferation by DNA quantification

A gradual increase in DNA content was observed during the progress of MSCs culturing in all the developed scaffolds. A higher DNA content (349 ng/ml) representing the higher

MSCs proliferation was obtained when SF/CS was loaded with 1% Glu in comparison to the DNA content shown by the SF/CS scaffold during the entire culture period of 21 days (fig. 5.18). The enhanced proliferation of MSCs shown by SF/CS/Glu scaffolds is due to the fact that Glu has facilitated a suitable microenvironment for the normal functioning of cell [26].

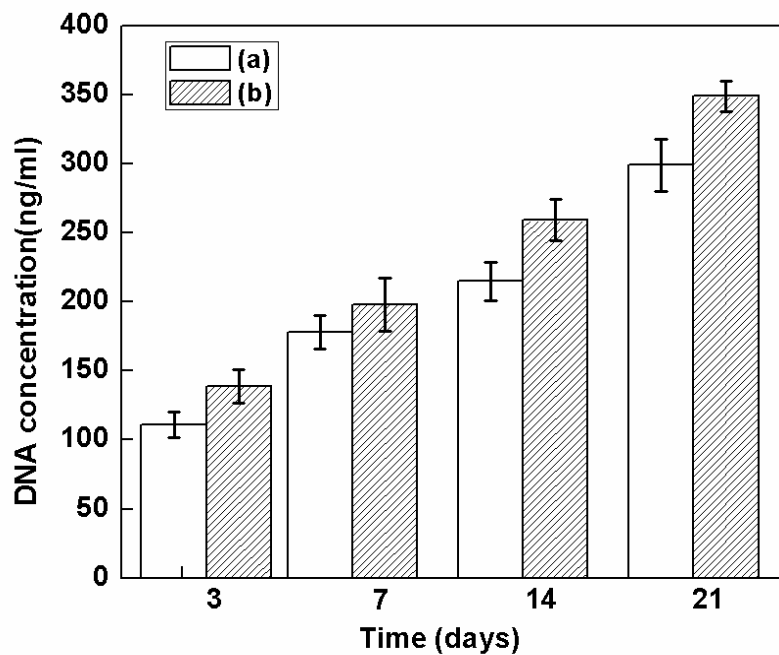


Figure 5.18: Proliferation in terms of DNA quantification of hMSC over (a) SF/CS (80: 20) scaffold, (b) SF/CS/Glu scaffolds with 1% (w/v) Glu. The hMSC proliferation on SF/CS scaffold increased with addition of Glu.

Cytoskeletal analysis by confocal microscopy

Confocal microscopy is a technique used to understand the cell spreading, proliferation in a scaffold matrix. It also enables to study the formation of F-actin and analyze the cell-scaffold interactions [96]. Figure 5.19 shows the uniform distribution of hMSCs on the SF/CS/Glu scaffolds observed under a confocal microscope. The cells were found to be well spread on the surface and also inside of the SF/CS/Glu scaffolds showing its superior cell compatibility thereby promoted cell-scaffold interaction than control (SF/CS 80:20). On the

14th day of culture, the number of viable cells observed is more on SF/CS/Glu scaffolds than SF/CS representing the higher cell proliferation shown by SF/CS/Glu scaffold due to the presence of disaccharide building blocks in Glu [81].

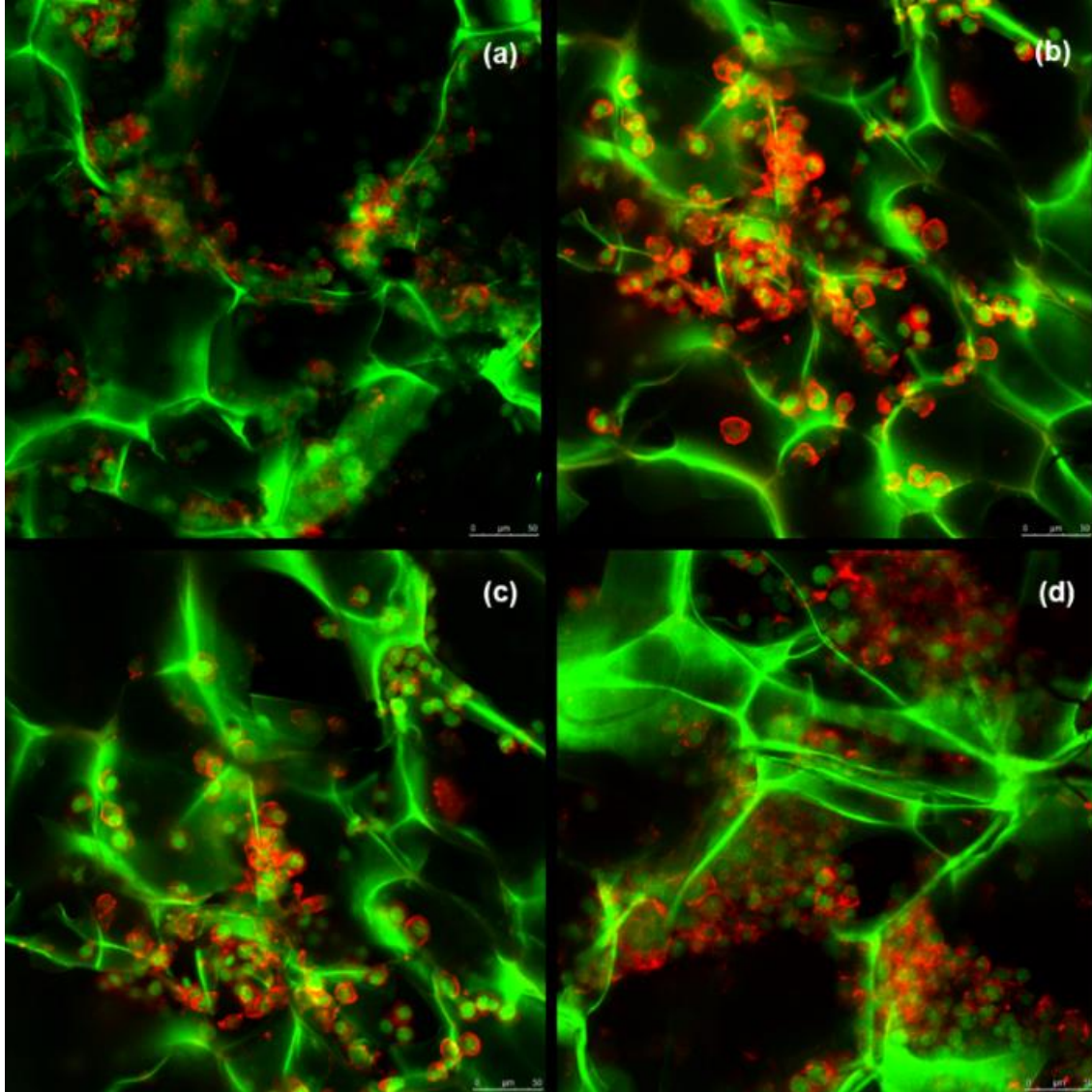


Figure 5.19: Confocal images showing the cytoskeletal arrangement on (a) SF/CS (80:20) scaffold; (b) SF/CS/Glu scaffolds with 1% (w/v) Glu. The cells were found to well spread on the surface and also inside of the SF/CS/Glu scaffolds.

GAG estimation

GAG estimation is an essential study which determines the ability of the cell seeded scaffold to support differentiation of cells to ECM synthesis [111]. The amount of GAG secreted by

MSCs over the SF/CS/Glu scaffolds during 21 days of culture is shown in figure 5.20. An increase in GAG content was observed with increase in culture time. However, GAG secreted by MSCs over SF/CS/Glu scaffolds was higher than the control (SF/CS) throughout the culture period. The corresponding amount of GAG secreted was measured to be 21 $\mu\text{g/ml}$ and 18 $\mu\text{g/ml}$ for SF/CS/Glu and SF/CS (80:20) respectively. The existence of GAG components in the SF/CS/Glu scaffold has enabled it to support better cellular activity, thereby an improved GAG production was achieved. Thus, this study demonstrated that the presence of Glu has enhanced cell proliferation and GAG secretion representing the differentiation ability of the scaffold [111]. This is also supported by the study as reported elsewhere [27].

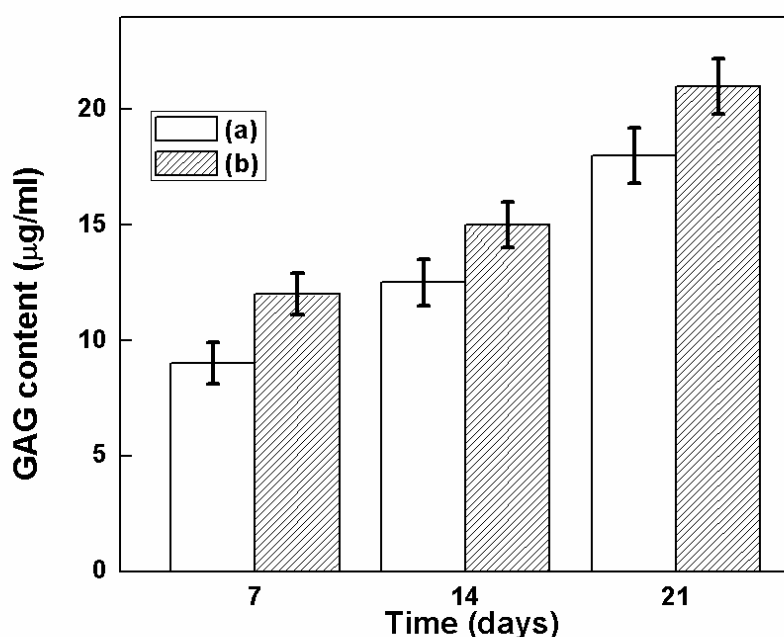


Figure 5.20: GAG analysis of (a) SF/CS (80:20) scaffold. (b) SF/CS/Glu scaffold with 1% (w/v) Glu. An increase in GAG content was observed with increase in culture time. The scaffold containing Glu showed higher GAG formation.

5.C DEVELOPMENT OF SILK FIBROIN/CHITOSAN / CHONDROITIN SULFATE SCAFFOLDS

In the previous chapter, the cell supportive property such as cell metabolic activity and GAG producing ability of MSCs seeded SF/CS scaffold was improved by the addition of Glu as a bioactive molecule. Chs is one of the naturally occurring GAG present in the aggrecan region of the cartilage tissue [21]. It is an important component of extracellular matrix. The anti-inflammatory activity, water and nutrient absorption activity, wound healing property and bioactivity at the cellular level of Chs are beneficial for cartilage tissue engineering [63]. The addition of Chs to the scaffold facilitates chondrogenesis of MSCs by providing a microenvironment that is favourable for the cellular growth and thus facilitates ECM formation [23].

Keeping the above beneficial effect of Chs, the present dissertation work has been focused on examining the effect of Chs on SF/CS scaffold properties in order to enhance cell proliferation and GAG secretion properties of SF/CS scaffolds. The results and discussion of this experimental work are described in this chapter.

5.3 Results and discussion

5.3.1 Scanning electron microscopy (SEM)

The morphology of the freeze dried SF/CS/Chs scaffolds prepared with different concentration of Chs is shown in figure 5.21. Table 5.5 shows the pore size range and average pore size of the SF/CS/Chs scaffolds. The pore morphology was observed to change from circular to oval shape when the concentration of Chs increases from 0.6 to 0.8wt%. On close observation, it has been found that all the scaffolds possess open pore structure with distinct pore walls and pore interconnectivity. The pore walls are more visible in scaffolds having Chs in the range between 0.8 - 1.2% (w/v). From the table it is observed that, a small change in pore diameter (109-103 μ m) was observed with increase in Chs (0.2-1.2 %w/v). This decrease in pore size is due to the hydrophilic behavior of Chs, combined with the CS present in the scaffold. Similarly, Naeimi et al reported a decrease in pore size of the SF porous scaffolds from 121.45 ± 3.00 – 60 ± 5.00 .after the addition of Chs. Liang et al also studied the variation in pore size of collagen scaffolds when loaded with Chs [23].

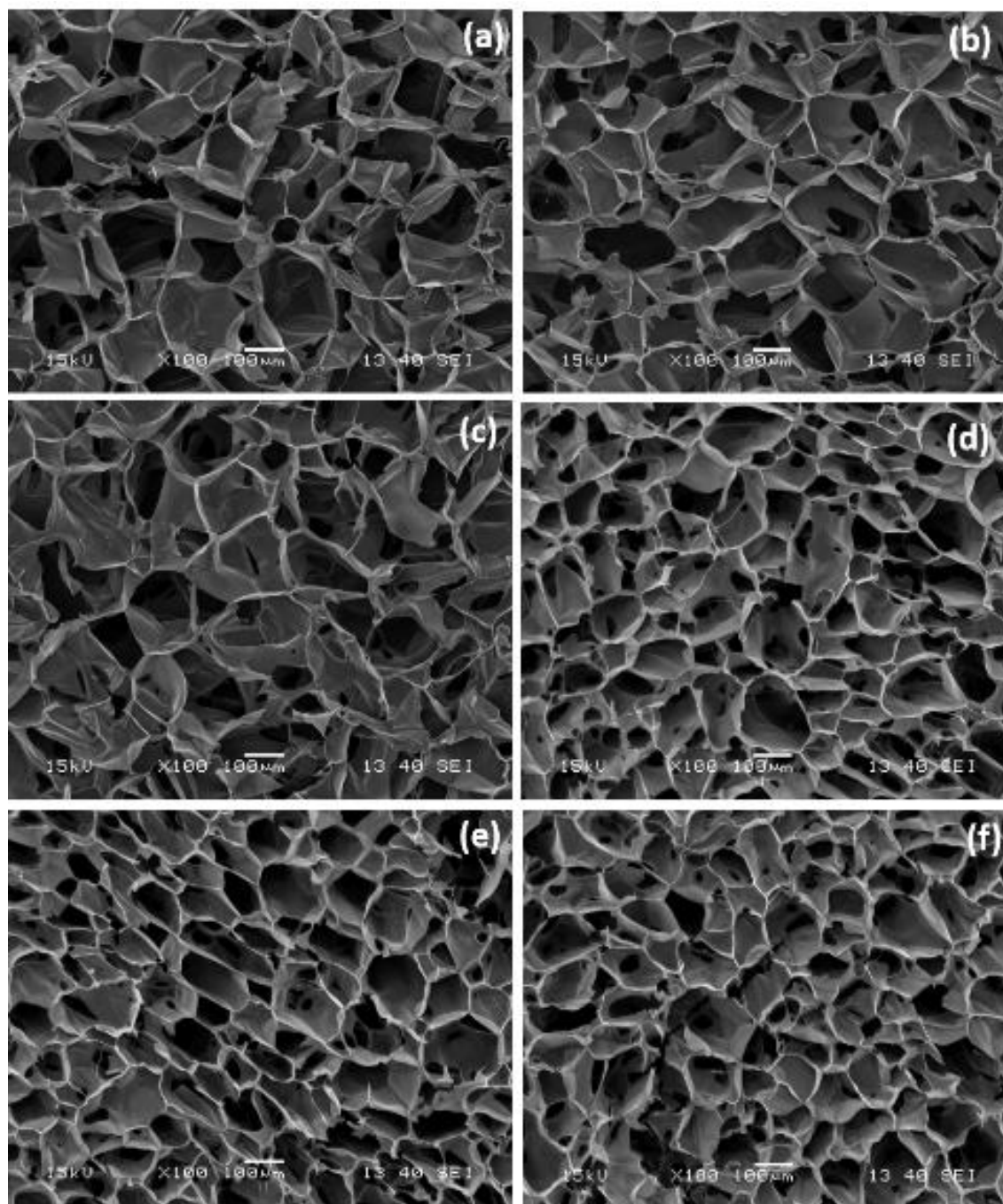


Figure 5.21: SEM images of SF/CS/Chs scaffolds with (a) (0.2), (b) (0.4), (c) (0.6), (d) (0.8), (e) (1) and (f) (1.2) % (w/v) of Chs respectively. All scaffolds possessed open porous network with highly interconnected pore structures.

5.3.2 Porosity

The measured porosity of the Chs added SF/CS scaffolds is tabulated in table 5.5. A minimal increase in porosity (85-87%) was evident with increase in Chs content from 0.2-

0.8% (w/v). A similar trend of increase in porosity with the addition of Chs to collagen scaffolds was reported earlier by Liang et al [117]. But further increase in porosity was not observed with further increase in Chs content (beyond 0.8%). Thus the obtained porosity with Chs added scaffolds is higher than the porosity of SF/CS scaffolds representing the superiority of the SF/CS/Chs scaffolds in terms of providing better cellular environment to the scaffold.

Table 5.5: Pore size, average pore size, and porosity of SF/CS/Chs scaffolds

Sample	Pore size (μm)	Average pore size (μm)	Porosity (%)
Chs 0.2 (w/v)	61-212	109 \pm 26.5	85 \pm 3.21
Chs 0.4 (w/v)	51-206	107 \pm 25.3	85.6 \pm 2.64
Chs 0.6 (w/v)	48-201	106 \pm 32.2	86.0 \pm 1.98
Chs 0.8 (w/v)	44-196	105 \pm 19.5	87 \pm 2.13
Chs 1 (w/v)	41-191	104 \pm 22.6	87.9 \pm 2.16
Chs 1.2 (w/v)	37-186	103 \pm 27.8	88.2 \pm 2.12

5.3.3 Structural analysis

FT-IR spectroscopy

Figure 5.22 represents the FT-IR spectra of the SF/CS/Chs scaffold. The absorption band at 1080cm^{-1} suggest the interaction between NH groups of SF and C=O and NH_2 groups of CS in the scaffold. The interaction between SF/CS and Chs, as represented at 1260cm^{-1} , corresponds to the S-O stretching between SF/CS and Chs [63]. Thus, FT-IR analysis indicates that Chs interacts at molecular level with SF/CS blend.

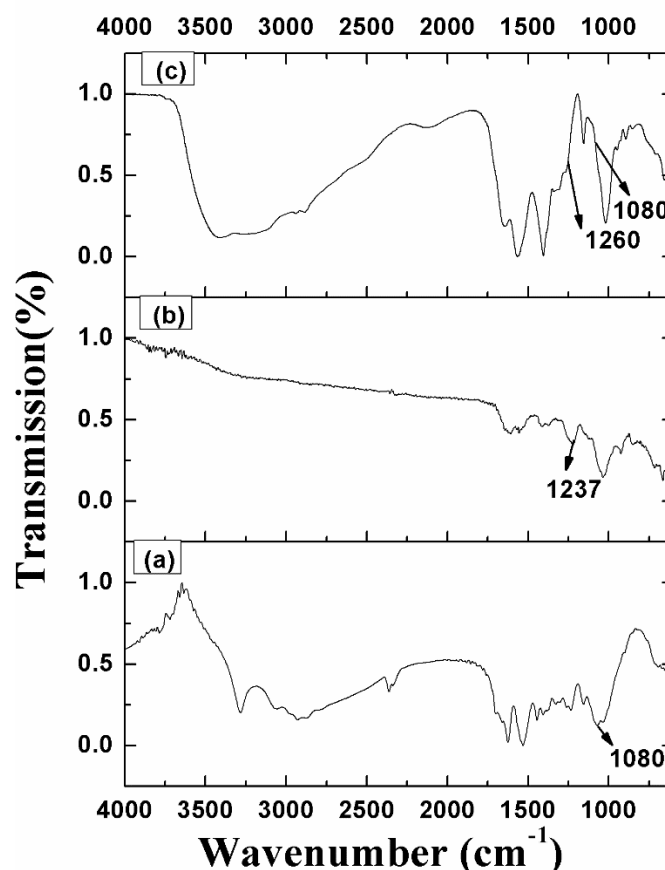


Figure 5.22: FT-IR spectra of (a) SF/CS (80: 20), (b) Chs powder and (c) SF/CS/Chs scaffolds. The additional band in SF/CS/Chs scaffold is due to the interaction of Chs with SF/CS blend.

5.3.4 Swelling behavior and water contact angle

A comparative study of the % swelling observed with SF/CS (80:20) and SF/CS/Chs scaffolds during 42 hrs of SBF treatment is shown in figure 5.23. All the scaffolds show higher % swelling (255%) than SF/CS scaffolds (219%) which may be attributed partly because of the increased porosity of SF/CS/Chs scaffold and partly hydrophilic nature of Chs [126]. There is an initial increase in swelling % of the scaffolds between 2-8 hrs which is due to the flow of SBF into the pores of the scaffold. As indicated, both SF/CS and SF/CS/Chs scaffolds attained state of swelling equilibrium after 10 hrs of study, which is due to the saturation of SBF into the porous scaffold matrix. The trend of swelling is SF/CS/Chs > SF/CS/Glu > SF/CS.

Table 5.6 shows the variation of contact angle of water on SF/CS/Chs scaffold with variation of Chs content in the scaffold. The contact angle of the SF/CS scaffold was improved after the addition of Chs to the scaffold as represented in table 5.6. The water contact angle of SF/CS (80:20) scaffolds is $54.2 \pm 0.3^\circ$. SF/CS/Chs (0.2 -1.2 w/v) showed a contact angle in the range 50.1 - 46.8° . With gradual increase in Chs content, the contact angle was found to be decreased which may be attributed to the fact that the hydrophilicity of Chs is enhancing the wettability of the SF/CS scaffold. A similar increase in swelling and water uptake of CS / hyaluronan composite sponges due to the addition of nano Chs was reported earlier by Anisha et al [63].

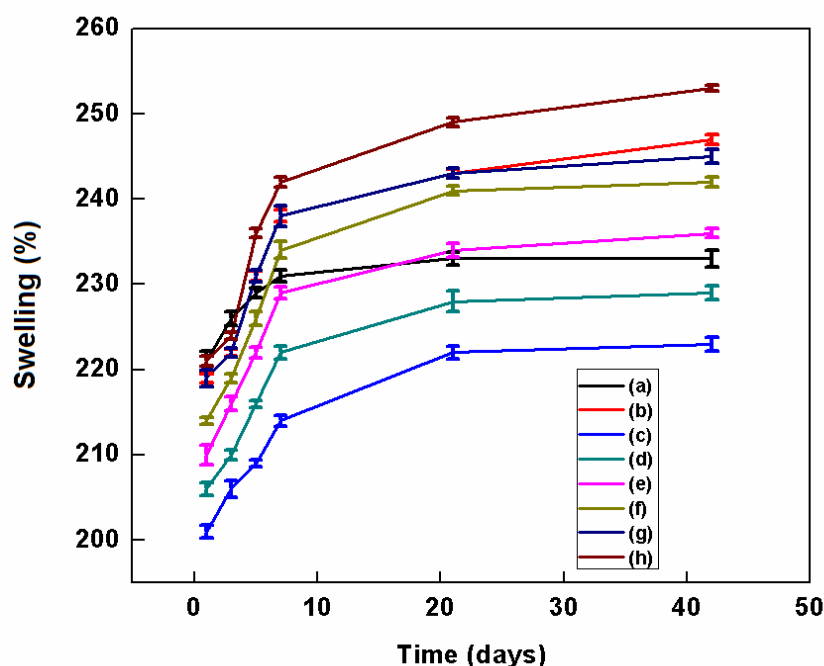


Figure 5.23: Swelling behaviour of (a) SF/CS (80:20), (b) SF/CS/Glu with 1% (w/v) Glu and SF/CS/Chs with (c) 0.2, (d) 0.4, (e) 0.6, (f) 0.8, (g) 1 & (h) 1.2 % (w/v) of Chs respectively. The rate of swelling increased between 2-8 hrs and after that they attained state of swelling equilibrium after 10 hrs of study.

Table 5.6: Contact angle of SF/CS/Chs scaffolds

Sample	Contact angle(degree)
SF/CS (80:20)	54.2±0.3
SF/CS/Chs 0.2 (w/v)	50.1±0.2
SF/CS/Chs 0.4 (w/v)	49.3±0.3
SF/CS/Chs 0.6(w/v)	48.7±0.1
SF/CS/Chs 0.8 (w/v)	47.4±0.7
SF/CS/Chs 1 (w/v)	47.1±0.8
SF/CS/Chs 1.2 (w/v)	46.8±0.6

5.3.5 In vitro degradation

Figure 5.24 depicts the in-vitro degradation pattern of SF/CS/Chs scaffolds. SF/CS/Chs scaffolds degraded at a faster rate (70%) in comparison to SF/CS/Glu (71%) and SF/CS (87.9%) scaffold. Initially the scaffolds showed a faster degradation, which is due to the rapid loss of scaffold material upon initial hours of contact with the SBF solution. With increase in time, there is a steady decrease in scaffold mass representing that the closure of pores resulting in lesser degradation. Increase in degradation rate may be due to the increase in scaffold porosity with increase in Chs content. The trend of degradation is SF/CS/Chs > SF/CS/Glu > SF/CS. A similar trend of increased degradation was observed earlier with incorporation of nano Chs with CS sponges [63].

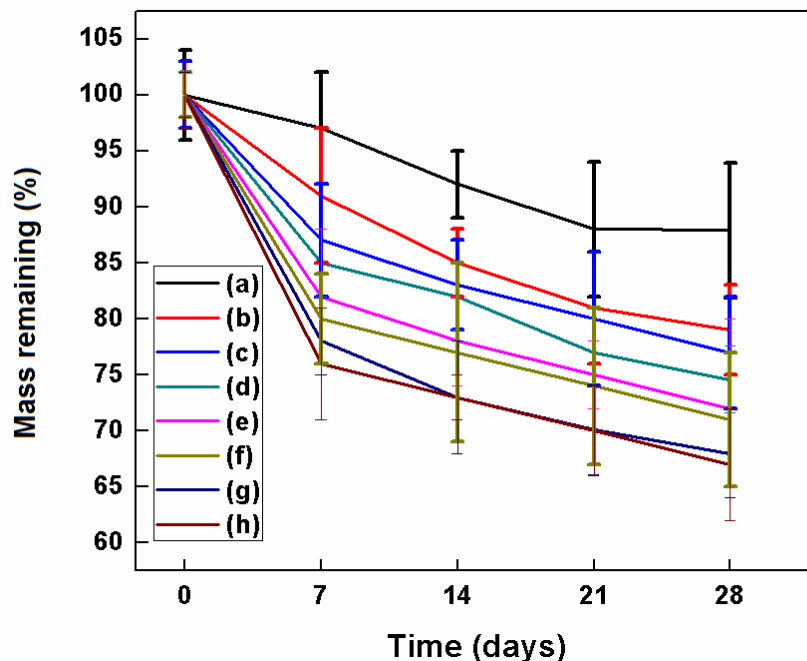


Figure 5.24: Degradation pattern of (a) SF/CS (80:20), (b) SF/CS/Glu with 1 % (w/v) Glu and SF/CS/Chs with (c) 0.2, (d) 0.4, (e) 0.6, (f) 0.8, (g) 1 & (h) 1.2 % (w/v) of Chs respectively. All the scaffolds showed an initial faster degradation and the rate of degradation increased with increase in Chs content.

5.3.6 Compressive strength

The compressive strength of the SF/CS/Chs scaffolds was measured as 201 ± 10 , 203 ± 11 , 203 ± 15 , 204 ± 13 , 200 ± 11 and 200 ± 12 with Chs content of 0.2, 0.4, 0.6, 0.8, 1 and 1.2% (w/v) respectively. As in case of Glu loaded scaffold, no significant change in the compressive strength due to addition of Chs was found.

5.3.7 In vitro cell culture

Cell attachment and morphology

Enhanced cell attachment and proliferation, in terms of increased cell spreading, were observed with all the SF/CS/Chs scaffolds compared to SF/CS (80:20) and a slightly lower than SF/CS/Glu 1 % (w/v) scaffolds as shown in figure.5.25. This enhanced cell proliferation achieved is due to the addition of Chs which is hydrophilic in nature thereby promotes cell attachment [21]. Also, a homogenous population of cells is seen in the SF/CS/Chs scaffolds.

In comparison, SF/CS/Chs scaffolds show lesser cell density than Glu loaded SF/CS scaffolds representing the superior cell supportive property of the later.

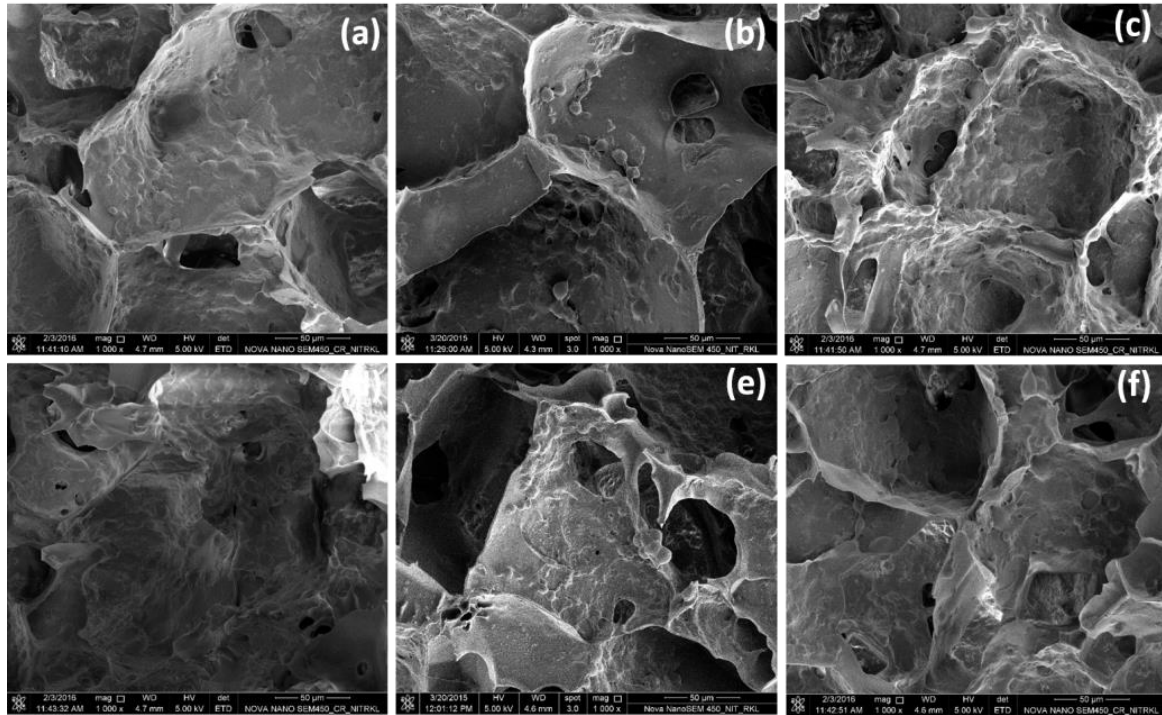


Figure 5.25: FE-SEM images showing the cell attachment & cell spreading over the scaffolds. (a) & (d) SF/CS (80:20), (b) & (e) SF/CS/Glu 1% (w/v), and (c) & (f) SF/CS/Chs 0.8% (w/v) scaffolds. A homogenous population of cells were present in the SF/CS/Chs scaffolds.

Cellular activity by MTT assay

The MTT assay results shows an increased trend in metabolic activity in SF/CS scaffold containing Chs during the progress of the culture as shown in figure 5.26. The metabolic activity of the SF/CS/Chs scaffold was higher than SF/CS scaffold representing the enhanced biocompatibility of Chs containing scaffold. But when compared to the SF/CS/Glu scaffolds, SF/CS/Chs scaffolds show lesser metabolic activity, as observed earlier in the cell attachment study.

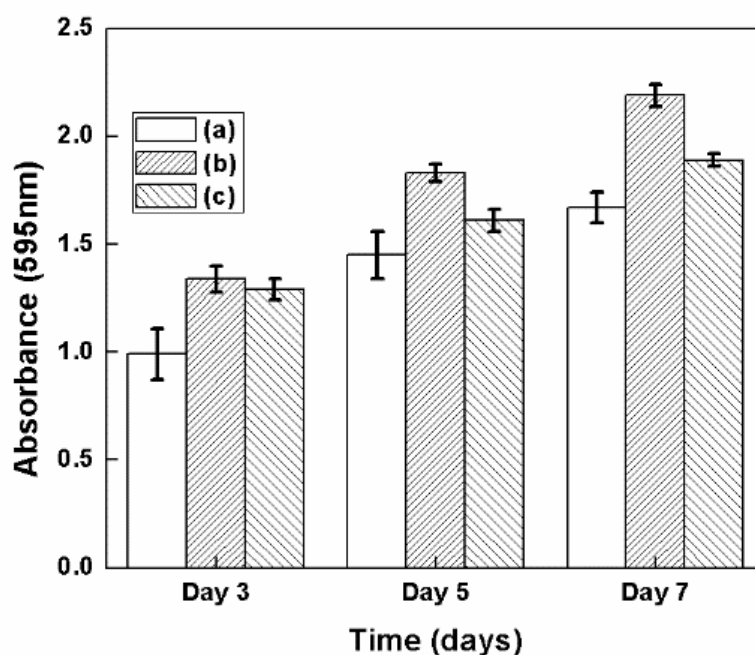


Figure 5.26: MTT assay of (a) SF/CS (80:20) blend scaffold, (b) SF/CS/Glu scaffold with 1% (w/v) Glu and SF/CS/Chs scaffold with (c) 0.8 % (w/v) of Chs. The metabolic activity of the SF/CS/Chs scaffold was higher than SF/CS scaffold but lower than SF/CS/Glu scaffolds.

Cellular proliferation by DNA quantification

The proliferation of hMSCs over the scaffold was measured quantitatively by DNA estimation. Figure 5.27 shows an increase in DNA content with time in all the developed scaffolds with a varying degree of DNA content. Among the scaffolds used under study, SF/CS/Chs scaffolds showed significantly higher DNA content (355 ng/ml) than the SF/CS (80:20) (299 ng/ml) and SF/CS/Glu (349 ng/ml) scaffolds representing enhanced proliferation rate of hMSCs on the scaffolds. The increase in proliferation rate achieved is attributed to the presence of Chs which influences hMSC proliferation and promotes cell polymer interactions [63]. The enhanced corneal stromal cell proliferation rate with addition of Chs to CS was also reported earlier by Yao et al [119].

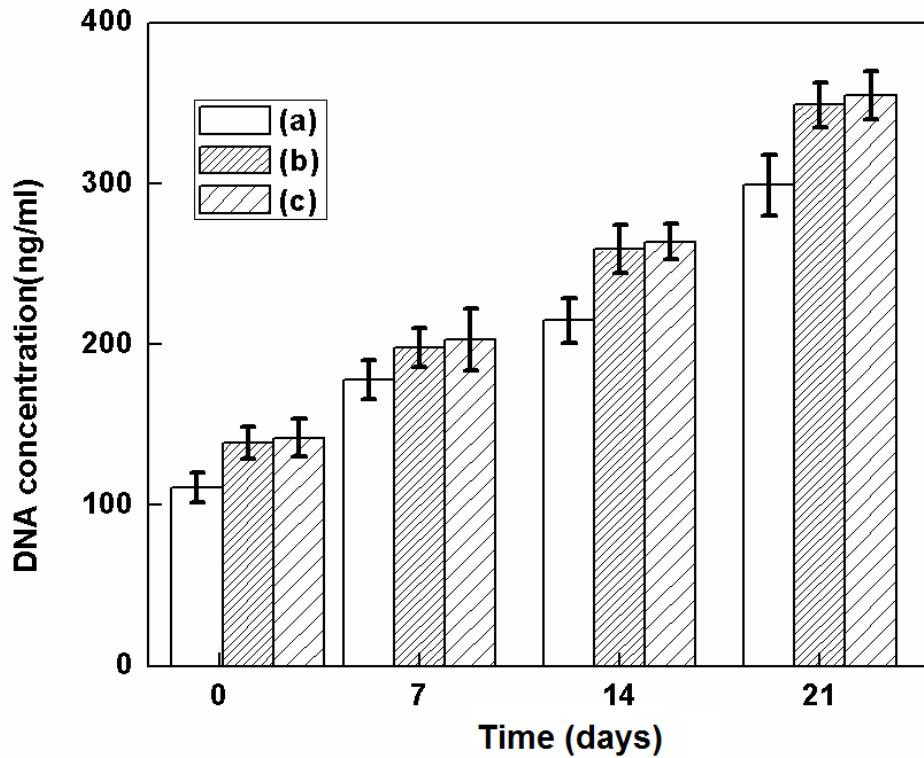


Figure 5.27: DNA assay of (a) SF/CS (80:20) blend scaffold, (b) SF/CS/Glu scaffold with 1% (w/v) Glu and (c) SF/CS/Chs scaffold with 0.8% (w/v) of Chs. SF/CS/Chs scaffold showed higher DNA content than the other scaffolds.

Cytoskeletal analysis by confocal microscopy

Understanding the cytoskeletal arrangement in a cell-scaffold construct is important to determine cell infiltration in the scaffolds [96]. Figure 5.28 shows the uniform distribution of hMSCs on the SF/CS/Chs scaffolds as observed from confocal microscopic images. Besides surface, the cells were also seen inside the scaffold matrix representing the superior interaction between Chs loaded scaffold (Fig.5.27). Also, the SF/CS/Chs scaffold shows reduced number of cells than the Glu loaded SF/CS scaffolds.

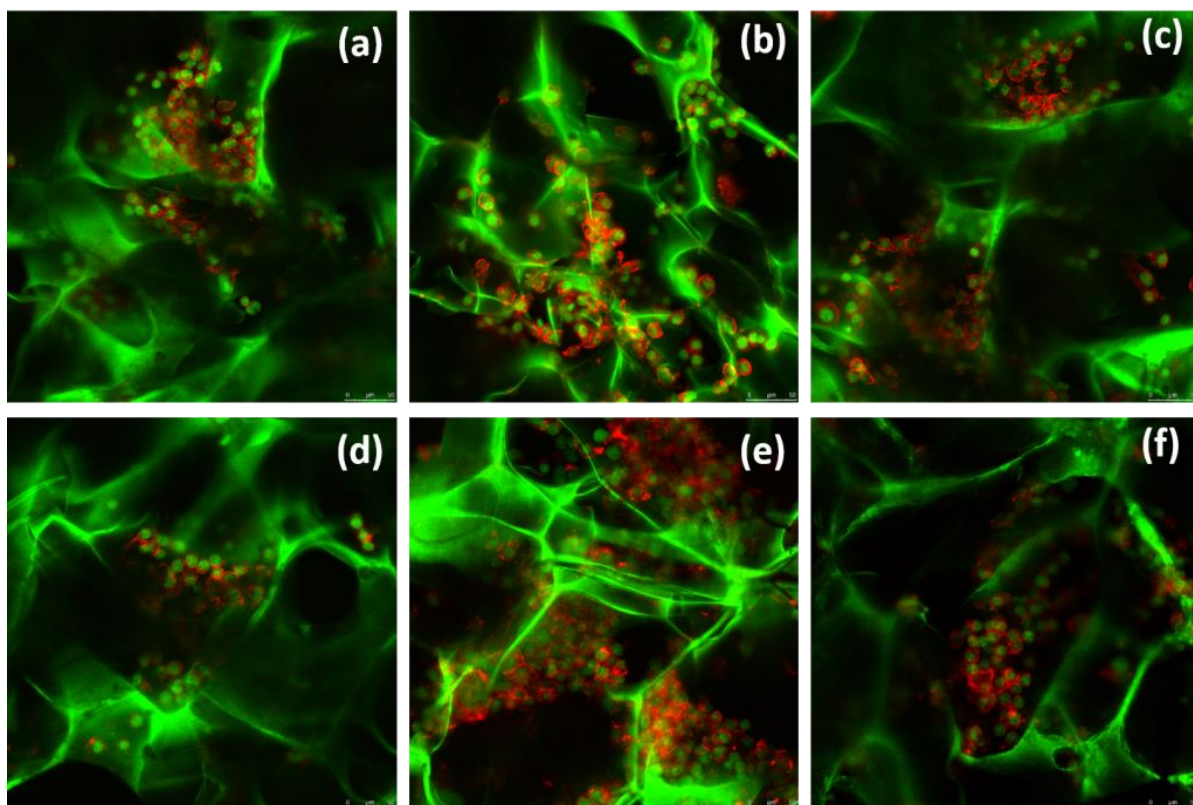


Figure 5.28: Confocal microscope images of scaffolds. (a) & (d) SF/CS (80:20), (b) & (e) SF/CS/Glu 1 % (w/v), and (c) & (f) SF/CS/Chs 0.8% (w/v) after 7 & 14 days of culture respectively. A uniform distribution of hMSCs on the SF/CS/Chs scaffolds was observed from confocal microscopic images. SF/CS/Chs scaffold showed reduced number of cells than the Glu loaded SF/CS scaffolds.

GAG assay

As described earlier, GAG assay is important to determine the initiation of hMSCs differentiation into chondrocytes that leads to ECM synthesis [111]. Figure 5.29 shows the GAG content in SF/CS/Chs scaffolds and SF/CS (80:20) scaffolds. A steady increase in GAG production is observed with all the scaffold groups. Scaffolds containing Glu and Chs showed higher GAG secretion than SF/CS scaffolds throughout the culture time. Initially, after 7 days of culture, the SF/CS/Glu scaffolds showed a slight increase in GAG content than the SF/CS and SF/CS/Chs scaffolds. But after 14 and 21 days of incubation, the SF/CS/Chs scaffolds showed higher GAG content than the other groups of scaffolds. SF/CS/Chs scaffolds showed higher GAG secretion of 23 μ g/mg after 21 days of culture than SF/CS (80:20) (18 μ g/mg) and SF/CS/Glu scaffolds (21 μ g/mg). The higher secretion

of GAG by the SF/CS/Chs scaffolds is due to the fact that Chs promotes differentiation and enhanced matrix production. A similar study was reported earlier with PEG and Chs based hydrogels by Varghese et al [81] in which the GAG secretion was found to gradually increase from 0.116 ± 0.011 g/g to 0.168 ± 0.008 g/g with the concentration of Chs in the PEG hydrogels.

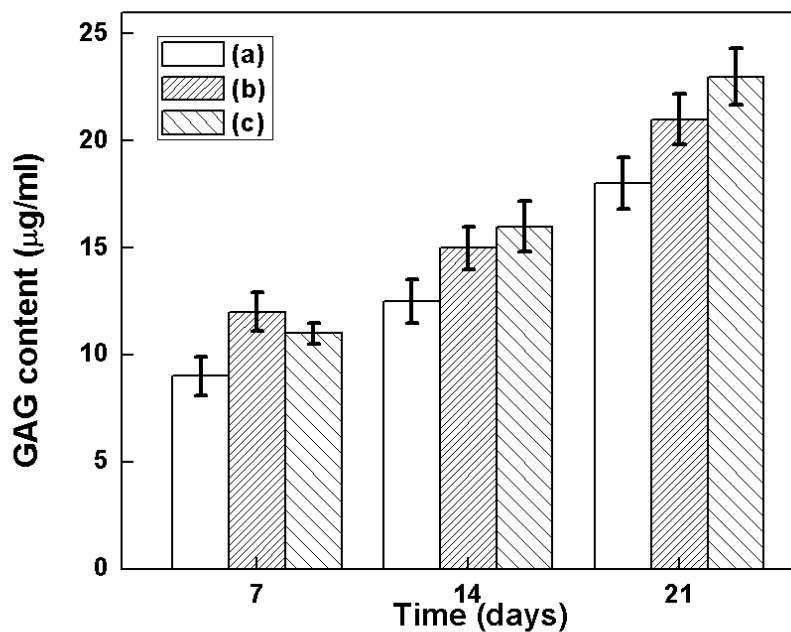


Figure 5.29: GAG estimation of (a) SF/CS (80:20) blend scaffold, (b) SF/CS/Glu scaffold with 1% (w/v) Glu and (c) SF/CS/Chs scaffold with 0.8% (w/v) of Chs. GAG secretion was found to be maximum for the SF/CS/Chs scaffolds.

5.D EFFECT OF ADDITION OF GLU AND CHS IN COMBINATION ON THE SCAFFOLD PROPERTY

In the previous chapters, the addition of Glu and Chs individually were found to be beneficial improving a set of desired properties of SF/CS blend scaffolds. Both glucosamine sulfate and chondroitin sulfate loaded SF/CS scaffolds has shown enhanced hydrophilicity, cell adhesion and cell proliferation, metabolic activity and more importantly GAG production. Messier et al has reported the utilization of Glu and Chs in combination for the regeneration of cartilage tissue using 1500/1200 mg of Glu and Chs respectively which reduced pain, improved the strength and movement of older people. The synergistic effects of both Glu and Chs towards cartilage regeneration was also reported [26]. The combination of Glu and Chs have alleviated pain, discomfort and improved the overall joint function in the patient groups [24,25].

Therefore, attempts have been made in the present chapter to investigate the effect of combination of Glu/Chs on the properties of the developed SF/CS scaffolds. To this end, three different weight percentage of Chs namely 0.5, 1 and 1.5 were added to the most efficient SF/CS/Glu 1%(w/v) solution developed in the previous section to prepare SF/CS/Glu/Chs porous scaffolds by freeze drying method. The combined effect of Glu (1%) and Chs (0.5, 1 & 1.5%) on various properties of SF/CS scaffold was assessed by physicochemical, mechanical and biological properties. This chapter describes the results and discussion on the above experimental research work.

5.4 Results and discussion

5.4.1 Scanning electron microscopy (SEM)

The open porous structure and high pore interconnectivity of the SF/CS/Glu/ Chs are depicted by SEM images, as shown in figure.5.30). The pore size range of 40-196 (avg. 106 ± 26.3), 44-204 (avg 107 ± 19.8) and 47-208 (avg 108 ± 31.2) μm with 0.5, 1.0, 1.5% (w/v) of Chs respectively was measured with the developed SF/CS/Glu/Chs hybrid scaffolds. The scaffolds show similar pore morphology with a little variation in their pore size with various compositions. Moreover, no significant change in pore size was observed between these scaffolds and the individual SF/CS/Glu and SF/CS/Chs scaffolds.

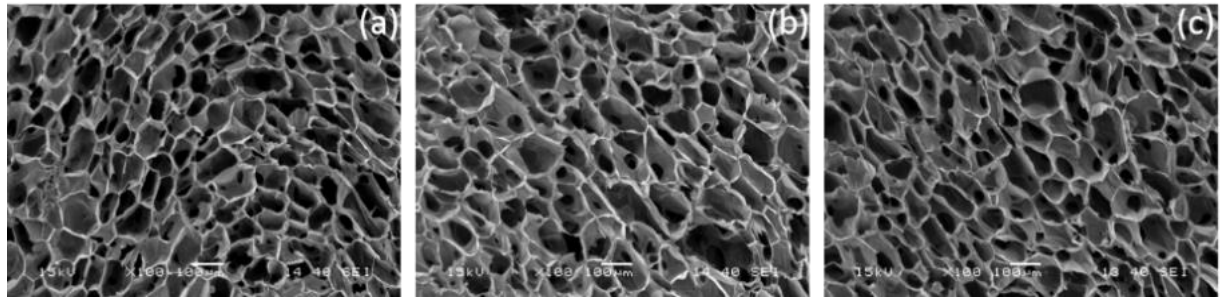


Figure 5.30: SEM images of SF/CS/Glu/Chs scaffold with (a) Chs (0.5) (b) Chs (1) (c) Chs (1.5) % (w/v). The scaffolds showed similar pore morphology with a little variation in their pore size with various compositions.

5.4.2 Porosity

The porosity of the developed SF/CS/Glu/Chs scaffolds was measured as 88.7 ± 1.12 , 90.2 ± 1.3 and 90.6 ± 2.1 with Chs content of 0.5, 1 and 1.5 % (w/v) respectively. A slight increase in porosity was achieved with the addition of Chs in comparison to SF/CS, SF/CS/Glu and SF/CS/Chs as shown in table 5.7. This increase in porosity may be explained as the presence of more hydrophilic groups in the scaffold material has enhanced the overall porosity of the scaffolds. This increase in porosity is beneficial to provide better microenvironment for cell-material interaction thereby facilitates neo tissue generation. Thus, these scaffolds show superior property in providing a highly porous scaffold matrix for cell support.

Table 5.7: Pore size, average pore size, and porosity of SF/CS/Glu/Chs scaffolds.

Sample	Pore size (μm)	Average pore size (μm)	Porosity (%)
Glu/Chs 0.5	40-196	106 ± 26.3	88.7 ± 1.12
Glu/Chs 1	44-204	107 ± 19.8	90.2 ± 1.3
Glu/Chs 1.5	47-208	108 ± 31.2	90.6 ± 2.1

5.4.3 Structural analysis

FT-IR spectroscopy

Figure 5.31 shows the FT-IR analysis of the SF/CS/Glu/Chs scaffolds. The band observed at 1080 cm^{-1} represents interaction between the SF and CS present in the scaffold. Bands at 1614 cm^{-1} indicate the interaction of Glu in the scaffolds. The band at 1260 cm^{-1} signifies the S-O stretching due to interaction between SF/CS blend and Chs. Thus FT-IR analysis confirms the intermolecular interaction between both Glu and Chs in the SF/CS scaffold.

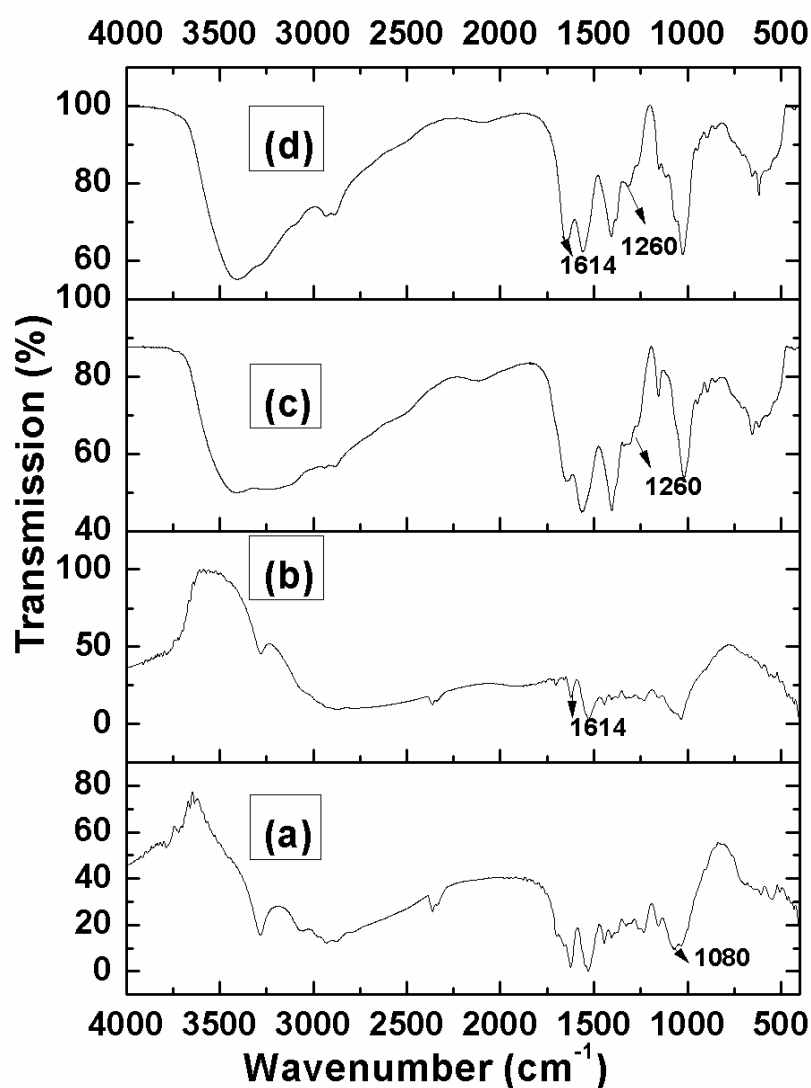


Figure 5.31: FT-IR spectra of (a) Pure SF/CS, (b) SF/CS/Glu (c) SF/CS/Chs (d) SF/CS/Glu/Chs scaffolds. The characteristic band of Glu & Chs was found in SF/CS/Glu/Chs representing the individual interaction of Glu & Chs with SF/CS blend.

5.4.4 Swelling behavior and water contact angle

Figure 5.32 shows the comparative study on the % swelling behavior of the developed scaffolds during the 42 hrs of swelling study. As observed from the figure, all the scaffolds showed an initial increase in swelling during the first few hrs but a steady swelling behavior (equilibrium state) was achieved with time, in about 10 hrs. Scaffolds with combination of Glu and Chs exhibited more swelling (263 %) than the scaffolds with individual Glu (246 %) and Chs content (243 %) and SF/CS (219 %). Also, the scaffolds with 0.5 % (w/v) showed least swelling among the SF/CS/Glu/Chs scaffolds (258 %) followed by 1 % (w/v) (258 %) and 1.5 % (w/v) (262%) of Chs content. This increased swelling rate of the SF/CS/Glu/Chs scaffolds can be attributed to the combined hydrophilicity of Glu and Chs. The trend of swelling is SF/CS/Glu/Chs > SF/CS/Chs > SF/CS/Glu > SF/CS.

The wettability of the SF/CS/Glu/Chs scaffolds was further confirmed by contact angle measurements. The hydrophilicity of the SF/CS/Glu scaffolds was slightly improved after the addition of Chs, as shown in table 5.8. SF/CS/Glu/chs (0.5-1.5 % w/v) showed a contact angle in the range 46.7-45.5 which is lower than the water contact angle measured with SF/CS/Glu 1% (w/v) scaffold is $49.5 \pm 0.8^\circ$. This represents the higher hydrophilicity, means higher wettability of the SF/CS/Glu/Chs scaffolds. Furthermore, decrease in contact angle with increase in Chs content was observed.

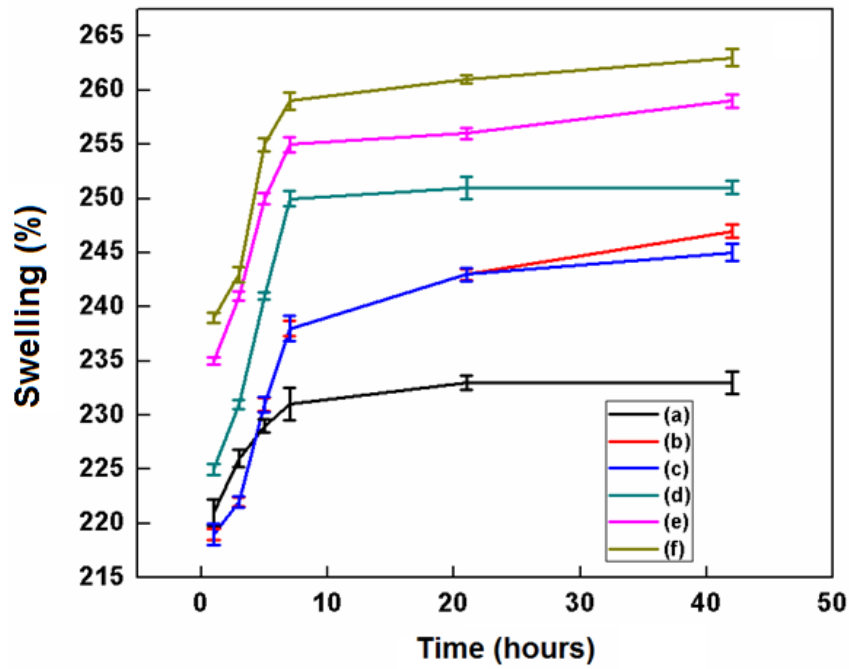


Figure 5.32: Swelling behaviour of (a) SF/CS (80:20) (b) SF/CS/Glu (1%) (c) SF/CS/Chs (0.8%) and SF/CS/Glu/Chs scaffolds with (d) 0.5 (e) 1 (f) 1.5 % (w/v) of Chs respectively. All the scaffolds showed an initial increase in swelling during the first few hrs but the swelling equilibrium was achieved after 10 hrs of SBF treatment.

Table 5.8: Contact angle of SF/CS/Glu/Chs scaffolds

Sample	Contact angle(degree)
SF/CS/Glu (1)	49.5±0.8
SF/CS/Glu/Chs (0.5)	46.7±0.1
SF/CS/Glu/Chs (1)	46.1±0.8
SF/CS/Glu/Chs (1.5)	45.5±0.8

5.4.5 In vitro degradation

The in-vitro degradation pattern of SF/CS/Glu/Chs scaffolds is depicted in figure 5.33. All the scaffolds degraded faster initially but reached a steady state of degradation after 7 days onwards. Glu and Chs in combination provided better scaffold degradation in comparison to the other scaffold groups. The SF/CS/Glu/Chs scaffolds showed faster degradation (57%) than the SF/CS/Chs (73%), the SF/CS/Glu (71%) and SF/CS (87.9%) scaffolds. However, scaffolds with Chs concentration of 1.5 % (w/v) showed the maximum degradation of 57%, followed by 61 and 67 % mass remaining with 1 and 0.5 % (w/v) respectively. Increase in degradation rate may be due to the increase in hydrophilic groups in the scaffold material with increase in Chs concentration. Overall, the trend of degradation is SF/CS/Glu/Chs > SF/CS/Chs > SF/CS/Glu > SF/CS.

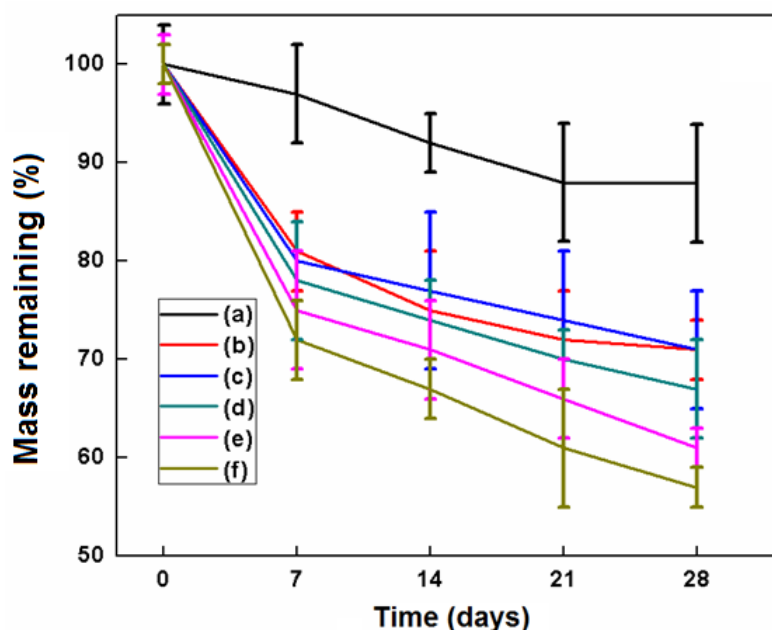


Figure 5.33: Degradation pattern of (a) SF/CS (80:20) (b) SF/CS/Glu (1%) (c) SF/CS/Chs (0.8%) and SF/CS/Glu/Chs scaffolds with (d) 0.5, (e) 1 & (f) 1.5 % (w/v) of Chs respectively. The degradation of SF/CS/Glu/Chs among the group with varied Chs content increased with increase in Chs content.

5.4.6 Compressive strength

The compressive strength of the SF/CS/Glu/Chs scaffolds with 0.5, 1 and 1.5 % (w/v) Chs were determined as 200 ± 12 , 200 ± 10 and 201 ± 11 kPa respectively. Though the addition of Chs to SF/CS scaffold increased the compressive strength, the variation in strength between the varied Chs content in the study range is not statistically significant. More importantly, the addition of Chs and Glu in combination did not hamper the mechanical integrity of the scaffold.

5.4.7 In vitro cell culture

Cell attachment and morphology

Scaffolds prepared with the combination of Glu and Chs showed a overall higher cell adhesion in comparison to the other scaffold groups namely SF/CS, SF/CS/Glu and SF/CS/Chs scaffolds as depicted from FESEM images in figure 5.34. This overall increase in cell adhesion is due to the synergistic effect of both Glu and Chs. The cells were found to attach well on the surface as well as inside the pores of the scaffolds.

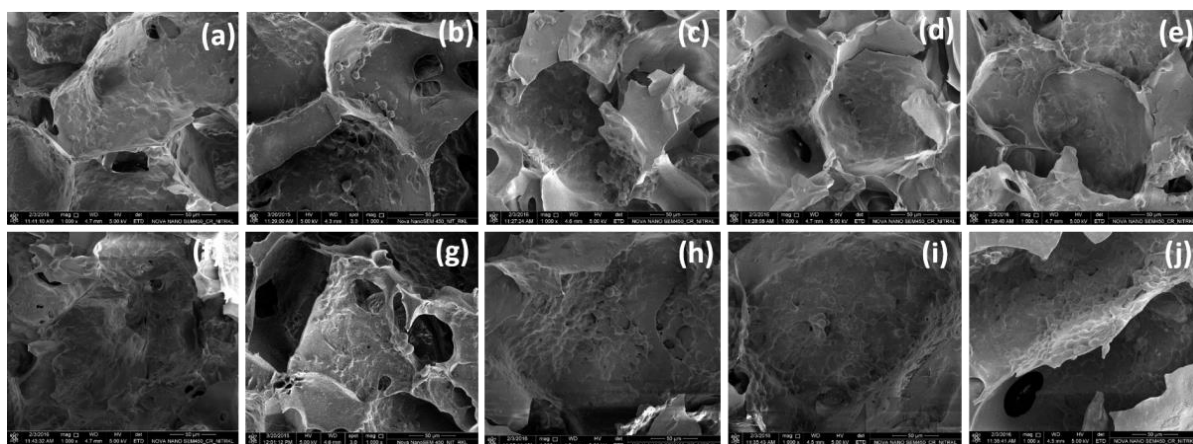


Figure 5.34: FE-SEM images of SF/CS/Glu/Chs scaffolds. (a) & (f) SF/CS(80:20), (b) & (g) SF/CS/Glu with 1% (w/v) of Glu, (c) & (h) SF/CS/Glu/Chs 0.5 % (w/v), (d) & (i) SF/CS/Glu / Chs 1 % (w/v), (e) & (j) SF/CS/Glu/Chs 1.5 % (w/v) scaffolds after 7 & 14 days of culture. The cells are found to attach well on the surface and also inside the pores of the scaffold.

Cellular activity by MTT assay

The cellular viability of the SF/CS/Glu/Chs scaffolds along with other scaffold groups was evaluated quantitatively by MTT assay as shown in figure 5.35. An increase in metabolic activity with culture period is evident with all the scaffolds with a varied degree of metabolic activity. However, SF/CS/Glu/Chs scaffolds showed better metabolic activity (2.3 ± 0.05) than the SF/CS/Chs (1.73 ± 0.03), SF/CS/Glu (2.15 ± 0.03) and SF/CS (1.67 ± 0.07) scaffolds. Between the various compositions prepared, SF/CS/Glu/Chs scaffolds with 0.5, 1 and 1.5 % (w/v) Chs showed O.D. values of 2.3 ± 0.05 , 2.25 ± 0.07 and 2.2 ± 0.07 respectively. This increase in metabolic activity can be explained on the basis of the combined beneficial effects of Glu and Chs than their addition to SF/CS scaffolds individually. Both these components possess cell attachment motifs [24] which have enhanced the metabolic activity of the cells.

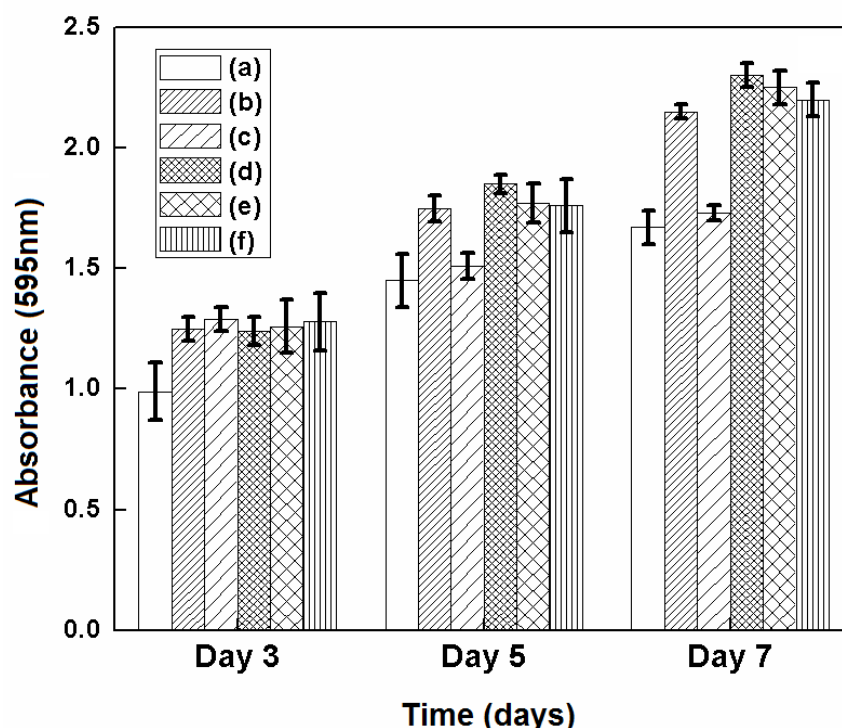


Figure 5.35: MTT assay of (a) SF/CS (80:20), (b) SF/CS/Glu (1%) (c) SF/CS/Chs (0.8%) and SF/CS/Glu (1%) with (d) 0.5, (e) 1 and (f) 1.5% (w/v) of Chs scaffolds. An increase in metabolic activity with culture period is evident with all the scaffolds with a varied degree of metabolic activity.

Cellular proliferation by DNA quantification

The cell proliferation was assessed by measuring the DNA content of the scaffolds. Figure 5.36 shows an increase in DNA content with progress of culture in all the developed scaffolds with a varying degree of DNA content. Among the scaffolds, SF/CS/Glu/Chs scaffolds showed a higher DNA content of 380 ng/ml over a period of 21 days compared to SF/CS/Chs (355 ng/ml), SF/CS/Glu (349 ng/ml) and SF/CS (80:20) scaffolds (299 ng/ml) representing an enhanced proliferation rate of hMSCs particularly over SF/CS scaffold containing both Glu and Chs. The increase in proliferation rate is attributed to the presence of more cell recognition binding sites or specific peptides on the surface of scaffold matrices due to the presence of Glu and Chs in combination which has enhanced the cell - polymer interactions.

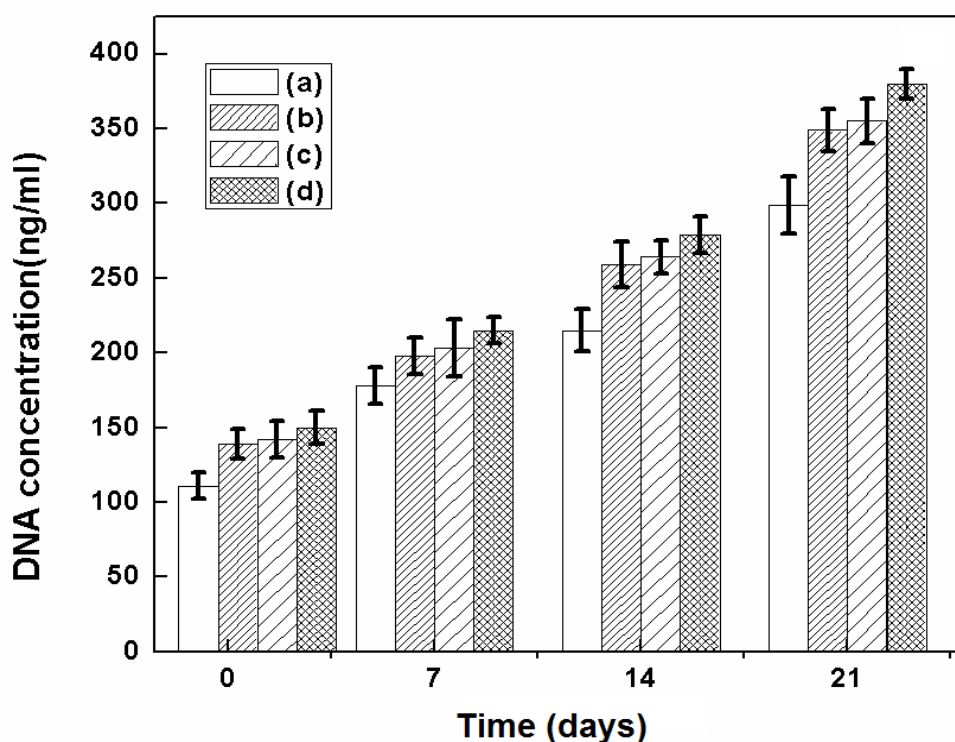


Figure 5.36: DNA quantification of (a) SF/CS(80:20) , (b) SF/CS/Glu (1%) , (c) SF/CS/Chs (0.8%), (d) Glu/Chs 0.5(% w/v) scaffolds. DNA content was found to increase in the SF/CS/Glu/Chs scaffold than the other developed scaffolds.

Cytoskeletal analysis by confocal microscopy

The enhanced distribution of hMSCs on the SF/CS/Glu/Chs scaffolds is depicted from the confocal images as shown in figure 5.37. Cells were found to be well attached and spread throughout the scaffolds in comparison with the other scaffolds. Furthermore, a significant population of cells were found to penetrate inside the scaffold pores representing better cell-material interaction than the SF/CS/Glu, SF/CS/Chs and SF/CS scaffolds.

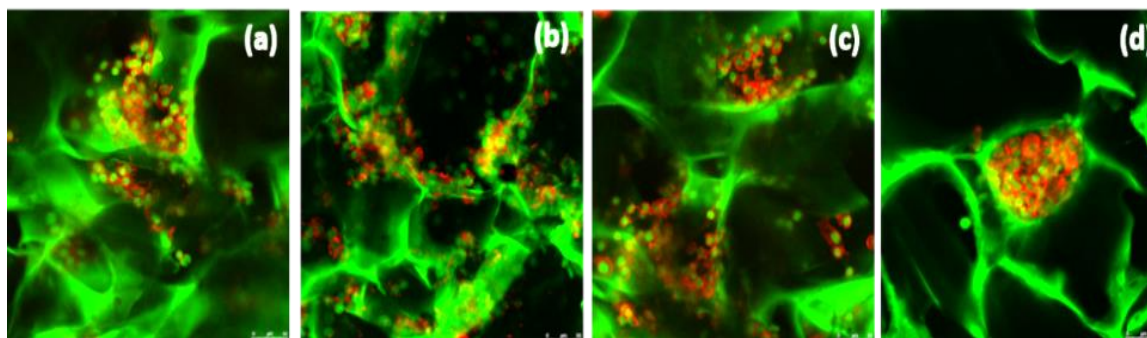


Figure 5.37: Confocal microscopy images (a) SF/CS (80:20), (b) SF/CS/Glu (1%), (c) SF/CS/Chs (0.8%), (d) Glu/Chs 0.5 (%w/v) scaffolds. after 7 days of culture. Significant cell population was observed in the SF/CS/Glu/Chs scaffolds.

GAG assay

GAG secretion was found to increase in all the scaffold groups with incubation time, as shown in figure 5.38. A significantly higher GAG secretion of $27\mu\text{g}/\text{mg}$ was achieved with SF/CS/Glu/Chs scaffold than the SF/CS (80:20) blend ($18\mu\text{g}/\text{mg}$), SF/CS/Glu ($21\mu\text{g}/\text{mg}$), SF/CS/Chs scaffolds ($23\mu\text{g}/\text{mg}$) respectively. In the initial culture period of 7 days, the scaffolds with Glu and Chs in combination showed higher GAG secretion than the other scaffolds groups. With increase in culture time from 7 to 21 days, a gradual steady increase in GAG secretion was observed in the SF/CS/Glu/Chs scaffolds. The existence of Glu, which is a precursor for GAG synthesis [24] and Chs which is an important GAG component has enhanced the GAG secretion of the scaffolds[21]. Moreover, since Chs enhances differentiation and matrix production, the synergistic effect of Glu with Chs has enabled hMSCs seeded on the scaffold to produce more GAG [80].

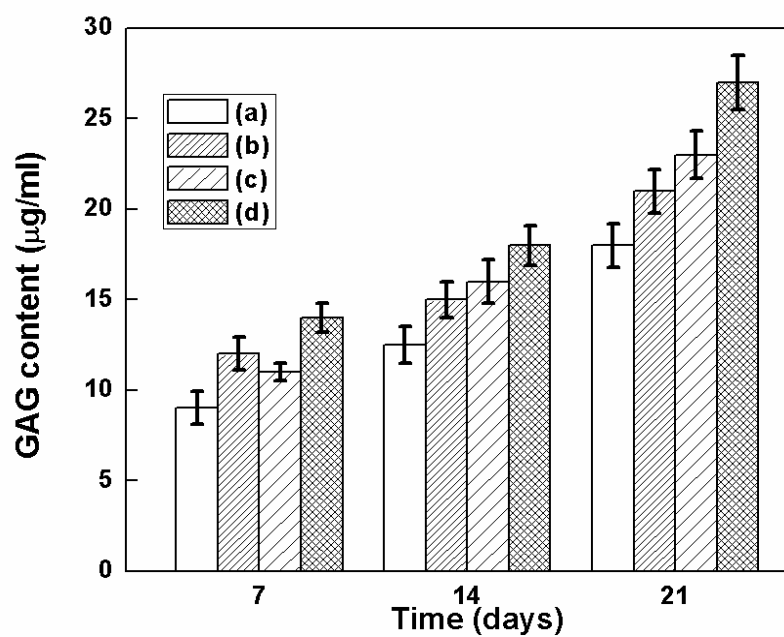


Figure 5.38: GAG analysis on (a) SF/CS (80:20), (b) SF/CS/Glu 1%(w/v) , (c) SF/CS/Chs 0.8%(w/v) and (d) SF/CS/Glu/Chs 0.5% (w/v) scaffolds. The presence of Glu & Chs in the SF/CS scaffold significantly increase the GAG secretion over culture period.

Chapter 6

Summary and Conclusion

Damaged and/or diseased cartilage tissue due to injury and degeneration are of frequent phenomena in medical field. Current clinical methods of cartilage repair or replacements often fail to provide long lasting and complete recovery. As a consequence, the patient can't restore normal cartilage function and thereby pain continues. In this context, tissue engineering offers a promising approach to repair and/or replacement of defect or disease providing restoration of normal cartilage function.

In tissue engineering, the design and fabrication of 3D scaffold from a suitable biomaterial is one of the key challenges. Though in the last decade, a variety of biomaterials have been explored for the development of scaffold targeting cartilage tissue regeneration, but not a single biomaterial is able to satisfy all desired scaffold properties which opens up further research in this area. SF and CS are the attractive biopolymers though they have their own limitation which restricts their use in tissue engineering. However, recently, the combination of SF/CS biopolymers thereby resulted in SF/CS blend scaffold with superior properties has been reported. However, these studies were limited to the use of a specific ratio of SF/CS with the aim of exploring the suitability of the blend as scaffold material. Therefore, a systematic research effort is necessary to develop scaffold from SF/CS blend to make it potential for cartilage tissue regeneration.

Keeping the above in view, the present research work aims to investigate the influence of different blend ratio of SF/CS on the scaffold properties to establish the most favourable blend ratio and further improvement of the properties of the SF/CS blend scaffold to facilitate cartilage tissue regeneration. The most interesting results obtained are described here.

- I. In the first phase of thesis work, different batches of 3D porous SF/CS scaffolds with varying blend ratios were prepared by freeze drying method. Among the scaffolds, SF/CS with 80:20 (v/v) was found to be the most favourable blend ratio. The scaffold possess open pore microstructures with interconnecting network of pores with desired pore size (71-201 μ m, porosity (82.2%) and compressive strength (190 kPa). The developed SF/CS scaffold was evaluated for its cell supportive property by in-vitro cell culture study using mesenchymal stem cells (MSCs) that were derived from umbilical cord blood. The scaffold was shown to provide suitable microenvironment for cell

attachment (SEM study) and cell proliferation (live dead assay) and metabolic activity (MTT assay). The differentiation ability of the scaffold towards cartilage specific ECM synthesis was indicated by the estimation of GAG by culturing hMSCs over the scaffold in chondrogenic media. Thus it has been established that the developed SF/CS (80:20) scaffold can be used as a potential artificial extracellular platform for cartilage tissue engineering applications.

- II. In this phase, the research was directed to improve the cell binding affinity and cartilage specific ECM formation ability of the SF/CS (80:20) scaffold by the incorporation of Glu as a precursor of GAG synthesis that resulted in SF/CS/Glu hybrid scaffold. Among the various compositions, SF/CS/Glu containing 1% of Glu was obtained as the most favourable composition that provided enhanced swelling (245%) and hydrophilicity (contact angle 49.5°) properties thereby exhibiting superior cell adhesion and cell proliferation. The scaffold was found to be superior to SF/CS scaffold in terms of cell supportive property. The addition of Glu further resulted in increased GAG synthesis ($21 \mu\text{g/ml}$), as observed during 21 days of culture in chondrogenic media indicating the enhanced chondrogenic specific ECM formation ability of scaffold.
- III. Chs is an important component of ECM. The addition of Chs to the scaffold favor cell adhesion, cell proliferation in chondrocyte cultures and ECM formation. Therefore, in this phase, efforts has been given to improve the above properties of the SF/CS scaffold by the addition of Chs. Among the various compositions, SF/CS with 0.8% Chs was the most favourable. The scaffold possess superior scaffold property than SF/CS scaffold. In comparison to SF/CS/Glu, SF/CS/Chs has shown a slightly higher cell proliferation and GAG secretion ($23 \mu\text{g/ml}$) ability. Therefore the scaffold is proven to promote cellular differentiation leading to ECM formation.
- IV. The synergistic effects of glucosamine sulfate and chondroitin sulfate towards cartilage regeneration has been reported by many reaserchers as they have been utilized for cartilage repair. Therefore, attempts have been made to investigate the effect of the addition of Glu and Chs by adding 0.5, 1 and 1.5% Chsin combination on the properties of SF/CS scaffold. To this end, SF/CS/Glu/Chs of different compositions were

prepared. Among these, SF/CS/Glu containing 0.5 % Chs was found to be best possessing superior hydrophilicity, cell adhesion, cell proliferation and cartilage specific ECM formation through GAG secretion (27 $\mu\text{g/ml}$) in comparison to other developed scaffolds.

Overall, in this study a novel 3D porous SF/CS/ blend scaffold has been developed which can be used as a base polymeric scaffold for various cartilage tissue engineering applications. The cell affinity and GAG secretion property of the SF/CS scaffolds were further improved by the addition of Glu and Chs individually. Furthermore, cell proliferation and secretion of cartilage specific ECM has been enhanced by the addition of Glu and Chs in combination. Therefore, it has been demonstrated in this dissertation work that the developed SF/CS based porous scaffolds, SF/CS/Glu/Chs in particular can serve as a potential artificial extra cellular scaffold matrix for cartilage tissue regeneration in future.

Suggested future work

The future studies are essential in analyzing the various differentiation studies using the developed scaffolds and optimizing the various parameters. Also, cell scaffold construct studies using a bioreactor can enable to monitor the potentiality of the scaffold. In vivo studies using a suitable animal model is important to understand the in vivo biocompatibility of the scaffolds.

References

1. X.Vial, and F.M. Andreopoulos, "Novel biomaterials for cartilage tissue engineering". *Curr Rheumatol Rev*, vol.5, no.1, pp.51-57, 2009.
2. C.Vinatier, C.Bouffi, C.Merceron, J.Gordeladze, J.M. Brondello, C.Jorgensen, P.Weiss, J.Guicheux, and D.Noël, "Cartilage tissue engineering: towards a biomaterial-assisted mesenchymal stem cell therapy", *Curr Stem Cell Res Ther*, vol.4, no.4, p.318, 2009.
3. L.Kock, C.C.van Donkelaar, and K.Ito, "Tissue engineering of functional articular cartilage: the current status", *Cell Tissue Res*, vol.347, no.3, pp.613-627, 2012.
4. J.A.Buckwalter and H.J. Mankin, "Articular cartilage: degeneration and osteoarthritis, repair, regeneration, and transplantation", *Instr Course Lect*, vol.47, pp.487-504, 1997.
5. J.Iwasa, L.Engelbretsen, Y.Shima and M.Ochi, "Clinical application of scaffolds for cartilage tissue engineering", *Knee Surg Sports Traumatol Arthrosc*, vol.17, no.6, pp.561-577, 2009.
6. D. Rana, T.S.Kumar and M. Ramalingam, "Cell-laden hydrogels for tissue engineering", *J Biomater Tissue Eng*, vol.4, no.7, pp.507-535, 2014.
7. U.A.Stock, and J.P.Vacanti, "Tissue engineering: current state and prospects", *Annu. Rev. Med*, vol.52, no.1, pp.443-451, 2001.
8. J.Melrose, C.Chuang, and J.Whitelock, "Tissue engineering of cartilages using biomatrices", *J. Chem.Technol, Biotechnol*, vol.83, no.4, pp.444-463, 2008.
9. S.N.Redman, S.F.Oldfield, and C.W.Archer,"Current strategies for articular cartilage repair", *Eur Cell Mater*, vol.9, no.23-32, pp.23-32, 2005.
10. L.E.Freed, G.C.Engelmayr, J.T.Borenstein, F.T.Moutos, and F.Guilak, "Advanced material strategies for tissue engineering scaffolds", *Adv Mater*, vol.21, no.32-33, pp.3410-3418, 2009.
11. J.Thiele, Y. Ma, S. Bruekers, S. Ma and W.T. Huck, "Designer hydrogels for cell cultures: a materials selection guide", *Adv Mater*, vol.26, no.1, pp.125-148, 2014.
12. R.Lanza, R.Langer, and J.P.Vacanti, eds, *Principles of tissue engineering*. Academic press, 2011.
13. R.A.Pérez, J.E.Won, J.C.Knowles, and H.W.Kim, "Naturally and synthetic smart composite biomaterials for tissue regeneration", *Adv Drug Deliver Rev*, vol.65, no.4, pp.471-496, 2013.
14. D. Puppi, F. Chiellini, A. M. Piras, and E. Chiellini. "Polymeric materials for bone and cartilage repair", *Prog. Polym. Sci*, vol.35, no. 4, pp. 403-440, 2010.
15. Z.She, B.Zhang, C.Jin, Q.Feng, and Y Xu, "Preparation and in vitro degradation of porous three-dimensional silk fibroin/chitosan scaffold", *Polym Degrad Stabil*, vol.93, no.7, pp.1316-1322, 2008.

16. N.Bhardwaj and S.C.Kundu, "Silk fibroin protein and chitosan polyelectrolyte complex porous scaffolds for tissue engineering applications", *Carbohydr Polym*, vol.85, no.2, pp.325-333, 2011.
17. Z.D.She, W.Q.Liu, and Q.L.Feng, "Preparation and cytocompatibility of silk fibroin/chitosan scaffolds", *Fr.Mater. Sci.China*, vol.3, no.3, pp.241-247, 2009.
18. H.Kweon, H. C.Ha, I. C. Um, & Y. H. Park, "Physical properties of silk fibroin/chitosan blend films", *J.App.polym. sci*, vol.80, no.7, pp.928-934, 2001.
19. M.Zang, Q.Zhang, G.Davis, G.Huang, M.Jaffari, C.N.Ríos, and A.B.Mathur, "Perichondrium directed cartilage formation in silk fibroin and chitosan blend scaffolds for tracheal transplantation", *Acta biomater*, vol.7, no.9, pp.3422-3431, 2011.
20. H.Suo, K.Xu, and X.Zheng. "Using glucosamine to improve the properties of photocrosslinked gelatin scaffolds", *J Biomater Appl*, vol.29, no.7, pp. 977-987, 2015.
21. H. J.Kwon and Y.Han. "Chondroitin sulfate-based biomaterials for tissue engineering", *Turkish J. Biol.*, vol.40, no.2, pp. 290-299, 2016.
22. J.Monfort, J.P.Pelletier, N.Garcia-Giralt, and J.Martel-Pelletier, "Biochemical basis of the effect of chondroitin sulphate on osteoarthritis articular tissues", *Ann. Rheum. Dis*, vol.67, no.6, pp.735-740, 2008.
23. M.Naeimi, M.Fathi, M.Rafienia and S.Bonakdar. "Silk fibroin-chondroitin sulfate-alginate porous scaffolds: Structural properties and in vitro studies", *J. Appl. Polym. Sci.*, vol.131, no.21, 2014.
24. J.Jerosch. "Effects of glucosamine and chondroitin sulfate on cartilage metabolism in OA: outlook on other nutrient partners especially omega-3 fatty acids", *Int J Rheumatol*, vol.2011, 2011.
25. C.Bottegoni, R.A.Muzzarelli, F.Giovannini, A.Busilacchi and A.Gigante. "Oral chondroprotection with nutraceuticals made of chondroitin sulphate plus glucosamine sulphate in osteoarthritis", *Carbohydr Polym*, vol.109, pp. 126-138, 2014.
26. S.P.Messier, S.Mihalko, F.Richard, R.F.Loesser, C.Legault, J.Jolla, J.Pfruender, B. Prosser, A.Adrian and J.D.Williamson. "Glucosamine/chondroitin combined with exercise for the treatment of knee osteoarthritis: a preliminary study", *Osteoarthr. Cartil.*, vol.15, no.11, pp. 1256-1266, 2007.
27. S.Gregory, N.D.Kelly. "The role of glucosamine sulfate and chondroitin sulfates in the treatment of degenerative joint disease" *Altern Med Rev.*, vol.3, no.1, pp. 27-39, 1998.
28. N.Bhardwaj and S.C.Kundu, "Chondrogenic differentiation of rat MSCs on porous scaffolds of silk fibroin/chitosan blends", *Biomaterials*, vol.33, no.10, pp. 2848-2857, 2012.
29. A.M.Altman, Y.Yan, N.Matthias, X.Bai, C.Rios and A.B.Mathur, "Human Adipose-Derived Stem Cells Seeded on a Silk Fibroin-Chitosan Scaffold Enhance Wound Repair in a Murine Soft Tissue Injury Model", *Stem Cells*, vol.27, no.1, pp.250-258, 2009.
30. A.M.Altman, V.Gupta, C.N.Ríos and A.B.Mathur, "Adhesion, migration and mechanics of human adipose-tissue-derived stem cells on silk fibroin-chitosan matrix", *Acta Biomater*, vol.6, no.4, pp.1388-1397, 2010.

31. N.Panda, A.Bissoyi, K.Pramanik, and A.Biswas, "Directing osteogenesis of stem cells with hydroxyapatite precipitated electrospun eri-tasar silk fibroin nanofibrous scaffold". *J.Biomat.Sci, Polym Ed*, vol. 25, no.13, pp.1440-1457, 2014.
32. N.Panda, A.Bissoyi, K.Pramanik, and A.Biswas, "Development of novel electrospun nanofibrous scaffold from P. ricini and A. mylitta silk fibroin blend with improved surface and biological properties" , *Mater. Sci.Engg C.*, vol.48, pp.521-532, 2015.
33. K.Bieback, S.Kern, H.Klüter, and H.Eichler, "Critical parameters for the isolation of mesenchymal stem cells from umbilical cord blood", *Stem cells*, vol.22, no.4, pp.625-634, 2004.
34. N.K.Mekala, R.R.Baadhe, S.R.Parcha, and D.Y.Prameela, "Osteoblast differentiation of umbilical cord blood-derived mesenchymal stem cells and enhanced cell adhesion by fibronectin", *Tissue Eng. Reg. Med.*, vol 9, no.5, pp.259-264, 2012.
35. S.H.Hwang, E.S.Son, Y.J.Park, C.S.Lee, and H.J.Chun, "Effect of cultured medium of human umbilical cord blood-derived mesenchymal stem cells on melanogenic enzyme activity in mouse B16 melanoma cells", *Tissue Eng. Reg. Med.*, vol.11, no.5, pp.414-422, 2014.
36. B.P.Chan, and K.W.Leong. "Scaffolding in tissue engineering: general approaches and tissue-specific considerations", *Eur Spine J*, vol.17, no.4, pp. 467-479, 2008.
37. W.M.Huang, C.L.Song, Y.Q. Fu, C.C Wang, Y.Zhao, H.Purnawali, H.B.Lu, C.Tang, Z.Ding, and J.L.Zhang. "Shaping tissue with shape memory materials." *Adv Drug Deliver Rev*, vol. 65, no. 4, pp.515-535, 2013.
38. P.X.Ma, and R.Langer, "Fabrication of biodegradable polymer foams for cell transplantation and tissue engineering". *Tissue engineering methods and protocols*. Springer, 1999.
39. D.W.Hutmacher, "Scaffolds in tissue engineering bone and cartilage", *Biomaterials*, vol.21, no.24, pp.2529-2543, 2000.
40. S.Sundelacruz, and D.L.Kaplan, "Stem cell-and scaffold-based tissue engineering approaches to osteochondral regenerative medicine", *Sem Cell Dev Biol*, vol. 20, no. 6, pp. 646-655, 2009.
41. B.M.Holzappel, J.C.Reichert, J.T.Schantz, U.Gbureck, L.Rackwitz, U.Nöth, F.Jakob, M.Rudert, J.Groll, and D.W.Hutmacher, "How smart do biomaterials need to be? A translational science and clinical point of view", *Adv Drug Deliver Rev*, vol.65, no.4, pp.581-603, 2013.
42. S.K.Grad, S.Gorna, S.Gogolewski, and M.Alini, "Scaffolds for cartilage tissue engineering: effect of pore size", *Eur Cells Mater*, vol 7, no.1, pp.1-3, 2004.
43. A.R.Amini, C.T.Laurencin, and S.P.Nukavarapu, "Bone tissue engineering: recent advances and challenges", *Crit Rev Biomed Eng*, vol.40, no.5, pp.363-408, 2012.
44. K.Numata, and D.L.Kaplan, "Silk-based delivery systems of bioactive molecules", *Adv Drug Deliver Rev*, vol.62, no.15, pp.1497-1508, 2010.

45. H. Park, J.S.Temenoff, T.A.Holland, Y.Tabata, and A.G.Mikos, "Delivery of TGF- β 1 and chondrocytes via injectable, biodegradable hydrogels for cartilage tissue engineering applications", *Biomaterials*, vol.26, no.34, pp.7095-7103, 2005.
46. Z.M.Huang, Y.Z.Zhang, M.Kotaki, and S.Ramakrishna, "A review on polymer nanofibers by electrospinning and their applications in nanocomposites", *Compos. Sci. Technol.* vol.63, no.15, pp.2223-2253, 2003.
47. N.Bhardwaj, and S.C.Kundu, "Electrospinning: a fascinating fiber fabrication technique", *Biotechnol. Adv.*, vol.28, no.3, pp.325-347, 2010.
48. L.A.Smith, and P.X.Ma, "Nano-fibrous scaffolds for tissue engineering", *Colloids Surf B Biointerfaces*, vol.39, no.3, pp.125-131, 2004.
49. Y.S.Nam, and T.G.Park, "Porous biodegradable polymeric scaffolds prepared by thermally induced phase separation", *J Biomed Mater Res A*, vol.47, no.1, pp.8-17, 1999.
50. A.G.Mikos, and J.S.Temenoff, "Formation of highly porous biodegradable scaffolds for tissue engineering", *Electron J Biotechnol*, vol.3, no.2, pp.23-24, 2000.
51. X.Wu, Y.Liu, X.Li, P.Wen, Y.Zhang, Y.Long, X.Wang, Y.Guo, F Xing, and J.Gao. "Preparation of aligned porous gelatin scaffolds by unidirectional freeze-drying method." *Acta Biomater*, vol.6, no.3, pp.1167-1177, 2010.
52. G.Chen, and W.Wang, "Role of freeze drying in nanotechnology", *Drying Technol*, vol.25, no.1, pp.29-35, 2007.
53. F.J.O'Brien, B.A.Harley, I.V.Yannas, and L.Gibson, "Influence of freezing rate on pore structure in freeze-dried collagen-GAG scaffolds", *Biomaterials*, vol.25, no.6, pp.1077-1086, 2004.
54. L.Qian, and H.Zhang, "Controlled freezing and freeze drying: a versatile route for porous and micro-/nano-structured materials", *J. Chem. Technol. Biotechnol*, vol.86, no.2, pp.172-184, 2011.
55. L.Wu, D.Jing, and J.Ding, "A room-temperature injection molding/particulate leaching approach for fabrication of biodegradable three-dimensional porous scaffolds", *Biomaterials*, vol.27, no.2, pp.185-191, 2006.
56. S.Yang, K.F.Leong, Z.Du, and C.K.Chua, "The design of scaffolds for use in tissue engineering: Part I. Traditional factors", *Tissue engg*, vol.7, no. 6, pp.679-689, 2001.
57. E.Sachlos, and J.T.Czernuszka. "Making tissue engineering scaffolds work. Review: the application of solid freeform fabrication technology to the production of tissue engineering scaffolds." *Eur Cell Mater*, vol. 5, no. 29, pp. 39-40, 2003.
58. D.W.Hutmacher, M.Sittinger, and M.V.Risbud, "Scaffold-based tissue engineering: rationale for computer-aided design and solid free-form fabrication systems", *Trends Biotechnol*, vol.22, no.7, pp.354-362, 2004.
59. S.Hofmann, S.Knecht, R.Langer, D.L.Kaplan, G.Vunjak-Novakovic, H.P.Merkle, and L.Meinel, "Cartilage-like tissue engineering using silk scaffolds and mesenchymal stem cells", *Tissue eng*, vol.12, no.10, pp.2729-2738, 2006.

60. Y.Wang, U.J.Kim, D.J.Biasioli, H.J.Kim, and D.L.Kaplan, "In vitro cartilage tissue engineering with 3D porous aqueous-derived silk scaffolds and mesenchymal stem cells", *Biomaterials*, vol.26, no.34, pp.7082-7094, 2005.
61. G.Portocarrero, G.Collins, and T. Livingston Arinzeh, "Challenges in cartilage tissue engineering", *J Tissue Sci Eng*, vol.4, no.1, pp.1-2, 2013.
62. A.M.Bhosale, and J.B.Richardson, "Articular cartilage: structure, injuries and review of management", *Br Med Bull*, vol.87, no.1, pp.77-95, 2008.
63. M.Peter, N.Ganesh, N.Selvamurugan, S.V.Nair, T.Furuike, H. Tamura, and R.Jayakumar, "Preparation and characterization of chitosan–gelatin/nanohydroxyapatite composite scaffolds for tissue engineering applications", *Carbohydr. Polym*, vol.80, no.3, pp.687-694, 2010.
64. B.S.Anisha, D.Sankar, A.Mohandas, K.P.Chennazhi, S.V.Nair and R.Jayakumar, "Chitosan–hyaluronan/nano chondroitin sulfate ternary composite sponges for medical use", *Carbohydr. Polym*, vol.92, no.2, pp.1470-1476, 2013.
65. D.Eyrich, H.Wiese, G.Maier, D. Skodacek, B.Appel, H.Sarhan, J.Tessmar, R.Staudenmaier, M.M. Wenzel, A.Goepferich, and, T. Blunk, "In vitro and in vivo cartilage engineering using a combination of chondrocyte-seeded long-term stable fibrin gels and polycaprolactone-based polyurethane scaffolds", *Tissue eng*, vol.13, no.9, pp.2207-2218, 2007.
66. A. A.Hegewald, J. Ringe, J. Bartel, I. Krüger, M. Notter, D. Barnewitz, C. Kaps, and M. Sittinger. "Hyaluronic acid and autologous synovial fluid induce chondrogenic differentiation of equine mesenchymal stem cells: a preliminary study", *Tissue Cell*, vol.36, no. 6, pp. 431-438, 2004.
67. J.F. Mano, G.A. Silva, H.S. Azevedo, P.B. Malafaya, R.A. Sousa, S.S. Silva, L.F. Boesel, J.M. Oliveira, T.C. Santos, A.P. Marques, and N.M. Neves, "Natural origin biodegradable systems in tissue engineering and regenerative medicine: present status and some moving trends", *J. R. Soc. Interface*, vol.4, no.17, pp.999-1030, 2007.
68. J.G. Hardy, and T.R. Scheibel, "Composite materials based on silk proteins", *Prog. Polym. Sci*, vol.35, no.9, pp.1093-1115, 2010.
69. R.Nazarov, H.J. Jin, and D.L.Kaplan, "Porous 3-D scaffolds from regenerated silk fibroin", *Biomacromolecules*, vol.5, no.3, pp.718-726, 2004.
70. A.S.Gobin, V.E.Froude and A.B.Mathur, "Structural and mechanical characteristics of silk fibroin and chitosan blend scaffolds for tissue regeneration", *J Biomed Mater Res A*, vol.74, no.3, pp.465-473, 2005.
71. A.Leal-Egaña, and T.Scheibel, "Silk-based materials for biomedical applications", *Biotech Appl Biochem*, vol.55, no.3, pp.155-167, 2010.
72. C.Vepari, and D.L.Kaplan, "Silk as a biomaterial", *Prog. Polym. Sci*, vol.32, no.8, pp.991-1007, 2007.
73. S.Lu, X.Wang, Q.Lu, X.Hu, N.Uppal, F.G.Omenetto, and D.L.Kaplan, "Stabilization of enzymes in silk films", *Biomacromolecules*, vol.10, no.5, pp.1032-1042, 2009.

74. M.K.Gupta, S.K.Khokhar, D.M.Phillips, L.A.Sowards, L.F.Drummy, M.P.Kadokia, and R.R. Naik, "Patterned silk films cast from ionic liquid solubilized fibroin as scaffolds for cell growth", *Langmuir*, vol.23, no.3, pp.1315-1319, 2007.
75. E.S.Sashina, A.M.Bochek, N.P.Novoselov, and D.A.Kirichenko. "Structure and solubility of natural silk fibroin." *Russ J Appl Chem*, vol. 79, no. 6, pp. 869-876, 2006.
76. S.E.Kim, J.H.Park, Y.W.Cho, H.Chung, S.Y.Jeong, E.B. Lee, and I.C.Kwon, "Porous chitosan scaffold containing microspheres loaded with transforming growth factor- β 1: implications for cartilage tissue engineering", *J. Control. Release*, vol. 91, no.3, pp.365-374, 2003.
77. J.P.Chen, S.H.Chen, and G.J.Lai, "Preparation and characterization of biomimetic silk fibroin/chitosan composite nanofibers by electrospinning for osteoblasts culture", *Nano. Res. Ltr*, vol. 7, no.1, pp.1-11, 2012.
78. W.Luangbudnark, J.Viyoch, W.Laupattarakasem, P.Surakunprapha, and P.Laupattarakasem, "Properties and biocompatibility of chitosan and silk fibroin blend films for application in skin tissue engineering", *Sci World J*, 2012.
79. P.K.Dutta, P.Kumar, J.Dutta, and V.S.Tripathi, "Chitin and chitosan: Chemistry, properties and applications", *J. scientific industrial res*, vol 63, no. 1, pp.20-31, 2004.
80. D.L.Nettles, S.H.Elder, and J.A.Gilbert, "Potential use of chitosan as a cell scaffold material for cartilage tissue engineering", *Tissue engg*, vol.8, no.6, pp.1009-1016, 2002.
81. S.Varghese, N.S.Hwang, A.C.Canver, P.Theprungsirikul, D.W.Lin, & J.Elisseff, "Chondroitin sulfate based niches for chondrogenic differentiation of mesenchymal stem cells", *Matrix.biol*, vol.27, no.1, pp. 12-21, 2008
82. C.G. Jackson, I.Wolinsky and J.A.Driskell, "Glucosamine and chondroitin sulphate", *Nutr.ergo. aids*, pp.115-27, 2004.
83. S.Deepthi, C.V.Viha, C.Thitirat, T.Furuike, H.Tamura, and R.Jayakumar, "Fabrication of chitin/poly (butylene succinate)/chondroitin sulfate nanoparticles ternary composite hydrogel scaffold for skin tissue engineering", *Polymers*, vol.6, no.12, pp.2974-2984, 2014.
84. I.S.Yeo, J.E.Oh, L.Jeong, T.S.Lee, S.J.Lee, W.H.Park, and B.M.Min, "Collagen-based biomimetic nanofibrous scaffolds: preparation and characterization of collagen/silk fibroin bicomponent nanofibrous structures", *Biomacromolecules*, vol.9, no.4, pp.1106-1116, 2008.
85. L.Zheng, H.Q.Lu, H.S.Fan, and X.D.Zhang, "Reinforcement and chemical cross-linking in collagen-based scaffolds in cartilage tissue engineering: a comparative study", *Iran Poly J.*, vol.22, no.11, pp.833-842, 2013.
86. G.E.Luckachan, and C.K.S.Pillai, "Biodegradable polymers-a review on recent trends and emerging perspectives", *J Polym Environ*, vol.19, no.3, pp.637-676, 2011.
87. D.Eyrich, H.Wiese, G.Maier, D.Skodacek, B.Appel, H.Sarhan, J.Tessmar, R.Staudenmaier, M.M. Wenzel, A.Goepferich, and, T. Blunk, "In vitro and in vivo cartilage engineering using a combination of chondrocyte-seeded long-term stable fibrin gels and polycaprolactone-based polyurethane scaffolds", *Tissue eng*, vol.13, no.9, pp.2207-2218, 2007.

88. K.Y.Chang, L.H.Hung, I.Chu, C.S.Ko, and Y.D.Lee, "The application of type II collagen and chondroitin sulfate grafted PCL porous scaffold in cartilage tissue engineering", *J.Biomed.Mat.Res Part A*, vol.92,no.2,pp.712-723, 2010.
89. C.S.Ko, J.P.Huang, C.W.Huang, and I.M.Chu, "Type II collagen-chondroitin sulfate-hyaluronan scaffold cross-linked by genipin for cartilage tissue engineering", *J. Biosci Bioengg*, vol.107, no.2, pp.177-182, 2009.
90. S.W.Kang, O.Jeon, and B.S.Kim, "Poly (lactic-co-glycolic acid) microspheres as an injectable scaffold for cartilage tissue engineering" .*Tissue engg*, vol.11, no. 3-4, pp.438-447, 2005.
91. C.Chung, and A.B.Jason, "Engineering cartilage tissue", *Adv drug del rev*, vol.60, no.2, pp.243 -262, 2008.
92. G.M.Peretti, M.A.Randolph, V.Zaporojan, L.J. Bonassar, J.W. Xu, J.C. Fellers and M.J. Yaremchuk, "A biomechanical analysis of an engineered cell-scaffold implant for cartilage repair". *Annals plastic surgery*, vol.46, no.5, pp. 533-537, 2001.
93. S.Yodmuang, S.L.McNamara, A.B.Nover, B.B.Mandal, M.Agarwal, T.A.N. Kelly, P.H.G. Chao, C.Hung, D.L.Kaplan, and G.Vunjak-Novakovic, "Silk microfiber-reinforced silk hydrogel composites for functional cartilage tissue repair", *Acta Biomater*, vol.11, pp.27-36, 2015.
94. A.M.Hopkins, L.De Laporte, F.Tortelli, E.Spedden, C.Staai, T.J.Atherton, J.A.Hubbell, and D.L. Kaplan, "Silk hydrogels as soft substrates for neural tissue engineering", *Adv. Funct. Mater*, vol.23, no.41, pp.5140-5149, 2013.
95. B. B.Mandal, A. S.Priya, and S. C.Kundu, "Novel silk sericin/gelatin 3-D scaffolds and 2-D films: fabrication and characterization for potential tissue engineering applications". *Acta Biomater*, vol.5, no.8, pp.3007-3020, 2009.
96. M.Garcia-Fuentes, A.J.Meinel, M.Hilbe, L.Meinel, and H.P. Merkle, "Silk fibroin/hyaluronan scaffolds for human mesenchymal stem cell culture in tissue engineering", *Biomaterials*, vol.30, no.28, pp.5068-5076, 2009.
97. B. B.Mandal, & S. C.Kundu, "Cell proliferation and migration in silk fibroin 3D scaffolds". *Biomaterials*, vol.30, no. 15, pp.2956-2965, 2009.
98. G. M.Nogueira, R. F.Weska, W. C.Vieira, B.Polakiewicz, A. C.Rodas, O. Z. Higa, and M. M. Beppu, "A new method to prepare porous silk fibroin membranes suitable for tissue scaffolding applications", *J.App. Polym.Sci*, vol.114, no.1, pp.617-623, 2009.
99. J.Zhan, X.Sun, F.Cui and X.Kong, "Preparation of 3-D porous fibroin scaffolds by freeze drying with treatment of methanol solutions", *Chin. Sci. Bull.*, vol.52, no.13, pp.1791-1795, 2007.
100. Q.Lv. and Q.Feng, "Preparation of 3-D regenerated fibroin scaffolds with freeze drying method and freeze drying/foaming technique", *J.Mat.Sci.Mat. Med*, vol.17, no.12, pp.1349-1356, 2006.
101. J.Nam, and Y. H.Park, "Morphology of regenerated silk fibroin: Effects of freezing temperature, alcohol addition, and molecular weight", *J.App. Polym.Sci*, vol. 81,no.12, pp. 3008-3021, 2001.

102. X.Y.Liu, C.C.Zhang, W.L.Xu, and C.X. Ouyang, "Controlled release of heparin from blended polyurethane and silk fibroin film", *Mat.Lett*, vol.63, no.2, pp.263-265, 2009.
103. C.Li, C.Vepari, H.J.Jin, H.J.Kim, and D. L. Kaplan, "Electrospun silk-BMP-2 scaffolds for bone tissue engineering", *Biomaterials*, vol. 27, no.16, pp.3115-3124, 2006.
104. K G.Lee, H.Kweon, J.H.Yeo, S.O.Woo, J.H.Lee, and Y.Hwan Park, "Structural and physical properties of silk fibroin/alginate blend sponges". *J.App. Polym.Sci*, vol. 93, no.5, pp.2174-2179, 2004.
105. G.Yang, L.Zhang, X.Cao, and Y.Liu, "Structure and microporous formation of cellulose/silk fibroin blend membranes: Part II. Effect of post-treatment by alkali", *J.Membrane Sci*, vol.210, no.2, pp.379-387, 2002.
106. S.Zeng, L.Liu, Y.Shi, J.Qiu, W.Fang, M. Rong, and W.Gao, "Characterization of Silk Fibroin/Chitosan 3D Porous Scaffold and In Vitro Cytology", *PloS one*, vol.10, no.6, e0128658, 2015.
107. D.N.Rockwood, R.C.Preda, T.Yücel, X.Wang, M.L.Lovett, and D.L.Kaplan, "Materials fabrication from Bombyx mori silk fibroin", *Nat. Protoc*, vol.6, no.10, pp.1612-1631, 2011.
108. V.Karageorgiou, and D.L.Kaplan, "Porosity of 3D biomaterial scaffolds and osteogenesis", *Biomaterials*, vol.26, no.27, pp.5474-5491, 2005.
109. S.Hofmann, C. W. P.Foo, F.Rossetti, M.Textor, G.Vunjak-Novakovic, D. L.Kaplan and L.Meinel, "Silk fibroin as an organic polymer for controlled drug delivery", *J. Control. Release*, vol.111, no.1, pp. 219-227, 2006.
110. M.Peter, N.Ganesh, N.Selvamurugan, S.V Nair, T.Furuike, H.Tamura, and R.Jayakumar, "Preparation and characterization of chitosan–gelatin/nanohydroxyapatite composite scaffolds for tissue engineering applications", *Carbo. Polym*, vol.80, no.3, pp.687-694, 2010.
111. F.Pati, H.Kalita, B.Adhikari, and S.Dhara, "Osteoblastic cellular responses on ionically crosslinked chitosan-tripolyphosphate fibrous 3-D mesh scaffolds", *J.Biomed.Mat.Res.Part A*, vol.101,no.9,pp.2526-2537, 2013.
112. N.Bhardwaj, Q.T.Nguyen, A.C.Chen, D.L.Kaplan, R.L.Sah & S.C.Kundu, "Potential of 3-D tissue constructs engineered from bovine chondrocytes/silk fibroin-chitosan for in vitro cartilage tissue engineering", *Biomaterials*, vol.32, no.25, pp.5773-5781, 2011.
113. B. B.Mandal, S. H.Park, E. S Gil, and D. L.Kaplan, "Multilayered silk scaffolds for meniscus tissue engineering", *Biomaterials*, vol.32, no.2, pp.639-651, 2011.
114. K.S.Han, J.E.Song, N.Tripathy, H.Kim, B.M. Moon, C.H. Park, and G. Khang, "Effect of pore sizes of silk scaffolds for cartilage tissue engineering", *Macromol Res*, pp. 1-7, 2015.
115. L.A.Lucia, O.Rojas The nanoscience and technology of renewable biomaterials. John Wiley & Sons. 2009; Jul 23:297.
116. S.H.Lee, and H Shin, "Matrices and scaffolds for delivery of bioactive molecules in bone and cartilage tissue engineering", *Adv drug del rev*, vol.59, no.4, pp.339-59, 2007.

117. J.S.Mojarrad, M.Nemati, H.Valizadeh, M.Ansarin, and S.Bourbour, "Preparation of glucosamine from exoskeleton of shrimp and predicting production yield by response surface methodology", *J. Agric. Food Chem*, vol.55, no.6, pp.2246-2250, 2007.
118. W.H.Liang, B.L.Kienitz, K.J.Penick, J.F.Welter, T.A.Zawodzinski, and H.Baskaran, "Concentrated collagen-chondroitin sulfate scaffolds for tissue engineering applications", *J.Biomed.Mat.Res. Part A*, vol.94, no.4, pp.1050-1060, 2010.
119. Z.A.Yaoa, and H.G.Wua, "Characterization of chitosan-chondroitin sulfate blended membranes and effects on the growth of corneal cells". *Adv. Mater. Lett*, vol.1, pp. 67-74, 2010.

Dissemination

Internationally indexed journals

1. Vishwanath, Varshini, Krishna Pramanik, and Amit Biswas. Optimization and evaluation of silk fibroin-chitosan freeze dried porous scaffolds for cartilage tissue engineering application. *Journal of Biomaterials Science, Polymer Edition*: 2016.27(7) 657-674.
2. Vishwanath, Varshini, Krishna Pramanik, and Amit Biswas. Development of a novel glucosamine incorporated silk fibroin-chitosan blend porous scaffolds. *Iranian polymer journal*: 2016 (1-9).

Conferences

1. V. Vishwanath, A. Biswas, K. Pramanik, “Freeze dried porous scaffolds for Cartilage tissue Engineering”, *Proceedings of Emerging issues in Chitin and Chitosan Research*, Institute of Himalayan Bioresource Technology, Palampur June 7-8 2013
2. V. Vishwanath, A. Biswas, K. Pramanik “Development and characterization of Silk based scaffold for Cartilage tissue engineering” Presented a poster at 2nd International conference on Nanotechnology at the Biomedical Interface (NANOBIO-12) Kochi, Kerala, India during Feb-2012
3. V. Vishwanath, A. Biswas, K. Pramanik “Porous scaffold for Cartilage Tissue Engineering” *Proceedings of National conference on Tissue Engineering: Prospects and challenges (TEPC-11)* organized by Tissue Engineering Group, NIT Rourkela in Jan-2011

Articles under review

1. Vishwanath, Varshini, Krishna Pramanik, and Amit Biswas. In vitro study of mesenchymal stem cells seeded on glycosaminoglycan incorporated silk fibroin-chitosan blend porous scaffolds for tissue engineering applications. UNDER REVIEW.(Journal of Applied Polymer Science)

Biography

Varshini Vishwanath is a PhD candidate in the Department of Biotechnology and Medical Engineering at National Institute of Technology Rourkela, India. She received her B.Tech (Biotechnology) in 2008 from SRM University, Kattangulathur, Tamilnadu (India). She also received her M.Tech (Medical Nanotechnology) from SASTRA University, Thanjavur (India). She started her Ph.D in NIT Rourkela in the year of 2010. Her interests include biomaterials processing and application for bone and cartilage tissue engineering, utilization of nanotechnology for enhanced tissue regeneration applications.

Personal Details:

Father's Name	Mr. M.Vishwanath
Mother's Name	Mrs. Usha Vishwanath
Gender	Female
Nationality	Indian
Language Known	English, Tamil, Hindi, Japanese

JOURNAL PUBLICATIONS

1. Vishwanath, Varshini, Krishna Pramanik, and Amit Biswas. Optimization and evaluation of silk fibroin-chitosan freeze dried porous scaffolds for cartilage tissue engineering application. Journal of Biomaterials Science, Polymer Edition: 2016.27(7) 657-674.
2. Vishwanath, Varshini, Krishna Pramanik, and Amit Biswas. Development of a novel glucosamine incorporated silk fibroin-chitosan blend porous scaffolds. Iranian polymer journal: 2016 (1-9).
3. Vishwanath, Varshini, Krishna Pramanik, and Amit Biswas. In vitro study of mesenchymal stem cells seeded on glycosaminoglycan incorporated silk fibroin-chitosan blend porous scaffolds for tissue engineering applications. UNDER REVIEW.(Journal of Applied Polymer Science)

CONFERENCE PAPERS

1. V. Vishwanath, A. Biswas, K. Pramanik, “Freeze dried porous scaffolds for Cartilage tissue Engineering”, Proceedings of Emerging issues in Chitin and Chitosan Research, Institute of Himalayan Bioresource Technology, Palampur June 7-8 2013
2. V. Vishwanath, A. Biswas, K. Pramanik “Development and characterization of Silk based scaffold for Cartilage tissue engineering” Presented a poster at 2nd International conference on Nanotechnology at the Biomedical Interface (NANOBIO-12) Kochi, Kerala, India during Feb-2012
3. V. Vishwanath, A. Biswas, K. Pramanik Porous scaffold for Cartilage Tissue Engineering” Proceedings National conference on Tissue Engineering: Prospects and challenges (TEPC-11) organized by Tissue Engineering Group, NIT Rourkela in Jan-2011